MONTANA STATE UNIVERSITY

Physiological heterogeneity and starvation in mature Pseudomonas aeruginosa biofilms
by Dongxin Karen Xu

A thesis submitted in partial fulfillment of the requirements for the degree of Doctor of Philosophy in Microbiology
Montana State University
© Copyright by Dongxin Karen Xu (1999)

Abstract:
Bacteria growing in biofilms are often found to be less susceptible to antimicrobial agents than bacteria grown planktonically. Slow growth and starvation were hypothesized to contribute to the reduced susceptibility of mature biofilms. In this study, spatial physiological heterogeneity of mature biofilms was visualized by molecular staining coupled with cryoembedding and cryosectioning. Frozen cross sections of biofilms that had been subjected to a period of phosphate starvation then stained for alkaline phosphatase activity with a fluorogenic stain demonstrated that alkaline phosphatase activity was induced only in a distinct band of approximately 30 μm adjacent to the gaseous interface. The localized pattern of alkaline phosphatase activity correlated well with dissolved oxygen penetration profile measured with an oxygen microelectrode. Biofilm sections stained with acridine orange and Fluorescent-In-Situ-Hybridization (FISH) revealed that faster-growing cells were located in the upper 20-25 μm layer of the biofilms, whereas the majority of cells in the lower part of the biofilms were slower growing. These molecular stains gave indications of different activity measurements in the biofilms.

The gene expression and protein level of the starvation sigma factor was studied to address the possible role of starvation in biofilm resistance. A rpoS-lacZ transcriptional fusion was used to compare the level of gene expression of Pseudomonas aeruginosa cells, grown planktonically and in biofilms. lmmunoblots were used to assay the levels of RpoS, under these different cultivation conditions. In 3-day continuously fed biofilms, rpoS gene expression was three fold higher per mg cell protein, than that of average stationary planktonic cells. In addition, the levels of RpoS in 3 and 4-day biofilms were similar to the level found in the stationary phase planktonic culture. These results demonstrated that the levels of RpoS were high in at least some regions of continuously fed mature biofilms. Since RpoS is involved in the regulation of general stress protection, induction of rpoS in biofilms may contribute to the increased resistance of biofilms.

Taken together, these results show that mature P.aeruginosa biofilms are characterized by striking physiological heterogeneity, including evidence of regions of diminished metabolic activity, slow growth, and starvation response.

PHYSIOLOGICAL HETEROGENEITY AND STARVATION IN MATURE *PSEUDOMONAS AERUGINOSA* BIOFILMS

by

Dongxin Karen Xu

A thesis submitted in partial fulfillment
of the requirements for the degree

of

Doctor of Philosophy

in

Microbiology

MONTANA STATE UNIVERSITY
Bozeman, Montana

July 1999

D378
X799

APPROVAL

of a thesis submitted by

Dongxin Karen Xu

This thesis has been read by each member of the thesis committee and has been found to be satisfactory regarding content, English usage, format, citations, bibliographic style, and consistency, and is ready for submission to the College of Graduate Studies.

7/28/99
Date

Chairperson, Graduate Committee

Approved for the Major Department

7/28/99
Date

Head, Major Department

Approved for the College of Graduate Studies

7-29-99
Date

Graduate Dean

STATEMENT OF PERMISSION TO USE

In presenting this thesis in partial fulfillment of the requirements for a doctoral degree at Montana State University, I agree that the Library shall make it available to borrowers under the rules of the Library. I further agree that copying of this thesis is allowable only for scholarly purposes, consistent with "fair use" as prescribed in the U. S. Copyright Law. Requests for extensive copying or reproduction of this thesis should be referred to University Microfilms International, 300 North Zeeb Road, Ann Arbor, Michigan 48106, to whom I have granted "the exclusive right to reproduce and distribute my dissertation for sale in and from microform or electronic format, along with the right to reproduce and distribute my abstract in any format in whole or in part".

Signature Yalk Xu

Date 7-28-99

This work is dedicated to my beloved father.

ACKNOWLEDGEMENTS

I could not have made my Ph.D through without the friendliest people I met in Montana State University. First and for the most, I would like to express my greatest appreciation to my mentors, Dr. Gordon A. McFeters and Dr. Philip S. Stewart, who gave me the opportunity and always were there when I needed help. Second, I would like to acknowledge my committee members, Dr. Gill Geesey, Dr. Cliff Bond, Dr. Joan Henson and Dr. Michael Franklin for their counsel and assistance.

I would also like to thank Wendy Cochran and Betsey Pitts for their friendship and encouragement. CBE graduate students and Biofilm Control Team members are appreciated for their parties and drinks after work. I want to thank Grace T. Wang for her accompany for the hiking and biking time in Montana.

Finally, I would like to thank my husband, Yi and my family. Their love and support made my life enjoyable and enabled me to overcome difficulties.

TABLE OF CONTENTS

Chapter		Page
1.	GENERAL INTRODUCTION	1
	Ubiquity of Biofilm Formation	1
	Biofilm Resistance	2
	Biofilm Physiology	3
	Physiological Heterogeneity and Starvation in Thick Biofilms	7
	In Situ Indicators of Physiological Activities	11
	Starvation, Stringent Response and Antimicrobial Susceptibility	16
	Regulation of Starvation Sigma Factor RpoS and Role of RpoS in Stress Response	18
	Objectives, Rationales and Experimental Design	21
	References Cited	23
2.	SPATIAL PHYSIOLOGICAL HETEOGENEITY OFALKALINE PHOSPHATASE IN *PSEUDOMONAS AERUGINOSA* BIOFILM IS DETERMINED BY OXYGEN AVAILABILITY	34
	Introduction	34
	Material and Methods	35
	Bacterial Strains, Media, and Growth Conditions	35
	Planktonic Culture Procedure	36
	Biofilm Culture Procedure	36
	Alkaline Phosphatase (APase) Activity and Total Protein Assay	37
	Staining Procedure	40
	Cryoembedding and Cryosectioning	40
	Microscopy	41
	Image Analysis	41
	Dissolved Oxygen Profile Measurement	42
	Results	42
	Planktonic and Biofilm APase Specific Activity	42
	Patterns of APase Expression in Biofilms	45
	Dissolved Oxygen Penetration Profile	48
	Discussion	53
	Acknowledgments	57
	References Cited	57
3.	SPATIAL PHYSIOLOGICAL HETEROGENEITY REVEALED BY ACRIDINE ORANGE STAINING AND FLUORESCENT-IN-SITU-HYBRIDIZATION (FISH)	61

Introduction 61
Materials and Methods 64
Bacterial Strains and Media 64
Planktonic Culture and Sampling Procedure 65
Biofilm Culture and Sampling procedure 65
Cryoembedding and Cryosectioning Procedure 66
Acridine Orange Staining Procedure 66
Hybridization of Whole Cells and Biofilms 66
Microscopy 67
Image Analysis 68
Results 68
AO Staining Result of Biofilm Sections 68
FISH Staining Result of Planktonic Cells and Biofilm Sections 69
Discussion 74
References Cited 76

4. PHYSIOLOGICAL HETEROGENEITY OF RESPIRATORY ACTIVITY REVEALED BY CTC STAINING 79
Introduction 79
Materials and Methods 81
Bacterial Strains, Media and Biofilm Growth Procedure 81
CTC Staining Procedure 81
Preparation of Biofilm Sections for Microscopy 82
Microscopy 82
Image Analysis 82
Results 83
Discussion 87
References Cited 89

5. ANALYSIS OF GENE EXPRESSION AND PROTEIN LEVELS OF THE STATIONARY PHASE SIGMA FACTOR, RpoS, IN CONTINUOUSLY-FED *PSEUDOMONAS AERUGINOSA* BIOFILMS 91
Introduction 91
Material and Methods 93
Bacterial Strains and Growth Media 93
Planktonic Culture Procedure 94
Biofilm Culture Procedure 95
β-galactosidase Activity and Total Protein Assay 95
SDS-PAGE and Western Blot 96
Statistical Analysis 98
Results 98
rpoS Expression in Planktonic Culture 98

rpoS Expression in Biofilms 99
Presence and Levels of RpoS in Mature Biofilms Grown in Complex and Minimal Media 102
Effect of oxygen limitation on RpoS buildup along growth .. 103
Discussion 103
Acknowledgements 111
References Cited 112

6. SUMMARY AND DISCUSSION 117
References Cited 123

APPENDIX Repeatibility of Biofilm Thickness among Different Chambers in Drip-flow Reactor 126
Biofilm Accumulation Curve 127
Quantification of Western Blots 128

LIST OF TABLES

Table		Page
2.1	Comparison of APase specific activity of planktonic *P.aeruginosa* with scraped biofilms under different conditions. Cell density is expressed as CFU/ml and CFU/cm^2 of planktonic and biofilm, respectively.	45
2.2	Thickness of the zone of APase expression under different gaseous conditions.	53
3.1	Summary of image analysis results of AO and FISH	74
4.1	Summary of image analysis result of CTC staining	87
5.1	Bacterial strains and plasmids	94
6.1	Active zones measured by different staining methods	120
7.1	Variability of biofilm thickness among different chambers of the drip-flow reactor	126
7.2	Raw data of the quantitative result of the two bands in Figure 5.3	129
7.3	Raw data of the quantitative result of the first band in Figure 5.3	129
7.4	Raw data of the quantitative result of the band in Figure 5.4	130
7.5	Raw data of the quantitative result of the band in Figure 5.5	130

LIST OF FIGURES

Figure		Page
2.1	Schematic diagram of drip-flow biofilm reactor	38
2.2	Photograph of the drip-flow chamber reactor	39
2.3	APase specific activity of plantonic *P.aeruginosa* in Response to phosphate starvation. APase specific activity is expressed as ΔA_{410} mg protein^{-1}min^{-1}. (□) represents APase specific activity under ambient air without disruption for 8 hours, (○) represents APase specific activity of a culture exposed to air, then pure nitrogen, and finally air again.	44
2.4	Photographs of *P.aeruginosa* biofilm cross-sections of biofilms induced for 0 (A), 8 (B), 24 (C), 36 (D) hours of phosphate starvation. The green-yellow color represents APase positive cells and the red color represents all cells. The image are oriented with the substratum at the bottom of the photographs. Bar represents 100μm.	46
2.5	Photographs of *P.aeruginosa* biofilm cross-sections stained for APase activity under different conditions. (A) high phosphate medium with ambient air; (B) low phosphate medium with ambient aerobic atmosphere; (C) low phosphate medium under pure nitrogen atmosphere; (D) low phosphate medium under pure oxygen atmosphere. The yellow colore represents APase positive cells and the red color represents all cells. The images are oriented with the substratum at the bottom of the photographs. Bar = 100μm.	49
2.6	A representative image analysis result of APase activity in *P.aeruginosa* biofilms with phosphate starvation under ambient aerobic condition. (◇) represents biofilm cells stained with tetramethyl rhodamine, while (□) represents APase positive cells. The substratum is at the "0" point.	51
2.7	Correlation of dissolved oxygen profile with image analysis result of APase activity under aerobic conditions. (◇) APase activity, (□) dissolved oxygen (-) trend line representing dissolved oxygen concentration. The substratum is at the "0" point.	52
3.1	A representative image of a 4-day old biofilm section stained with acridine orange. Orange color	

represents high RNA, whereas green color represents low RNA. The substratum is at the bottom of the photograph. Bar = 100μm. 70

3.2 Photographs of *P.aeruginosa* planktonic cells stained with Eub338probe (A) and anti-Eub338 probe (B). X 40 magnification. 71

3.3 A representative image of a 4-day old *P.aeruginosa* biofilm section stained with Eub338 probe (A) and anti-Eub338 probe (B). The substratum was oriented at the bottom of the photograph. Bar = 100μm. 72

3.4 Image analysis of a FISH/DAPI stained *P.aeruginosa* biofilm section. (◊) represents FISH fluorescence intensity, (-) represents DAPI fluorescence intensity Substratum is at the "0" point. 73

4.1 Photographs of a 4-day old *P.aeruginosa* biofilm stained with CTC/DAPI. (A) DAPI staining visualized with U cubic filter; (B) CTC-formazan formed across biofilm visualized with G cubic filter; (C) CTC/DAPI staining simultaneously visualized with B cubic filter. The substratum is oriented at the bottom of the photographs. Bar = 100 μm. 84

4.2 Image analysis result of CTC/DAPI staining of a 4-day old *P.aeruginosa* biofilm. (□) represents CTC staining and (◇) represents DAPI staining. Substratum is at "0" point. ....., 86

5.1 *rpoS* expression in planktonic KX101 and KX101c during growth in full strength LB. The cell density is expressed as $\log OD_{600}$, specific β-galactosidase activity is expressed as $\Delta A_{410} ml mg^{-1} min^{-1}$; (Δ) and (△) represents $\log OD_{600}$ and specific β-galactosidase activity of KX101, respectively; (~) and (□) represents $\log OD_{600}$ and specific β-galactosidase activity of KX101c, respectively. 100

5.2 Comparison of *rpoS* expression in stationary-phase planktonic culture and biofilms grown in 1/5-strength LB medium. The first bar at the left is the average level of *rpoS* expression of planktonic culture within 20-hour stationary phase (excluding the lowest level of *rpoS* expression). (n=4 for planktonic, stationary; n=3 for 3-day and 3.5-day biofilms; bar = S.D.) 101

5.3 Western blot analysis of RpoS levels in 1/5LB grown

planktonic and biofilm cultures. The arrow indicates RpoS. The positions of molecular mass markers (in kilodaltons) are indicated on the left. Lane 1: stationary-phase PAO1; lane 2: stationary-phase SS24; lane 3-5: mid-log, transition, stationary phase ERC1; lane 6-8: 2.5, 3, 3.5-day ERC1 biofilms; lane 9: 3.5-day SS24 biofilm. 104

5.4 Western blot analysis of RpoS level in 1g/L glucose minimal media grown planktonic and biofilm cultures. The positions of molecular mass marker (in kilodaltons) are indicated on the left. Lane1: stationary-phase SS24; lane 2-4: mid-log, transition, stationary phase ERC1; lane 5-7: 3, 3.5, 4-day ERC1 biofilms. 105

5.5 Western blot analysis of RpoS level in 0.1g/L glucose minimal media grown biofilms. The positions of molecular mass marker (in kilodaltons) are indicated on the left. Lane 1-3: mid-log, transition, stationary-phase ERC1 grown in 1g/L glucose minimal medium; lane 4-6: 3, 4, 4.5-day ERC1 biofilms grown in 0.1g/L glucose minimal medium. 106

5.6 Effect of oxygen limitation on growth and RpoS accumulation. The upper panel shows the growth curve of LB medium under ambient air or nitrogen. The growth is expressed as $\log OD_{600}$; (◇) represents the growth of ERC1 under ambient air condition without interruption (control culture); (□) represents the growth of ERC1 under ambient air condition for 3.5 hours before pure nitrogen was introduced and left inside the culture flask (experimental culture). The arrow indicates when pure nitrogen was introduced. The lower panel shows western blots of samples taken from the cultures above: A) lane 1: stationary-phase PAO1 as positive control, lane 2-6 corresponding to samples 1-5 from experimental culture; B) lane 1: stationary-phase PAO1 as positive control, lane 2-6 corresponding to samples 1-5 from control culture. 107

7.1 Accumulation curve of biofilms grown in drip-flow reactor 127

7.2 Summary intensity of the two bands in Figure 5.3 131

7.3 Intensity of the 1st band in Figure 5.4. 131

7.4 Intensity of the band in Figure 5.5. 132

7.5 Intensity of the band in Figure 5.6. 132

Parts of the thesis have been published or submitted for publication to meet the requirement of the major department. Chapter 2 has been published in October, 1998, Applied and Environmental Microbiology, 64(4): 1526-1531 (2nd author) and 64(10): 4035-4039 (1st author). Chapter 5 has been submitted to Applied and Environmental Microbiology, 1999 (1st author).

ABSTRACT

Bacteria growing in biofilms are often found to be less susceptible to antimicrobial agents than bacteria grown planktonically. Slow growth and starvation were hypothesized to contribute to the reduced susceptibility of mature biofilms. In this study, spatial physiological heterogeneity of mature biofilms was visualized by molecular staining coupled with cryoembedding and cryosectioning. Frozen cross sections of biofilms that had been subjected to a period of phosphate starvation then stained for alkaline phosphatase activity with a fluorogenic stain demonstrated that alkaline phosphatase activity was induced only in a distinct band of approximately 30 μm adjacent to the gaseous interface. The localized pattern of alkaline phosphatase activity correlated well with dissolved oxygen penetration profile measured with an oxygen microelectrode. Biofilm sections stained with acridine orange and Fluorescent-In-Situ-Hybridization (FISH) revealed that faster-growing cells were located in the upper 20-25 μm layer of the biofilms, whereas the majority of cells in the lower part of the biofilms were slower growing. These molecular stains gave indications of different activity measurements in the biofilms.

The gene expression and protein level of the starvation sigma factor was studied to address the possible role of starvation in biofilm resistance. A *rpoS-lacZ* transcriptional fusion was used to compare the level of gene expression of *Pseudomonas aeruginosa* cells, grown planktonically and in biofilms. Immunoblots were used to assay the levels of RpoS, under these different cultivation conditions. In 3-day continuously fed biofilms, *rpoS* gene expression was three fold higher per mg cell protein, than that of average stationary planktonic cells. In addition, the levels of RpoS in 3 and 4-day biofilms were similar to the level found in the stationary phase planktonic culture. These results demonstrated that the levels of RpoS were high in at least some regions of continuously fed mature biofilms. Since RpoS is involved in the regulation of general stress protection, induction of *rpoS* in biofilms may contribute to the increased resistance of biofilms.

Taken together, these results show that mature *P.aeruginosa* biofilms are characterized by striking physiological heterogeneity, including evidence of regions of diminished metabolic activity, slow growth, and starvation response.

CHAPTER 1

GENERAL INTRODUCTION

Ubiquity of Biofilm Formation

Bacteria in natural aquatic populations have a marked tendency to interact with surfaces and form biofilms. The real significance of bacterial biofilms has gradually emerged since their first description (Zobell & Anderson, 1936), and the first recognition of their ubiquity (Costerton et al., 1978). Biofilms are found in natural aquatic environments (Lock et al., 1984), in industrial aquatic systems and on medical biomaterials. They are involved in biodeterioration of materials, including the digestion of insoluble nutrients by bacterial populations in the digestive tracts of higher animals and protective and pathogenic association with tissue surfaces (Costerton et al., 1987). It has become increasingly clear that the biofilm mode of growth (sessile) predominates in natural ecosystems both in medical and non-medical situations. In an exhaustive survey of the sessile and planktonic bacterial populations of 88 streams and rivers, the sessile populations exceeded the planktonic populations by 3-4 logarithm units in pristine alpine streams and by 200 fold in sewage effluent (Lock et al., 1984). In the investigation of medical-devices-associated infections, extensive bacterial biofilms were

found by scanning and transmission electron microscopy on transparent dressings, sutures, wound drainage tubes, intraarterial and intravenous catheters (Peters et al., 1981), cardiac pacemakers (Marrie & Costerton, 1982), Foley urinary catheters (Nickel et al., 1985a) and urine collection systems.

Biofilm Resistance

It is well documented that biofilms are generally less susceptible to antimicrobial agents than their free-living counterparts (Brown and Gilbert, 1993; Costerton, 1984; LeChevallier et al., 1988). Treatment with traditional concentrations of biocides kills planktonic microorganisms but leaves the biofilm populations virtually unaffected (Ruseska et al., 1982; LeChevallier et al., 1988). Millions of dollars each year have been wasted in ineffectual treatments. There are also numerous reports about the biofilm resistance to antibiotics (Nickel et al., 1985a; Nickel et al., 1985b; Evans & Holmes, 1987; Anwar et al., 1989). The resistance of biofilms to antibiotics was demonstrated (Nickel et al., 1985b) by the inability of tobramycin to kill *Pseudomonas aeruginosa* cells embedded in a biofilm at antibiotic levels more than 50 times the MIC for the same strain grown in a liquid culture.

A bacterial cell initiates the process of irreversible adhesion by binding to the surface using exopolysaccharide glycocalyx polymers (Costerton et al., 1987). Cell division then produces sister cells that are bound within the glycocalyx matrix, initiating

the development of adherent microcolonies. The eventual production of a continuous biofilm on the surface is a function of cell division within microcolonies and new recruitment of bacteria from the planktonic phase (Malone & Caldwell, 1983). The biofilm finally consists of single cells and microcolonies of sister cells all embedded in a highly hydrated, predominantly anionic matrix (Sutherland, 1977) of bacterial exopolymers and trapped extraneous macromolecules. These so-called extracellular-polymers (EPS) may protect the biofilm cells from the onslaught of antimicrobial agents by serving as a diffusional barrier (Anwar et al., 1992; Hoyle et al., 1992). The reduced penetration of antimicrobial agents results from the binding, absorption or reaction of the antimicrobial agents within the biofilms (de Beer et al., 1994; Nichols et al., 1988). de Beer et al. (1994) measured the chlorine penetration into biofilms during disinfection using chlorine microelectrode and found the limited penetration was caused by neutralization of the chlorine in the biofilm matrix. Monochloramine was also observed to be more effective than free chlorine for inactivation of biofilm bacteria due to its lower reaction rates resulting in greater penetration power (LeChevallier et al., 1988).

Biofilm Physiology

While reduced penetration of antimicrobial agents could explain some cases of biofilm resistance, transport limitation is not sufficient to explain all biofilm recalcitrance. Nichols (1989) mathematically modeled the penetration of two antibiotics into a

Pseudomonas aeruginosa biofilm. The amino-glycoside, tobramycin and a β-lactam, cefsuldin, were used. Based on their model the authors concluded that transport limitation of the antibiotics was not the only factor reducing the susceptibility of this biofilm. Using ATR/FT-IR, Vrany et al. (1997) observed that the transport of the fluoroquinolones, levofloxacin and ciprofloxacin, was rapid (<20min) for a 15-25 μm thick *P.aeruginosa* biofilm. Differences in levels of recalcitrance observed for this biofilm system were suggested to be due to a less susceptible physiological status which bacteria assume during biofilm life (Vrany et al., 1997). Stewart (1996) recently argued that, for most antibiotics, transport limitation was insufficient to explain the reduced susceptibility of biofilms because most antibiotics do not react or sorb sufficiently within the biofilm. Therefore, physiological and genetic modifications of biofilms resulting in biofilm resistance are receiving more and more attention (Anwar et al., 1992; Gilbert et al., 1990).

How solid surfaces may influence bacterial activity is an important question in microbial ecology. For over 50 years researchers have been trying to address the question and it appears to be complex, particularly in natural environments. Most measurements deal directly or indirectly with the efficiency of substrate utilization. It is speculated that biofilm bacteria have a nutritional advantage over the planktonic cells. Surfaces in aquatic environments rapidly adsorb organic molecules. These organic molecules are a source of nutrients for the attached bacteria. Griffith and Fletcher (1991) reported the adsorption of bovine serum albumin (BSA) by particles, derived

from diatoms. Attached bacteria degraded 100% of the protein absorbed, while the planktonic cells were unable to utilize the BSA. McFeters et al. (1990) found a shorter lag time and greater specific activity in the degradation of nitrilotriacetate by attached bacteria than by bacteria in the bulk aqueous phase. Other investigations have produced different results. Fowler (1988) found that growth of *Escherichia coli* was improved after surface adsorption, but only at a nutrient (glucose) concentration less than 25 ppm. Jeffery & Paul (1986) reviewed a number of studies and found an increase in metabolic activities for surface-associated bacteria at low or zero nutrient concentrations.

There are several review articles addressing the changes of physiological activity in biofilm bacteria (van Loosdrecht et al., 1990; Costerton et al., 1995; Marshall & Goodman, 1994). However, during the 1984 Dahlem Workshop on Microbial Adhesion and Aggregation, the discussion group on activity on surfaces concluded: "Attachment to a surface can undoubtedly affect the activity of microorganisms, although sometimes in ways that are not readily predictable on our current knowledge" (Breznak, 1984). In the review article by van Loosdrecht et al, this statement was claimed to be still true. Although they examined the current work on microbial activity case by case, due to the great diversity in experimental set-up and parameters involved, the conclusion drawn was: "The presence of surfaces may positively or negatively (or not at all) affect microbial substrate utilization rates and growth yields. The results often depend on the nature of the organisms, the kind and concentration of substrate, and the nature of the

solid surface. In interpreting the effect of surfaces on bioconversion processes, all possible physical and chemical interactions (e.g., diffusion ad- and desorption, ion-exchange reactions, conformation changes, etc.) of a given compound and its possible metabolites with a given surface have to be considered before general conclusions can be drawn".

The effects of adhesion on microbial physiology at genetic level have just begun to come under investigation using molecular approaches. The application of reporter gene technology has allowed in situ studies of gene expression directly at surfaces and has provided possibilities of identification of genes "switched on" or "switched off" at surfaces (Davies et al., 1993; Hoyle et al., 1993; Marshall et al., 1994). Using an *algC-lacZ* transcriptional fusion, Davies et al. (1993) found *algC* expression was upregulated in bacterial cells at the time of adhesion and often ceased when cells were surrounded by large amounts of alginate. Dagostino et al. (1991) employed reporter gene technology to demonstrate the "switching on" of genes at polystyrene surfaces in mutants that failed to express the genes in either liquid or semisolid media. Using the plasmid vector pJO100 (Östling et al., 1991) to transfer the transposon mini-*Mu* containing the promoterless *lacZ* into the marine *Pseudomonas* S9, mutants were selected that failed to express β-galactosidase in liquid or on semisolid media but produced the enzyme at a solid-liquid interface.

Hodgson et al. (1995) developed a perfused biofilm fermenter to achieve growth rate control in adherent population cells. Whole cell proteins of *Staphylococcus aureus*

were isolated from biofilm cells and chemostat-grown cells and analyzed by SDS polyacrylamide gel electrophoresis (PAGE). SDS-PAGE demonstrated significant differences between the protein profiles of biofilm and chemostat controls cultured at equivalent growth rates. The differences include the repression of a 48 KDa protein and increased expression of a 21 KDa protein in the biofilm.

Physiological Heterogeneity and Starvation in Thick Biofilms

A major factor in biofilm growth that is different from planktonic growth is that biofilms are usually mass transport limited. The three factors that govern concentrations of a particular solute in a biofilm are 1) external mass transport to the biofilm, 2) diffusion within the biofilm, and 3) reaction or consumption of the solute by biofilm cells. Nutrient concentrations at the liquid-biofilm interface can be much lower than bulk liquid concentration due to a diffusion boundary layer (Characklis et al., 1990). Biofilms are predominantly water and diffusion into a biofilm should be relatively rapid, except that the presence of EPS and other cellular materials may impede the diffusion of nutrients. Reaction/ consumption plays an important role that leads to the depletion of a nutrient in the biofilm. Mass transport limitation within the biofilm results in a concentration gradient, where cells embedded deeper may experience starvation for nutrients. Thus in a thick aging biofilm the physiological status of biofilm cells is hypothesized to be heterogeneous and is determined by the location of each individual cell within the

multiple layers of cells (Wentland et al., 1996). Cells located in the upper regions of the biofilm may have easy access to nutrients, including oxygen, and have fewer problems with the discharge of metabolic waste products. These cells are speculated to be metabolically active. In contrast, cells of the same species deep within the biofilm are likely to be less metabolically active.

Concentrations of oxygen, hydrogen sulphide, nitrous oxide and hydrogen ions (pH) can be measured within biofilms by microsensors with tip diameters down to a few micrometers. The size of the tip is so small that it provides an accurate measurement of concentration profiles in biofilms without disturbing the system. The use of such sensors has revealed steep concentration gradients, not only in the biofilm itself, but also in the aqueous phase above it (Lewandowski, 1994; Revsbech, 1989). In natural systems, this spatial differentiation generates a range of habitats providing niches for different physiological types of bacteria. A level of organization may develop in which cells of different species form consortia with integrated metabolic processes. Ritz (1969) examined the species composition of the sections of dental plaque by probing with fluorescent antibodies. The aerobic *Neisseria* were found to be most abundant in young plaque and in the upper layers of mature plaque. *Veillonella* (anaerobes) were limited to the inner two-thirds of the plaque.

There is also some evidence showing the spatial physiological heterogeneity and growth rate limitation within the biofilm as a result of restriction for a particular nutrient that fails to fully penetrate the biofilm. Tresse et al. (1995) entrapped viable cells of

Escherichia coli in agar gel layers to form artificial biofilm-like structures. Killing assays of immobilized bacteria by latamoxef and tobramycin were performed under different oxygenation conditions of the culture medium and compared with suspended cells. Under moderate aeration, agar-entrapped bacteria displayed higher resistance to the two antibiotics than suspended cells. In anaerobic conditions, suspended bacteria were highly resistant to the two antibiotics. Sustained oxygenation enhanced tobramycin efficacy against suspended and immobilized cells. These results show that oxygen deficiency in the gel layer contributes to the enhanced antibiotic resistance of biofilm-like cells. Oxygen concentration gradients in biofilms have been experimentally demonstrated many times using dissolved oxygen microelectrodes (de Beer et al., 1994).

Acridine orange (AO) stains double stranded nucleic acids green and single stranded nucleic acid orange. An actively-growing cell will have a higher RNA/DNA ratio than a less active cell, and therefore will have higher orange/green fluorescence intensity ratio after staining with AO. Wentland (1995) sampled colony-biofilms at different growth phases and stained the cryosections with AO. He found that mid-exponential phase colonies had high overall growth rates ($\mu > 1 hr^{-1}$) and were bright orange; stationary phase colonies had cells at the colony edges that fluoresced orange thus indicating high growth rates while cells in the interior of the colony fluoresced green indicating slower growth.

Kinniment and Wimpenny (1992) measured the distribution of adenylate concentrations and adenylate energy charge across *Pseudomononas aeruginosa* biofilms. The method involved freezing and sectioning of the intact biofilm, followed by extraction and assay of the adenylates in the sectioned material. Results indicated an increase in adenylate energy charge of about 0.2 units from the bottom to the surface of the biofilm and total adenylates formed a peak just below the interface. Energy charge values were generally low throughout the biofilm, reaching a maximum of only 0.6 units. Of the adenylates measured, AMP was the predominant nucleotide, especially in the deeper parts of the biofilm.

The same researchers along with Scourfield (Wimpenny et al., 1993) also used transmission electron microscopy (TEM) to examine biofilm growth. Scourfield (1990) grew the Bowden dental plaque community in the Cardiff constant-depth film fermenter (CDFF) as a model biofilm and investigated the structure with TEM. Examination by TEM of the dental biofilm and the above-mentioned *Pseudomonas aeruginosa* biofilm showed that healthy cells are present in the upper two-thirds of the biofilm. Below this the majority of cells appeared to be lysed. It was remarkable that there was a sharp division between the two zones. They suggested that in steady-state biofilm, nutrients diffuse downwards to a reproducible position below which cells were starved and/or anaerobic.

In Situ Indicators of Physiological Activities

The ability of microorganisms to grow and form colonies on solid culture media has been used as the traditional approach to study bacterial viability. Conventional microbiological methods for assessing the viability of bacteria within biofilms are based on the mechanical removal of cells from substrata followed by enumeration by colony formation. However, these methods not only require at least 24 hours incubation but also often underestimate bacterial activity (Morita, 1985; Brock, 1987). Most importantly, spatial relationships that are inherently complex and important in studying biofilm ecology will be lost by culture-dependent approaches.

To reveal spatial physiological heterogeneity in situ, fluorogenic probes can be utilized to stain biofilm before or after cryoembedding and cryosectioning depending upon the probes and targeting activities. Cryoembedding and cryosectioning is a simple technique developed by Yu et al. (1994) to mechanically remove biofilms from the substratum with minimal disruption of the structure and enable the imaging of sections of thick biofilms under light and epifluorescent microscopes.

There are extensive fluorescent reagents originally used by cellular biologists to observe the activities of cells (Mason, 1993; Haugland, 1992) and some have been exploited in microbiological applications. The compounds, 4,6-diamidino-2-phenylindole (DAPI), propidium iodide, ethidium bromide and Hoechst 33342 are all fluorescent nucleic acid stains that have been applied by microbiologists to determine a 'total

bacterial count' in a range of circumstances (Porter and Feig, 1980; Swannell and Williamson, 1988).

Fluorescent dyes also exist for different cellular functions. 5-cyano-2,3-ditolyl tetrazolium (CTC) has recently been applied with flow cytometry to determine respiratory activity (Kaprelyants and Kell, 1993). This compound is related to 2-(*p*-iodophenyl)-3-(*p*-nitrophenyl)-5-phenyl tetrazolium chloride (INT) which has been extensively used to microscopically discriminate actively respiring bacterial in a wide range of ecological and environmental studies (Rodriguez et al., 1992; Zimmermann et al, 1978). Both CTC and INT act as artificial electron acceptors. INT is converted to insoluble red (nonfluorescent) crystals of INT-formazan within metabolically active bacteria. Results obtained with INT correlated well with cellular ATP content in a study of pure and mixed microbial cultures (Stubberfield and Shaw, 1990). However, when cells are on opaque surfaces the microscopic examination of INT-formazan crystals is virtually impossible since the transmission of visible light through the specimen is required. On the other hand CTC can be utilized to observe respiring bacteria on an opaque surface since CTC is reduced to its fluorescent formazan crystals by succinate dehydrogenase of the respiratory pathway in *E. coli* (Smith and McFeters, 1996). CTC has been used to visualize respiring autochthonous bacteria in drinking water and biofilms (Schaule et al., 1993). Recently CTC was coupled with an immunomagnetic method to observe respiring *E. coli* O137 from hamburger (Pyle et al., 1999).

Cell biologists have extensively used indicators of membrane potential ($\Delta\Psi$) for nearly 20 years (Wu and Cohen, 1993; Loew, 1993). $\Delta\Psi$ is linked to the energy status of the cell (Diaper et al., 1992; Kaprelyants and Kell, 1992). Some studies have shown that $\Delta\Psi$ changes in eukaryotic cells during cellular proliferation with respect to their phase in the cell cycle (Darzynkiewicz et al., 1981). $\Delta\Psi$ can be evaluated in bacteria by using fluorescent probes developed in mammalian cells. Commonly used fluorescent probes include rhodamine 123 (Rh123) and 3,3'–dihexyloxacarbocyanine iodide [$DiOC_6(3)$]. Rh123 is a cationic fluorescent dye that is concentrated in mitochondria by the relatively high negative potential across the energized mitochondrial membrane (Johnson et al., 1981). In bacterial cells Rh123 is accumulated in an uncoupler-sensitive fashion via transmembrane potential (Haugland, 1992). Different studies have shown that Rh123 is a sensitive $\Delta\Psi$ probe for $Gram^+$ bacteria. However, the uptake of this fluorochrome dye by $Gram^-$ bacteria is low because their outer membrane is less permeable to it (Diaper et al., 1992; Kaprelyants, 1992; Matsuyama, 1984). Some recent methods described a pretreatment for staining $Gram^-$ bacteria with Rh123 (Kaprelyants, 1992; Yu and McFeters, 1994; Yu and McFeters, 1994). To eliminate the pretreatment problem, some other dyes have been exploited. For example, $DiOC_6(3)$ is a lipophilic cationic dye that has been shown to be satisfactory to evaluate the $\Delta\Psi$ of *E. coli* cells and to follow $\Delta\Psi$ changes during cells growth and throughout the cell cycle (Monfort and Baleux, 1996).

Acridine orange (AO) has been available for over 100 years and is one of the most commonly used fluorogenic dyes in microbial ecology and environmental microbiology as part of the acridine orange direct count (AODC). Some suggested that the reaction of bacteria with AO will allow discrimination of faster and slower growing cells, as mentioned above. McFeters et al. (1991) confirmed this assumption using purified DNA, ribosomes, bacteriophage-infected cells and *Escherichia coli* under a range of defined physiological circumstances. However, he also suggested that when applying the AO staining reactions as an indicator of physiological activity, the relevant variables including drying, fixation and chlorination should be understood.

Another more direct molecular method for measuring ribosomal RNA (rRNA) is oligonucleotide probes. The use of rRNA sequence divergence to infer phylogenetic relationships and as the basis for developing determative hybridization probes is now well established (Amann et al., 1990a; Amann et al., 1990b; Olsen et al., 1986; Woese, 1987). A popular method is the use of fluorescent-dye-labeled oligonucleotides complementary to rRNAs for the visualization of single cells with fluorescent microscopy (Stahl et al., 1989). This technology has been largely devoted to the detection of microorganisms. Coupled with image analysis, fluorescent-in-situ-hybridization (FISH) has been developed to infer cellular ribosomal (rRNA) content. In some bacteria cellular rRNA content shows good correlation with growth rate (Schaechter et al., 1958). Delong et al. (1989) first demonstrated the application of FISH for the estimation of growth rate of *Escherichia coli* in pure culture. Poulsen et al. (1993) observed good correlation

between growth rate and FISH signal intensity of a sulfate-reducing bacterium isolated from an anaerobic fixed-bed bioreactor. He then used this quantitative FISH method to estimate the growth rate of this specific population of sulfate-reducing bacteria in multispecies biofilms. There was also a study to estimate the growth rate of *Escherichia coli* colonizing the large intestine of streptomycin-treated mice (Poulsen et al., 1995).

Other approaches to study the activity of attached bacteria in situ include microautoradiography (Ellis, 1999; Stewart et al., 1991), microcalorimetry and microelectrodes. Radiolabeling and microautoradiography were applied by Fletcher (1979) and Karel (1989) to investigate the activity of attached bacteria. Microcalorimetry has been used to measure heat output by surface-associated microorganisms and provide an estimate of total metabolic activity. Microelectrodes, which have been developed primarily for determining variations in pH and oxygen concentration in structural microbial mats, are useful tools for dissecting the different physiological activities of surface-associated microbial populations (Revsbech et al. 1983; Revsbech and Ward ,1984).

There is the problem of finding which parameter to measure in order to provide a valid indication of metabolic activity. For example, Lisle et al. (1999) found that using several fluorescent stains and probes could permit a more comprehensive determination of the site and extent of injury in bacterial cells following sublethal disinfection with chlorine.

Starvation, Stringent Response and Antimicrobial susceptibility

Most antibiotics target specific machinery that maintains a viable cell such as cell wall synthesis, protein synthesis, nucleic acid synthesis and cell membrane function. The synthetic functions, which some of these antibiotics target such as cell wall synthesis and protein synthesis are directly related to growth. Bacteria are known for their ability to alter their sensitivity to certain antibiotics and disinfectants with changes in growth rate (Brown et al., 1988; Eng et al., 1991; Gilbert et al., 1990). In some instances the coupling between growth and susceptibility is absolute (Tuomanen et al., 1986); this is the basis for the classical method of counterselection for auxotropic mutants. In studies performed by Harakeh et al. (1985) *Yersinia enterocolitica* and *Klebsiella pneumoniae* were shown to be less susceptible to chlorine dioxide when they were grown at submaximal rates. *Pseudomonas aeruginosa* cells grown to stationary phase were found to be less susceptible to either 0.25% (v/v) acetic acid or 31 mg/L glutaraldehyde treatment than cells growing in the exponential phase (Carson et al.,1972). Matin et al. (1989) also suggested that nutrient-deprived *Escherichia coli* and *Salmonella typhimurium* cells were more resistant to disinfectants' and to osmotic stress. The *E.coli* MAR (Multiple-Antibiotic-Resistance) operon is upregulated in inverse proportion to growth rate (Maira et al., 1998).

The growth of heterotrophic bacteria in natural environments is inhibited by periods of insufficient levels of energy and nutrients (Stenstrom et al., 1989). The

survival strategies of bacteria in their natural environments under starvation conditions have been identified (Roszak & Colwell, 1987a) and suggest that the bacterial cultures undergo a series of physiological changes which enable the survival of some of the cells. Rapid multiple divisions of starved cells, which lead to the formation of ultramicrobacteria (<0.3 μm in diameter) have been observed (Novitsky & Morita, 1976). Roszak and Colwell (1987) suggested that ultrabacteria are exogenously dormant forms, responding to unfavorable environmental conditions, are sporelike bacteria. The similarity in responses to nutrient limitation of both sporeforming and nonsporeforming bacterial species may be due to the possession by both groups of the stringent response (SR) gene, *relA*. The SR is a phenotypic adaptation to conditions of amino acid limitation (Cashel, 1987). The gene product of *relA* is (p)ppGpp synthetase I, which phosphorylates GDP and GTP to ppGpp and pppGpp. It is apparent that *relA*-competent cells are unusual because they appear to have an enhanced resistance to many antibiotics. This resistance may be due solely to the reduced rates of metabolism, which could explain the lack of susceptibility to cell wall- and DNA- active antibiotics observed by Stenstrom et al. (1989). Alternatively, some products of the SR may serve to protect intracellular targets from action of antibiotics. In particular, the known binding affinity of (p)ppGpp for ribosomes may protect the cell against the action of amino-glycoside antibiotics.

Regulation of Starvation Sigma Factor RpoS and Role of RpoS in Stress Response

Bacteria are subject to an array of stresses within their natural environment, and it has been demonstrated previously that stationary-phase and starved cells survive these insults better than their exponential-phase counter parts (Jenkins et al., 1988). In *E.coli*, this is due in part to the alternative sigma factor, RpoS (σ^S), which accumulates in stationary-phase cells (Lange and Hengge-Aronis, 1991). Regulation of RpoS levels in *E. coli* cells was believed to occur at three levels (Takayanagi et al., 1994; Lange and Hengge-Aronis, 1994): transcription, translation, and protein stability. Using *rpoS-lacZ* reporter fusions (Mulvey et al., 1990), *rpoS* transcriptional expression in cells was shown to be low in early exponential phase and to increase gradually two-to threefold during exponential phase. The most substantial increase to 20-fold above basal levels occurred during and after the transition to stationary phase (Mulvey et al., 1990; Lange and Hengge-Aronis, 1991). In minimal medium, unexplained strain-specific differences have arisen. One report indicated that *rpoS* expression did not occur in minimal medium (Lange and Hengge-Aronis, 1994). Starvation also elicits an increase in *rpoS* expression depending on the missing component. Starvation for carbon resulted in limited expression, whereas starvation for nitrogen (Mulvey et al., 1990) or phosphate (Lange and Hengge-Aronis, 1991) resulted in maximal expression of *rpoS*. Anaerobiosis reduced the growth rate and stimulated *rpoS* expression during exponential growth in Luria-Bertani (LB) medium (Mulvey et al., 1990). *rpoS* transcription is inversely

correlated with growth rate and is negatively controlled by cAMP-CRP. *rpoS* expression begins to increase during slow growth and will stop immediately before growth ceases.

Another level of RpoS regulation is posttranscriptional, at the levels of translation and protein stability. The induction of RpoS upon a shift to high osmolarity was shown to result from stimulation of translation and a change in the half-life of RpoS from 3 to 50 minutes (Muffler et al., 1996). RpoS was found to be a highly unstable protein in exponentially growing cells (with a half-life of 1.4 minutes), that was stabilized (with a half-life of 10.5 minutes) in stationary phase (Zgurskaya et al., 1997). By quantifying the relative *rpoS* mRNA levels by RNA_{ase} protection assay, Zgurskaya and Matin (1997) recently found the increase in RpoS level during stationary phase was solely due to a large increase in its stability. In *Pseudomonas aeruginosa*, there is not much known about RpoS regulation. Latifi et al. (1996) reported a hierarchical quorum-sensing cascade in *P. aeruginosa* involved in the activated expression of *rpoS*. They showed that expression of *rpoS* was abolished in a *P. aeruginosa lasR* mutant and in the pleiotropic *N*-(*3-oxododecanoyl*)-L-homoserine lactone (BHL)-negative mutant. In a heterologous (*E. coli*) background, a *rpoS-lacZ* fusion was regulated directly by RhlR/BHL. A density-dependent phenotype in *P. aeruginosa* biofilms was shown recently by Davies et al (1998). In biofilm, due to the likelihood of slow growth and density-dependent signaling, it is hypothesized that there will be RpoS upregulation.

In *E. coli* RpoS is a master regulator responsible for the gene expression in stationary phase and starvation conditions (Loewen and Hengge-Aronis, 1994). It

controls a large group of genes. Analysis of two-dimensional gels has revealed that 18 (Lange and Hengge-Aronis, 1991) to 32 (McCann et al., 1991) proteins are missing or are present in smaller amounts, as well as the presence of some new proteins in an *rpoS* mutant. The identified RpoS-controlled proteins encompass a diverse group of functions, including prevention and repair of DNA damage (*katE*, *katG*, *xthA*, *dps*, *aidB*), cell morphology (*bolA*, *ficA*), modulation of virulence genes in *Salmonella*, *Shigella*, and *E.coli*, osmoprotection and thermotolerance (*otsBA*, *treA*, *csiD*, *htrE*), glycogen synthesis (*glgS*), anaerobically induced genes (*appY*, *appCBA*, *hyaABCDEF*) and membrane and cell envelope functions (*osmB*, *osmY*, *cfa*) (Loewen and Hengge-Aronis, 1994). Several of the genes listed above are involved in stress protection. Protection against H_2O_2 involves *katE* and *katG*, encoding the catalases HPII and HPI, respectively, which destroy H_2O_2 before it can cause damage. Dps forms nuclease-resistant complexes with DNA that also presumably protect the cells from killing by H_2O_2 (Almiron et al., 1992). The RpoS-dependent *otsBA* operon encodes trehalose-6-phosphate synthase (OtsA) and trehalose-6-phosphate phosphatase (OtsB), which together produce large amounts of trehalose in osmotically stressed cells (Giaever et al., 1988). Trehalose acts as an osmoprotectant, and consequently, *otsBA* and *rpoS* mutants exhibit an osmosensitive growth phenotype. Trehalose also acts as a thermoprotectant in a wide variety of species (Van Laere, 1989), presumably through its membrane and protein-protecting properties (Crowe et al., 1984; Crowe et al., 1988). A mutation in the RpoS-dependent *csiD* gene (Weichart et al., 1993) causes a similar

heat-sensitive phenotype in addition to causing pleiotropic changes in protein patterns on 2-D gels. In addition, RpoS was reported to protect *E. coli* cells from the electrophile *N*- ethylmaleimide (Ferguson et al., 1998).

Objectives, Rationales and Experimental Design

The main goal of the study is to achieve a comprehensive understanding of spatial physiological heterogeneity and nutrient limitation in thick biofilms, thereby providing a basis for continued investigation of physiological mechanisms of the biofilm recalcitrance to antimicrobial agents.

The specific objectives are presented below:

Objective 1. To demonstrate spatial physiological heterogeneity in a model biofilm with different fluorescent probes which indicate RNA content, protein synthesis and respiratory activity and determine if this spatial physiological heterogeneity is caused by an oxygen gradient in the biofilm (Chapter 2, 3, 4).

Rationale. There is limited work demonstrating the spatial physiological heterogeneity in thick biofilms. Systematic studies of spatial physiological heterogeneity will provide a comprehensive understanding of biofilm physiological ecology and provide an explanation for recalcitrance of thick biofilms to antimicrobial agents.

Objective 2. To investigate the gene expression and protein levels of the starvation sigma factor RpoS in the biofilms.

Rationale. The speculation of starvation and the evidence of quorum-sensing phenomena in the biofilms lead us to hypothesize that the starvation sigma factor is upregulated in the aging biofilms. This would provide a mechanism of recalcitrance of aging biofilms at a genetic and molecular level.

Experimental Design.

A continuous flow reactor that has been shown to be suitable for growing biofilms and is convenient for physiological analysis was used to generate thick biofilms. To study spatial physiological heterogeneity in the biofilms, biofilms were stained with a fluorogenic alkaline phosphatase substrate, acridine orange, fluorescent-in-situ-hybridization for ribosomal RNA and CTC. These techniques gave an indication of active protein synthesis, RNA/DNA ratio, RNA content and respiratory activity, respectively. The stained biofilm sections were observed microscopically and image analysis was performed to quantify patterns of heterogeneity.

To investigate gene expression of *rpoS*, a plasmid carry *rpoS-lacZ* was transformed into the *P. aeruginosa* ERC strain. Biofilms bearing the plasmid were grown and analyzed for β-galactosidase activity. Western blots were performed to measure RpoS levels.

References Cited

Almiron, M., A. Link, D. Furlong, and R. Kolter. 1992. A novel DNA binding protein with regulatory and protective roles in starved Escherichia coli. *Genes Dev.* **6**: 2646-2654.

Amann, R. I., B. Binder, S. W. Chisholm, R. Olsen, R. Devereux, and D. A. Stahl. 1990a. Combination of 16S rRNA-targeted oligonucleotide probes with flow cytometry for analyzing mixed microbial populations. *Appl. Environ. Microbiol.* **56**: 1919-1925.

Amann, R. I., L. Krumholz, and D. A. Stahl. 1990b. Fluorescent oligonucleotide probing of whole cells for determinative, phylogenetic, and environmental studies in microbiology. *J. Bacteriol.* **172**: 762-770.

Anwar, H., T. Biesen, M. Dasgupta, K. Lam, and J. W. Costerton. 1989. Interaction of biofilm with antibiotics in a novel chemostat system. *Antimicrob. Agent Chemother.* **33**: 1824-1826

Anwar, H., J. L. Strap, and J. W. Costerton. 1992a. Establishment of aging biofilms: possible mechanism of bacterial resistance to antimicrobial therapy. *Antimicrob. Agents Chemother.* **36**: 1347-1351.

Anwar, H., J. L. Strap, and J. W. Costerton. 1992b. Kinetic interactions of biofilm cells of *Staphylococcus aureus* with cephalexin and tobramycin in a chemostat system. *Antimicrob. Agent Chemother.* **36**: 890-893.

Breznak, J. A. 1984. Activity on surfaces: group report, Dahlem Conference, p. 203-221. In K. C. Marshall (ed.), Microbial adhesion and aggregation. Springer – Verlag, Berlin.

Brock, T. D. 1987. The study of microorganisms in situ: progresses and problems. *Symp. Soc. Gen. Microbiol.* **41**: 1-17.

Brown, M. R. W., D. G. Allison, and P. Gilbert. 1988. Resistance of bacterial biofilms to antibiotics: a growth-rate related effect? *J. Antimicrob. Chemother.* **22**: 777-780

Brown, M. R. W., and P. Gilbert. 1993. Sensitivity of biofilms to antimicrobial agents. *J. Appl. Bacteriol. Symp. Suppl.* **74**: 87S-97S.

Carson, L. A., M. S. Favero, W. W. Bond, and N. J. Peterson. 1972. Factors affecting comparative resistance of naturally occuring and subcultured *Pseudomonas aeruginosa* to disinfectants. *Appl. Microbiol.* **23**: 863-869.

Cashel, M., and K. E. Rudd. 1987. The strigent response, p. 1410-1438. In F.C. Neidhardt, J.L. Ingraham, K.B.Low, B.Magasanik, M.Schaechter, and H.E.Umbarger (ed.), *Escherichia coli* and *Salmonella typhimurium*: Cellular and Molecular Biology, Vol. 2, ASM, Washington, D.C.

Characklis, W. G., M. H. Turakhia, and N. Zelver. 1990. Transport and interfacial transfer phenomena. p. 265-340. In W. G. Charackis and K. C. Marshall. (ed.), Biofilms, John Wiley and Sons Inc, New York

Costerton, J. W., G. G. Geesey, and K.-J. Cheng. 1978. How bacteria stick. *Sci. Am.* **238**: 86-95.

Costerton, J. W. 1984. The formation of biocide-resistant biofilms in industrial, natural and medical systems. *Dev. Ind. Microbiol.* **25**: 363-372.

Costerton, J. W., K.-J. Cheng, G. G. Geesey, T. I. Ladd, Nickel, J. C. Dasgupta, and M. Marrie. 1987. Bacterial biofilms in nature and disease. Ann. Rev. Microbiol. 41: 435-64.

Costerton, J. W., Z. Lewandowski, D. E. Caldwell, D. R. Korber, and H. M. Lappin-Scott. 1995. Microbial Biofilms. *Annu. Rev. Microbiol.* **49**: 711-45.

Crowe, J. H., L. M. Crowe, and D. Chapman. 1984. Preservation of membranes in anhydrobiotic organisms: the role of trehalose. *Science* **223**: 701-3.

Crowe, J. H., L. M. Crowe, J. F. Carpenter, A. S. Rudolph, and C. Aurell-Wistrom. 1988. Interactions of sugars with membranes. *Biochim. Biophys. Acta Biomembr. Rev.* **947**: 367-84

Dagostino, L., A. E. Goodman, and K. C. Marshall. 1991. Physiological responses induced in bacteria adhering to surfaces. *Biofouling* **4** : 113-119

Darzynkiewicz, Z., L. Staiano-Coicoand, and M. R. Melamed. 1981. Increased mitochondrial uptake of rhodamine 123 during lymphocyte stimulation. *Proc. Natl. Acad. Sci.* USA **78**: 2383-2387

Davies, D. G., A. M. Chakrabarty, and G. G. Geesey.1993. Exopolysaccharide production in biofilms: substratum activation of alginate gene expression by *Pseudomonas aeruginosa. Appl. Environ. Microbiol.* **59**: 1181-86.

Davies, D. G., M. R. Parsek, J. Pearson, B. H. Iglewski, J. W. Costerton, and E. P. Greenberg.1998. The involvement of cell-to-cell signals in the development of a bacterial biofilm. *Science.* **280**: 295-298

de Beer, D., R. Srinivasan, and P. S. Stewart. 1994. Direct measurement of chlorine penetration into biofilm during disinfection. *Appl. Env. Microbiol.* **60**: 4339-4344.

Delong, E. F., G. S. Wickham, and N. R. Pace. 1989. Phylogenetic stains: ribosomal RNA-based probes for identification of single cells. *Science.* **243**: 1360-1363.

Diaper, J. P., K. Tither, and C. Edwards.1992. Rapid assessment of bacterial viability by flow cytometry. *Appl. Microbiol. Biotechnol.* **38**: 268-272.

Eng, R. H. K., F. T. Padberg, S. M. Smith, E. N. Tan, and C. E. Cherabin. 1991. Bactericidal effects of antibiotics on slowly growing and nongrowing bacteria. *Antimicrob. Agents. Chemother.* **35**: 1824-1828

Evans, R.C., and C. J. Holmes. 1987. Effect of vancomycin hydrochloride on *Staphylococcus epidermidis* biofilm associated with silicone elastomer. *Antimicrob. Agents. Chemother.* **31**: 889-894

Ferguson, G. P., R. I. Creighton, Y. Nikolaev and I. R. Booth. 1998. Importance of RpoS and Dps in survival of exposure of both exponential- and stationary-phase *Escherichia coli* cells to the electrophile *N*-ethylmaleimide
J. Bacteriol. **180**: 1030-1036

Fletcher, M. 1979. A microautoradiographic study of the activity of attached and free-living bacteria. *Arch. Microbiol.* **122**: 271-274.

Fowler, H. W. 1988. Microbial adhesion to surfaces. In Wimpenny, J. W. T. (ed.) *Handbook of Laboratory Model Systems for Microbial Ecosystems*, Vol. 2, pp. 139-153. CRC Press, Boca Raton.

Giaever, H. M., O. B. Styrvold, I. Kaasen, and A. R. Storm. 1988. Biochemical and genetic characterization of osmoregulatory trehalose synthesis in *Escherichia coli. J. Bacteriol.* **170**: 2841-2849

Gilbert, P., P. J. Collier, and M. R. W. Brown. 1990. Influence of growth rate on susceptibility to antimicrobial agents: biofilms, cell cycle, dormancy and stringent response. *Antimicrob. Agents Chemother.* **34**: 1865-1868.

Griffith, P. C. and M. Fletcher. 1991. Hydrolysis of protein and model dipeptide substrates by attached and nonattached marine *Pseudomonas* sp. Strain NCIMB 2021. *Appl. Environ. Microbiol.* **57**: 2186-2191.

Harakeh, M. S., J. D. Berg, J. C. Hoff, and A. Matin. 1985. Susceptibility of chemostat grown *Yersinia enterocolitica* and *Klebsiella pneumoniae* to chlorine dioxide. *Appl. Environ. Microbiol.* **49**: 69-72.

Haugland, R. P. 1992. Handbook of fluorescent probes and research chemicals.

Haugland, R. P. 1992. Molecular probes, Molecular Probes, Eugene, Oregon.

Hodgson, A. E., S. M. Nelson, M. R. W. Brown, and P. Gilbert. 1995. A simple in vitro model for growth control of bacterial biofilms. *J. Appl. Bacteriol.* **79**: 87-93.

Hoyle, B. D., J. Alcantara, and J. W. Costerton. 1992. *Pseudomonas aeruginosa* biofilm as a diffusion barrier to piperacillin. *Antimicrob. Agent Chemother.* **36**: 2054-2056.

Hoyle, B. D., L. J. Williams, and J.W. Costerton. 1993. Production of mucoid exopolysaccharide during development of *Pseudomonas aerugionsa* biofilms. *Infect. Immun.* **61**: 777-80.

Jeffrey, W. H., and J. H. Paul. 1986. Activity of an attached and free-living *Vibrio* sp. As measured by thymidine incorporation, *p*-iodonitrotetrazolium reduction and ATP/DNA ratio. *App. Environ. Microbiol.* **51**: 150-156.

Jenkins, D. E., J. E. Schultz, and A. Matin. 1988. Starvation induced cross-protection against heat or H_2O_2 challenge in *Escherichia coli. J. Bacteriol.* **170**: 3910-3914

Johnson, L. V., M. L. Walsh, B. J. Bockus, and L. B. Chen. 1981. Monitoring of relative mitochondrial membrane potential in living cells by fluorescence microscopy. *J. Cell. Biol.* **88**: 526-535.

Kaprelyants, A. S. and D. B. Kell. 1992. Rapid assessment of bacterial viability and vitality by rhodamine 123 and flow cytometry. *J. Appl. Bacteriol.* **72**: 410-422.

Kaprelyant, A. S. and D. B. Kell. 1993. The use of 5-cyano-2,3-ditolyl tetrazolium chloride and flow cytometry for the visualization of repiratory activity in individual cells of *Micrococcus luteus. J. Microbiol. Methods* **17**: 115-122.

Karel, S. F. and C. R. Robertson. 1989. Autoradiographic determination of mass-transfer limitations in immobilized cell reactors. *Biotechnol. Bioeng.* **34**: 320-336

Kinniment, S. L., and J. W. T. Wimpenny. 1992. Measurements of the distribution of adenylate concentrations and adenylate energy charge across *Pseudomonas aeruginosa* biofilms. *Appl. Environ. Microbiol.* **58**: 1629-1635.

Lange, R., and R. Henge-Aronis. 1994. The cellular concentration of the σ^S subunit of RNA polymerase in *Escherichia coli* is controlled at the levels of transcription, translation, and protein stability. *Genes Dev.* **8**: 1600-1612

Latifi, A., M. Foglino, K. Tanaka, P. Williams, and A. Lazdunski. 1996. A hierarchical quorum-sensing cascade in *Pseudomonas aeruginosa* links the transcriptional activators LasR and RhlR (VsmR) to expression of the stationary-phase sigma factor RpoS. *Mol. Microbiol.* **21**: 1137-1146.

LeChevallier, M. W., C. D. Cawthon, and R.G. Lee. 1988. Inactivation of biofilm bacteria. *Appl. Env. Microbiol.* **54**: 2492-2499.

Lewandowski, Z. 1994. Dissolved oxygen gradients near microbially colonized surfaces. In Biofouling and Biocorrosion in Industrial Water Systems. Ed. G. Geesey, Z. Lewandowski and H-C. Flemming. p 175-188. CRC Press, Inc., Florida.

Lisle, J. T., B. H. Pyle, and G. A. McFeters. 1999. The use of multiple indices of physiological activity to access viability in chlorine disinfected *Escherichia coli* O157: H7. *Lett. Appl. Microbiol.*: In Press

Lock, M. A., R. R. Wallace, J. W. Costerton, R. M. Ventullo, and S. E. Charlton. 1984. River epilithon: towards a structural-functional model. *Oikos* **44**: 10-22.

Loew, L. M. 1993. Potentiometric membrane dyes. pp. 150-160. In Mason, W. T., Ed., Fluorescent and Luminescent Probes for Biological Activity. Academic Press, London.

Loewen, P. C., and R. Hengge-Aronis. 1994. The role of the sigma factor σ^S (KatF) in bacterial global regulation. *Annu. Rev. Microbiol.* **48**: 53-80.

Maira, T., S. B. Levy, D. G. Allison and P. Gilbert. 1998. 98th General Meeting of American Society for Microbiology Abstract, p. 528, V-89.

Malone, J. S., and D. E. Caldwell. 1983. Evaluation of surface colonization kinetics in continuous culture. *Microb. Ecol.* **9**: 299-306

Marrie, T. J., and J. W. Costerton. 1982. A scanning and transmission electron microscopic study of an infected endocardial pacemaker lead. *Circulation* **66**: 1339-43

Marshall, K. C. and A. E. Goodman. 1994. Effects of adhesion on microbial cell physiology. *Colloids and Surfaces B: Biointerfaces*, **2**: 1-7.

Mason, W. T. 1993. Fluorescent and luminescent probes for biological activity. Academic Press, London

Matin, A., E. A. Anger, P. H. Blum, and J. E. Schultz. 1989. Genetic basis of starvation survival in non-differentiating bacteria. *Annu. Rev. Microbiol.* **43**: 293-316

Matsuyama, T. 1984. Staining of living bacteria with rhodamine 123. *FEMS Microbiol. Lett.* **21**: 153-157

McCann, M. P., J. P. Kidwell, and A. Matin. 1991. The putative σ factor *katF* has a central role in development of starvation-mediated general resistance in *Escherichia coli. J. Bacteriol.* **173**: 4188-94

McFeters, G. A., T. Egli, E. Willberg, A. Alder, M. Suozzi, and M. Giger. 1990. Activity and adsorption of nitrilotriacetate (NTA)-degrading bacteria: fields and laboratory studies. *Wat. Res.* **24**: 875-881.

McFeters, G. A., A. Singh, S. Byun, P. R. Callis, and S. Williams.1991. Acridine orange staining reaction as an index of physiological activity in *Escherichia coli. J. Microbiol. Meth.* **13**: 87-97

Monfort, P. and B. Baleux. 1996. Cell cycle characteristics and changes in membrane potential during growth of *Escherichia coli* as determined by a cyanine fluorescent dye and flow cytometry. *J. Microbiol. Meth.* **25**: 79-86.

Morita, R. Y. 1985. Starvation and miniaturization of heterotrophs, with special emphasis on maintenance of starved viable state. pp. 113-130. In Fletcher, M. and Floodgate, G. D., eds, Bacteria in their natural environments, Academic Press, Inc., London

Muffler, A., D. D. Traulsen, R. Lange, and R. Hengge-Aronis. 1996. Posttranscriptional osmotic regulation of the σ^S subunit of RNA polymerase in *Escherichia coli. J. Bacteriol.* **178**: 1607-1613.

Mulvey, M. R., J. Switala, A. Borys, and P. C. Loewen.1990. Regulation of transcription of *katE* and *katF* in *Escherichia coli. J. Bacteriol.* **172**: 6713-20.

Nichols, W. W., S. M. Dorrington, M. P. E. Slack, and H. L. Walmsley. 1988. Inhibition of tobramycin diffusion by binding to alginate. *Antimicrob. Agents Chemother.* **32**: 518-523.

Nichols, W. W. 1989. Susceptibility of biofilms to toxic compounds. In Structure and Function of Biofilms. Eds. W. G. Characklis and P. A. Wilderer. pp. 321-331. John Wiley & Sons, Inc., publication.

Nickel, J. C., S. K. Grant, and J. W. Costerton.1985a. Electron microscopic study of an infected Foley catheter. *Can. J. Surg.* **28**: 50-54

Nickel, J. C., I. Ruseska, and J. W. Costerton. 1985b. Tobramycin resistance of cells of *Pseudomonas aeruginosa* growing as a biofilm on urinary catheter material. *Antimicrob. Agents Chemother.* **27**: 619-24.

Novitsky, J. A., and R. Y. Morita. 1976. Morpholoigical characterization of small cells resulting from nutrient starvation of a psychrophilic marine vibrio. *Appl. Environ. Microbiol.* **32**: 617-622.

Olsen, G. J., D. J. Lane, S. J. Giovannoni, N. R. Pace, and D. A. Stahl. 1986. Microbial ecology and evolution: a ribosomal RNA approach. *Annu. Rev. Microbiol.* **40**: 337-365.

Östling, J., A. E. Goodman, and S. Kjelleberg. 1991. Behavior of IncP-1 plasmids and a mini*Mu* transposon in a marine Vibrio sp.: isolation of starvation inducible lac operon fusions. *FEMS Microbiol. Ecol.* **86**: 83

Peters, G., R. Locci, and G. Pulverer. 1981. Microbial colonization of prosthetic devices. II. Scanning electron microscopy of naturally infected intravenous catheters. *Zentralbl. Bakteriol. Mikrobiol. Hyg. I Abt. Orig. B* **173**: 293-99

Porter, K. G. and Y. S. Feig. 1980. The use of DAPI for identifying and counting aquatic microflora. *Limnol. Oceanogr.* **25**: 943-948.

Poulsen, L. K., T. R. Licht, C. Rang, K. A. Krogfelt, and S. Molin. 1995. Physiological state of *Escherichia coli* BJ4 growing in the large intestines of streptomycin-treated mice. *J. Bacteriol.* **177**: 5840-5845.

Pyle, B. H., S. C. Broadway, and G. A. McFeters. 1999. Sensitive detection of *Escherichia coli* O157: H7 in food and water by immunomagnetic separation and solid-phase laser cytometry. *Appl. Environ. Microbiol.* **65**: 1966-1972.

Revsbech, N. P., B. B. Jorgensen, and T. H. Blackburn. 1983. Microelectrode studies of the photosynthesis and O_2, H_2S, and pH profiles of a microbial mat. *Limnol. Oceanogr.* **28**: 1062-1074.

Revsbech, N. P., and D. M. Ward. 1984. Microelectrode studies of interstitial water chemistry and photosynthetic activity in a hot spring microbial mat. *Appl. Environ. Microbiol.* **48**: 270-75.

Revsbech, N. P. 1989. Microsensors: spatial gradients in biofilms. In Characklis, W. G. & Wilderer, P. A. (eds.) Structure and Function of biofilms, pp. 129-144, Wiley, New York

Ritz, H. L. 1969. Fluorescent antibody staining of *Neisseria*, *Streptococcu*, and *Veillonella* in frozen sections of human dental plaque. *Arch. Oral Biol.***14**: 1073-1083.

Rodriguez, G. G., D. Philips, K. Ishiguro, and H. F. Ridgway. 1992. Use of a fluorescent redox probe for direct visualization of actively respiring bacteria. *Appl. Environ. Microbiol.* **58**: 1801-1808.

Roszak, D. B., and R. R. Colwell. 1987a. Survival strategies of bacteria in the natural environment. *Microbial Rev.* **51**: 365-379.

Ruseska, I., J. Robbins, E. S. Lashen, J. W. Costerton. 1982. Biocide testing against corrosion-causing oilfield bacteria helps control plugging. *Oil Gas J.*

Schaechter, M., O. Maaloe, and N. O. Kjeldgaard. 1958. Dependency on medium and temperature of cell size and chemical composition during balanced growth of Salmonella typhimurium. *J. Gen. Microbiol.* **19**: 592-606.

Schaule, G., H.-C. Fleming, and H. F. Ridway. 1993. Use of 5-cyano-2,3-ditolyl-tetrazolium chloride for quantifying planktonic and sessile respiring bacteria in drinking water. *Appl. Environ. Microbiol.* **59**: 3850-3857.

Scourfield, M. A. 1990. An investigation into the structure and function of model dental plaque communities using a laboratory film fermenter. PhD thesis, University College Cardiff, Wales.

Smith, J. J. and G. A. McFeters.1996. Effects of substrates and phosphate on INT (2-(4-iodophenyl)-3-(4-nitrophenyl)-5-phenyl tetrazolium chloride) and CTC (5-cyano-2,3-ditolyl tetrazolium chloride) reduction in *Escherichia coli. J. Appl. Bacteriol.* **80**: 209-215.

Stahl, D. A., R. Devereux, R. I. Amann, B. Flesher, C. Lin, and J. Stromley. 1989. Ribosomal RNA based studies of natural microbial diversity and ecology, p. 669-673. *In* Y. Hattoir, Y. Ishida, Y. Maruyama, R. Y. Morita, and A. Uchida (ed.), Recent advances in microbial ecology. Proceedings of the 5th International Symposium on Microbial Ecology. Japan Scientific Societies Press, Tokyo.

Stenstrom, T.-A., P. Conway, and S. kjelleberg. 1989. Inhibition by antibiotics of the bacterial response to long-term starvation of Salmonella typhimurium and the colon microbiota of mice. *J. Appl. Bacteriol.* **67**: 53-59.

Stewart, P. S., S. F. Karel, and C. R. Robertson. 1991.Characterization of immobilized cell growth rates using autoradiography. *Biotechnol. Bioeng.* **37**: 824-833.

Stewart, P. S. 1996. Theoretical aspects of antibiotic diffusion into microbial biofilms. *Antimicrob. Agent. Chemother.* **40**: 2517-2522.

Stubberfield, L. C. F. and P. J. A. Shaw. 1990. A comparison of tetrazolium reduction and FDA hydrolysis with other measures of microbial activity. *J. Microbiol. Meth.* **12**: 151-162.

Sutherland, I. W. 1977. Bacterial exopolysaccharide – their nature and production. In Surface carbohydrates of the prokaryotic Cell, ed. I. W. Sutherland, pp. 27-96. London: Academic.

Swannell, R. P. J. and F. A. Williamson. 1988. An investigation of staining methods to determine total cell numbers and the number of respiring microorganisms in samples from the field and laboratory. *FEMS Microbiol. Ecol.* **53**: 315-324.

Takayanagi, Y., K. Tanaka, and H. Takahashi. 1994. Structure of the 5' upstream region and the regulation of the *rpoS* gene of *Escherichia coli. Mol. Gen. Genet.* **243**: 525-531

Tresse, O., T. Jouenne, and G.-A. Junter. 1995. The role of oxygen limitation in the resistance of agar-entrapped, sessile-like *Escherichia coli* to aminoglycoside and β-lactam antibiotics. *J. Antimicrob. Chemother.* **35**: 521-526.

Tuomanen, E., R. Cozns, W. Tosch, O. Zak, and A. Tomasz. 1986. The rate of killing of Escherichia coli by β-lactam antibiotics is strictly proportional to the rate of bacterial growth. *J. Gen. Microbiol.* **132**: 1297-1304

Van Laere, A. 1989. Trehalose reserve and/or stress metabolite? *FEMS Microbiol. Rev.* **63**: 201-10

Van Loosdrecht, M. C. M., J. Lyklema, W. Norde, and A. J. B. Zehnder. 1990. Influence of interfaces on microbial activity. *Microbiol. Rev.* **54**: 75-87

Vrany, J. D., P. S. Stewart and P. A. Suci. 1997. Comparison of recalcitrance to ciprofloxacin and levofloxacin exhibited by Pseudomonas biofilms displaying rapid-transport characteristics. *Antimicrob. Agents. Chemother.* **41**: 1352-1358

Weichart, D., R. Lange, N. Henneberg, R. Hengge-Aronis. 1993. Identification and characterization of stationary phase-inducible genes in *Escherichia coli. Mol. Microbiol.* **10**: 407-20

Wentland, E. J. 1995. Visualization and quantification of spatial variations in growth rate within *Klebsiella pneumoniae.* Master thesis, Montana State University-Bozeman, MT

Wentland, E. J., P. S. Stewart, C. T. Huang, and G. A. McFeters. 1996. Spatial variations in growth rate within *Klebsiella pneumoniae* colonies and biofilm. *Biotechnol. Prog.* **12**: 316 –321

Wimpenny, J. W. T., S. L. Kinniment, and M. A. Scourfield. 1993. The physiology and Biochemistry of biofilm. *Society for Applied Bacteriology Technical Series,* **30**, pp. 51-94.

Woese, C. R. 1987. Bacterial evolution. *Microbiol. Rev.* **51**: 221-271.

Wu, J.-Y. and L. B. Cohen.1993. Fast multisite optical measurement of membrane potential, pp. 405-419. In Mason, W. T., Ed., Fluorescent and Luminescent Probes for Biological Activity. Academic Press, London.

Yu, F. P. and G. A. McFeters. 1994a. Physiological responses of bacteria in biofilms to disinfection. *Appl. Environ. Microbiol.* **60**: 2462-2466

Yu, F. P. and G. A. McFeters. 1994b. Rapid in situ assessment of physiological activities in bacterial biofilms using fluorescent probes. *J. Microbiol. Meth.* **20**: 1-10.

Yu, F. P., G. M. Callis, P. S. Stewart, T. Griebe and G. A. McFeters. 1994c. Cryosectioning of biofilm for microscopic examination. *Biofouling* **8**: 85-91.

Zgurskaya, H. I., M. Keyhan, and A. Matin. 1997. The σ^S level in starving *Escherichia coli* cells increased solely as a result of its increased stability, despite decreased synthesis. *Mol. Microbiol.* **24**: 643-651.

Zimmermann, R., R. Iturriaga, and J. Becker-Birck.1978. Simultaneous determination of the total number of aquatic bacteria and the number thereof involved in respiration. *Appl. Environ. Microbiol.* **36**: 926-935.

Zobell, C. E., and D. Q. Anderson.1936. Observations on the multiplication of bacteria in different volumes of stored seawater and the influence of oxygen tension and solid surfaces. *Bio. Bull. Woods Hole* **71**: 324-42.

CHAPTER 2

SPATIAL PHYSIOLOGICAL HETEROGENEITY OF ALKALINE PHOSPHATASE IN *PSEUDOMONAS AERUGINOSA* BIOFILM IS DETERMINED BY OXYGEN AVAILABILITY

Introduction

It has long been observed that biofilms are much less susceptible to antimicrobial agents than are their planktonic counterparts (Brown and Gilbert 1993; Costerton 1984; LeChevallier et al. 1988; Nickel et al. 1985), but the underlying basis for this recalcitrance is not well established. As introduced in Chapter 1, physiological and genetic modification of biofilms are hypothesized to be a mechanism of biofilm resistance. In a thick aging biofilm, the deep-internal portions of biofilms are hypothesized to experience starvation and slow growth due to nutrient limitation. The biofilm cell growth is hypothesized to be spatially heterogeneous. The purpose of the work in this chapter was to test the dual hypotheses that physiological status varies spatially within the biofilm and that, in the case of a *P. aeruginosa* model biofilm, physiological activity is controlled by oxygen availability. As a physiological indicator, we have used the expression of alkaline phosphatase upon exposure to phosphate starvation, which reflects the capacity for de-novo protein synthesis. Oxygen delivery was controlled by varying the composition of the gaseous environment and measured directly using an oxygen microelectrode.

Materials and Methods

Bacterial Strains, Media, and Growth Conditions.

A pure culture of *Pseudomonas aeruginosa* ERC1 was used thoroughout. It was isolated from an industrial water system, identified with API NFT (bioMérieux Vitek, Inc., MO, USA) and retained in the culture collection of the Center for Biofilm Engineering. The 16S rDNA of the isolate was PCR amplified with 27F (sequence: 5' – AGA GTT TGA TCC TGG CTC AG – 3', corresponds to the *Escherichia coli* 16S rRNA position 8 to 27) as a forward primer and 1392R (sequence: 5' – ACG GGC GGT GTG TAC – 3', corresponds to the *Escherichia coli* 16S rRNA position 1392 to1406) as a reverse primer and commercially sequenced at University of Montana (Missoula, MT). When the sequence was aligned with the most similar Ribosomal Database Project (Maidak et al. 1994) sequence using Genetic Data Environment 2.3 Software, the percent similarity between *P.aeruginosa* strain NIH18 and ERC1 was 99.0%. MOPS (morpholinopropanesulfonic acid) minimal medium prepared as described by Neidhardt et al. (1974) was used in both planktonic and biofilm experiments. High phosphate medium contained 1g/L Na_2HPO_4 while low phosphate medium contained 0.01g/L Na_2HPO_4. Glucose (1.0 and 0.1g/L) was used as sole carbon source in the planktonic and biofilm culture medium, respectively. All the experiments were carried out at room temperature, 22.2 ± 3.0°C.

Planktonic Culture Procedure.

P.aeruginosa overnight cultures were harvested by centrifugation at 7,500 rpm for 10 minutes, washed twice with low phosphate medium, and resuspended in 100ml low phosphate medium to induce phosphate starvation. The low phosphate culture was stirred for 24 hours. Two-milliliter aliquots were withdrawn every hour for alkaline phosphatase and total protein assays. To test the effect of anoxic conditions on alkaline phosphatase production, a low phosphate culture was left in ambient air for 2.5 hours, then connected to pure nitrogen through a bacterial air vent for 3 hours, then changed back to ambient air for another 2.5 hours. Two-milliliter aliquots were withdrawn every 30 minutes.

Biofilm Culture Procedure.

A drip-flow plate reactor was designed to cultivate biofilms (Figure 2.1). It was then modified to a chamber reactor (Figure 2.2). Stainless steel slides in petri dishes were continuously bathed with medium dripping onto the biofilm at a constant flow rate of 50ml/hour. After inoculation with an overnight culture ($3x10^8$ cells/ml in 0.1g/L glucose MOPS medium) and incubation for 24 hours, the reactor was fed with high phosphate medium for another 72 hour, then replaced with low phosphate medium. The bacterial air vent of the reactor was either connected to pure nitrogen (120~130 ml/min), pure oxygen (120~130 ml/min), or exposed to ambient air to create different gaseous environments. All the biofilm experiments were duplicated.

Alkaline Phosphatase (APase) Activity and Total Protein Assay.

In planktonic experiments, 2 ml aliquots were sampled and centrifuged, then resuspended in 1ml TEP solution (10mM Tris-Cl, pH 8.0; 1mM EDTA, pH 8.0; 1mM PMSF, phenylmethylsulfonyl fluoride). In biofilm experiments, attached cells were scraped into 20ml PBS buffer using a rubber policeman. After being treated with a homogenizer (Tissuemizer, Type SDT 1810, Tekmar Co., Cincinnati, OH) with 13,500 r.p.m speed output in an ice bath for 3 minutes, 2 ml aliquots were suspended in 1 ml TEP solution. Bacterial suspensions in TEP solution were disrupted by ultrasonic treatment using an ultrasonic cell disrupter (TORBEO, 36810 series, Cole-Parmer, IL) and then centrifuged. The supernatant was used for enzyme and total protein assays. APase activity was determined by the rate of hydrolysis of *p*-NPP (*p*-nitrophenyl phosphate) to *p*-nitrophenol, measured by absorbance at 410nm. The change of colorimetric intensity was monitored over a 4-minute interval. Total protein was determined with Sigma (Sigma Inc., St.Louis, MO) Diagnostic kit No. 690, which is a modified micro-Lowry method.

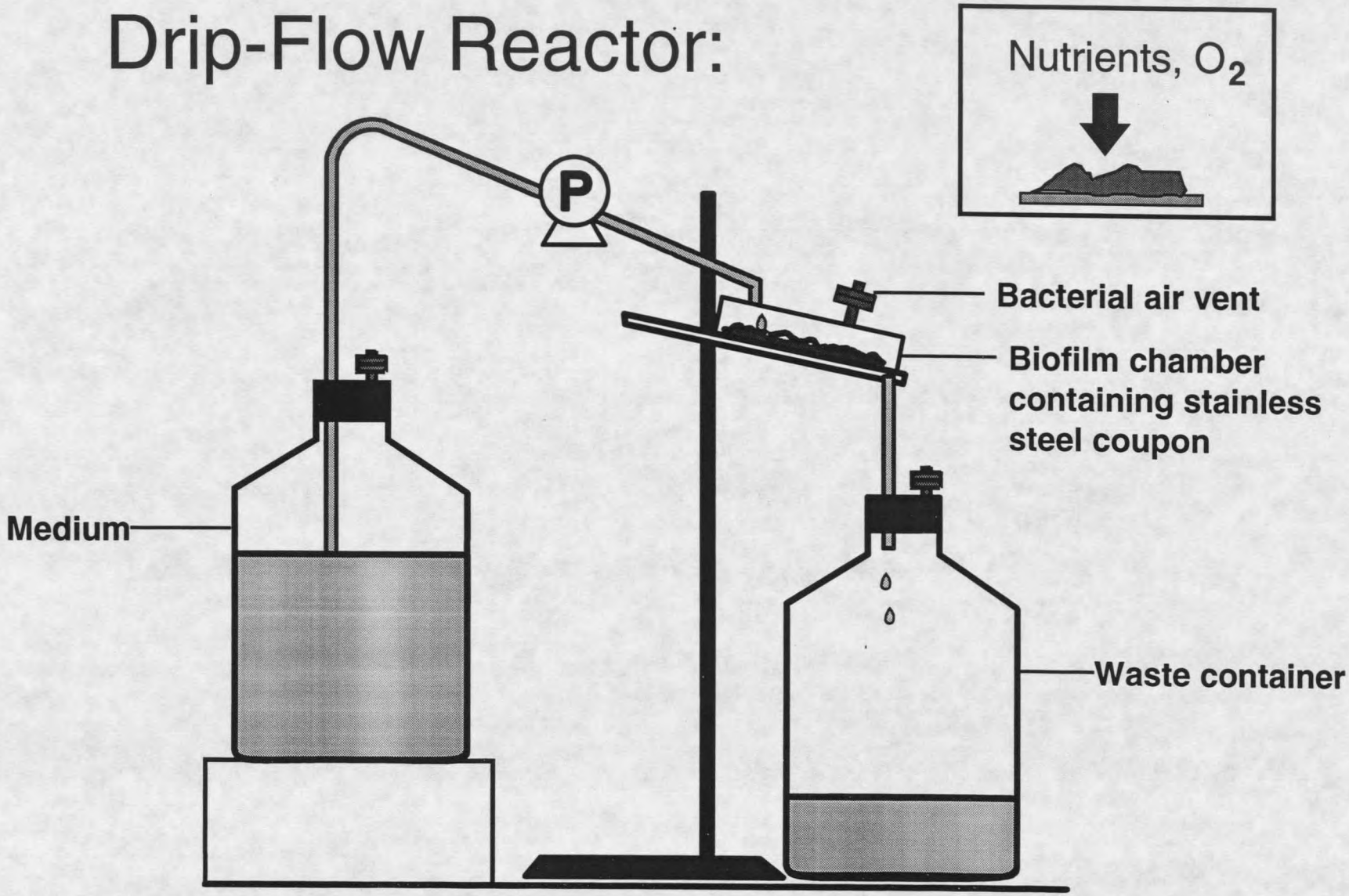


Figure 2.1. Schematic diagram of drip-flow biofilm reactor

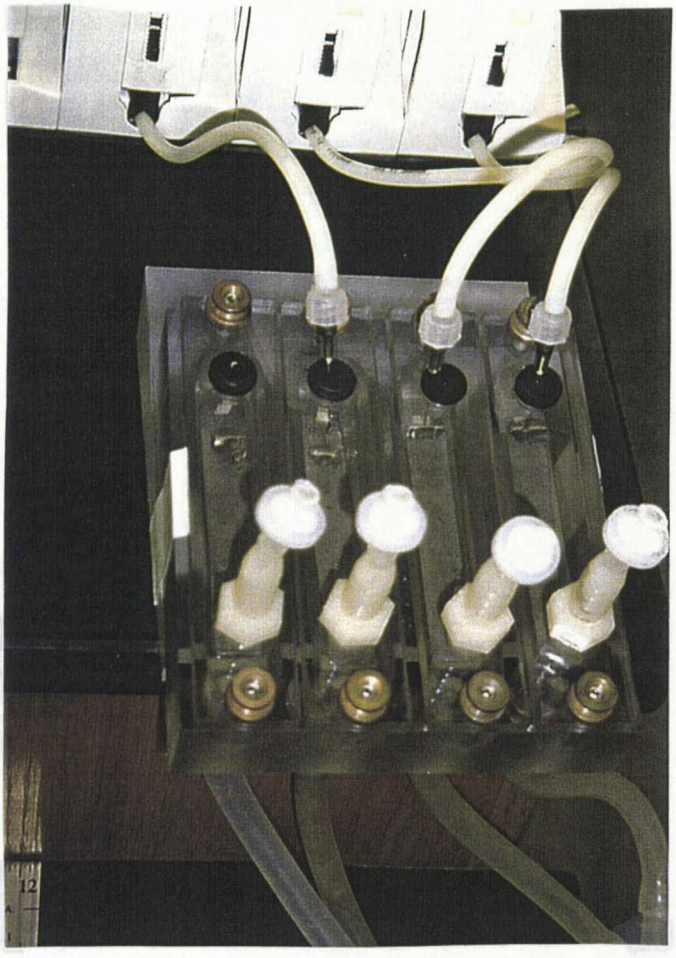


Figure 2.2. Photograph of the drip-flow chamber reactor

Staining Procedures.

ELF-97 phosphatase substrate (Molecular Probes, Eugene, OR) is a water-soluble weakly blue fluorescent stain. Upon cleavage by APase, the substrate yields a bright yellow-green fluorescent precipitate that exhibits excellent photostability since photobleaching is insignificant. Therefore bacterial cells with or without APase can be simultaneously visualized as yellow-green and blue fluorescence, respectively, using epifluorescence microscopy. The biofilms were stained ex-situ in a homemade staining box with 5 ml staining solution at 35°C for 45 minutes. For microscopic examination and photography, biofilm frozen sections were counterstained with 5 μL of 10 μg/ml propidium iodide (PI) to improve the contrast of APase positive and negative cells. After PI counterstaining, cells with APase activity exhibited yellow-green fluorescence while the cells without APase activity were red using the U filter. For image analysis, biofilm sections were counterstained with 5 μL of 1 μg/L of tetramethylrhodamine.

Cryoembedding and Cryosectioning.

Biofilm samples were cryoembedded with Tissue-Tek OCT compound (Miles Inc., Elkhart, IN) as described previously (Yu et al. 1994). Embedded samples were sectioned using a Leica CM 1800 cryostat (Leica Inc., Deerfield, IL). The 5μm-thick sections were mounted on Superfrost Plus microscopic slides (Fisher Scientific, Pittsburgh, PA).

Microscopy.

An Olympus BH-2 microscope (Lake Success, NY) with epifluorescence illumination was used for the examination of the biofilm sections. After ELF staining, weakly blue and intense yellow-green fluorescence was visualized using an Olympus U filter cubic unit containing an excitation filter (334-365nm), a dichroic mirror (DM-400), and a barrier filter (L-420).

Image Analysis.

After counterstaining with tetramethylrhodamine, cells containing APase activity (green) and all cells (red) were selectively captured with an Olympus U and G filter cubic unit, respectively. The G filter cubic unit contained an excitation filter (BP-545), a diachronic mirror (DM-570), and a barrier filter (O-590). The images captured at the same spot by different filters were digitalized by a cooled color CCD camera (Optronics, Goleta, CA) and saved as 8-bit gray scale TIFF files. The fluorescence intensity was determined by MARK image analysis software. The "MARK" program (Murga et al., 1995) was developed by Dr. Gary Harkin of the Center for Biofilm Engineering at Montana State University and it was used on a UNIX operating system. Selected areas of the APase and tetramethyl-rhodamine images were bracketed and superimposed to compare each pixel and determine the intensities across the biofilm cross-section using the built-in "cross-section" function of the program. The data processed by the UNIX

system was stored as ASCII files and was FTPed to a PC-based system. The ASCII files were opened in Microsoft Excel and graphs were generated.

Dissolved Oxygen Profile Measurement.

Oxygen profiles were measured using a combined Clark type dissolved oxygen microelectrode. The electrode was constructed as described by Revsbech (1989). Microelectrode measurements were conducted using a micromanipulator (Model M3301L, World Precision Instruments, New Haven, CT) equipped with a stepper motor (Model 18503, Oriel, Stratford, CT). Custom data acquisition software was used to control the microelectrode movement. The microelectrode was introduced into biofilm from the top perpendicular to the substratum of stainless steel slides. Data was collected at 10 μm increments and 2 seconds intervals. Current produced by the electrode was collected and converted to oxygen concentration by the software.

Results

Planktonic and Biofilm APase Specific Activity.

APase activity was below detectable levels in bacteria grown planktonically in high phosphate medium. After inducing phosphate starvation by transfer to low phosphate medium, APase was readily measured in planktonic bacteria. APase specific activity kept increasing during the first 8 hours of phosphate starvation (Figure 2.3).

When pure nitrogen was introduced after 2.5 hour-induction in air, alkaline phosphatase production was immediately arrested. Accumulation of enzyme activity resumed immediately after switching back to air (Figure 2.3). When bacterial biofilm was subjected to the same duration of low phosphate medium under ambient aerobic conditions, the level of APase specific activity was approximately one fifteenth that of planktonic bacteria (Table 2.1). Biofilm induction of APase was totally blocked when pure nitrogen was administered during the induction period whereas pure oxygen increased APase activity specific activity approximately 2-fold (Table 2.1).

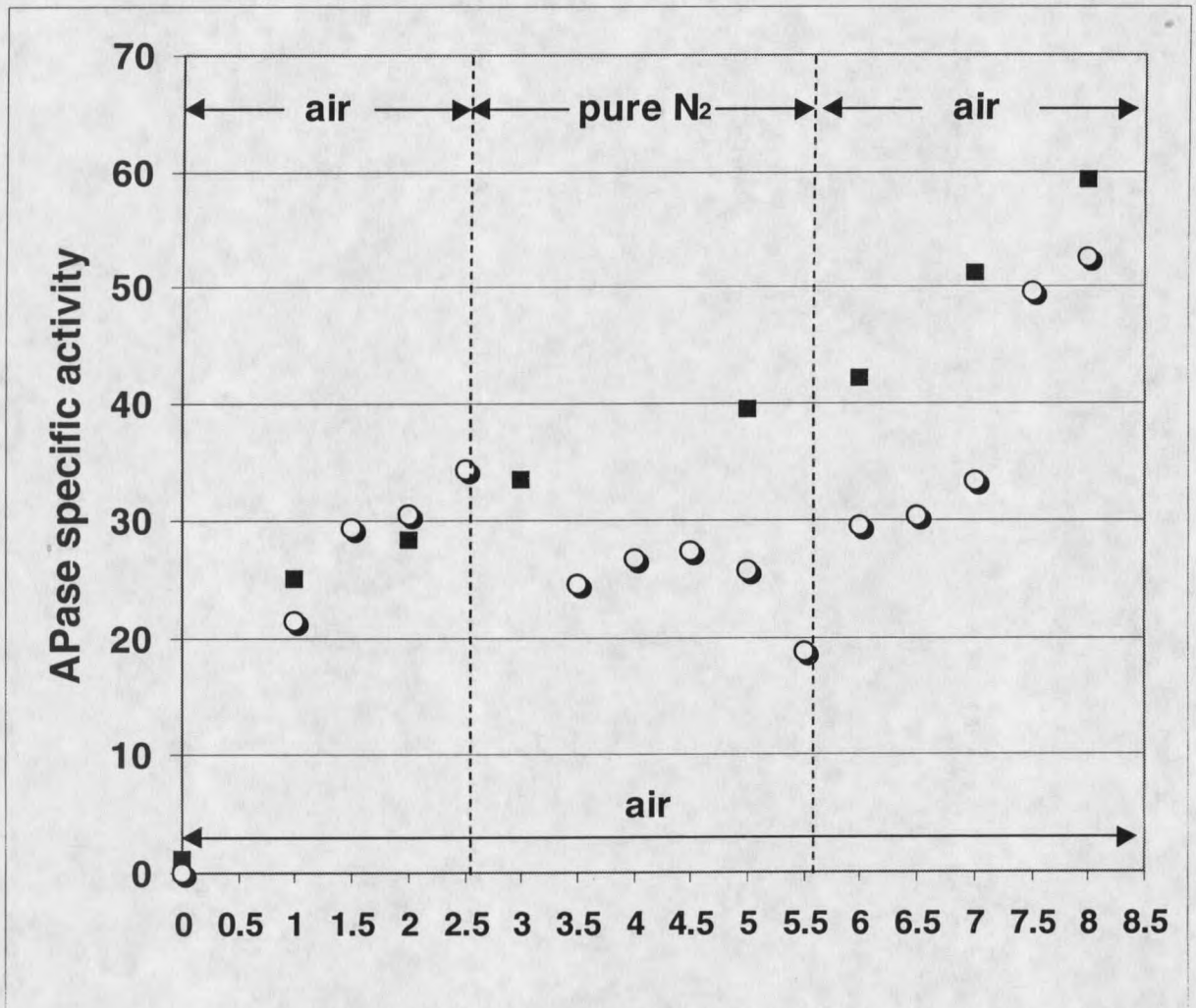


Figure 2.3. APase specific activity of planktonic *P.aeruginosa* in response to phosphate starvation. APase specific activity is expressed as ΔA_{410} mg protein^{-1}min^{-1}. (■) represents APase specific activity under ambient air without disruption for 8 hours, (○) represents Apase specific activity of a culture exposed to air, then pure nitrogen, and finally air again.

Table 2.1. Comparison of APase specific activity of planktonic *P.aeruginosa* with scraped biofilms under different conditions. Cell density is expressed as CFU/ml and CFU/cm^2 of planktonic and biofilm, respectively.

Condition	Enzyme specific activity (ΔA_{410} $mgprotein^{-1}min^{-1}$)	Cell density
Planktonic, HP 8h	0	1.52×10^9
Planktonic, LP 8h	59.19	2.6×10^8
biofilm, LP +air 8h	3.95 ± 0.56	$4.26 \pm 0.96 \times 10^9$
biofilm, LP + pure N_2 8h	0.13 ± 0.079	$4.43 \pm 1.43 \times 10^9$
biofilm, LP + pure O_2 8h	7.49 ± 0.83	$4.72 \pm 0.53 \times 10^9$

Patterns of APase Expression in Biofilms.

Staining with a fluorogenic phosphatase substrate revealed a distinct, spatially non-uniform pattern of APase expression within *P. aeruginosa* biofilm after induction by switching to low phosphate medium. A control biofilm grown continuously with high phosphate medium showed no alkaline phosphatase activity (Figure 2.4A). APase was expressed in a sharply delineated band adjacent to the biofilm-bulk fluid interface after inducing phosphate starvation for 8 hours (Figure 2.4B). Even though biofilms were

induced for a longer period of starvation for 24 hours and 36 hours, the APase band did not expand significantly (Figure 2.4C & D).

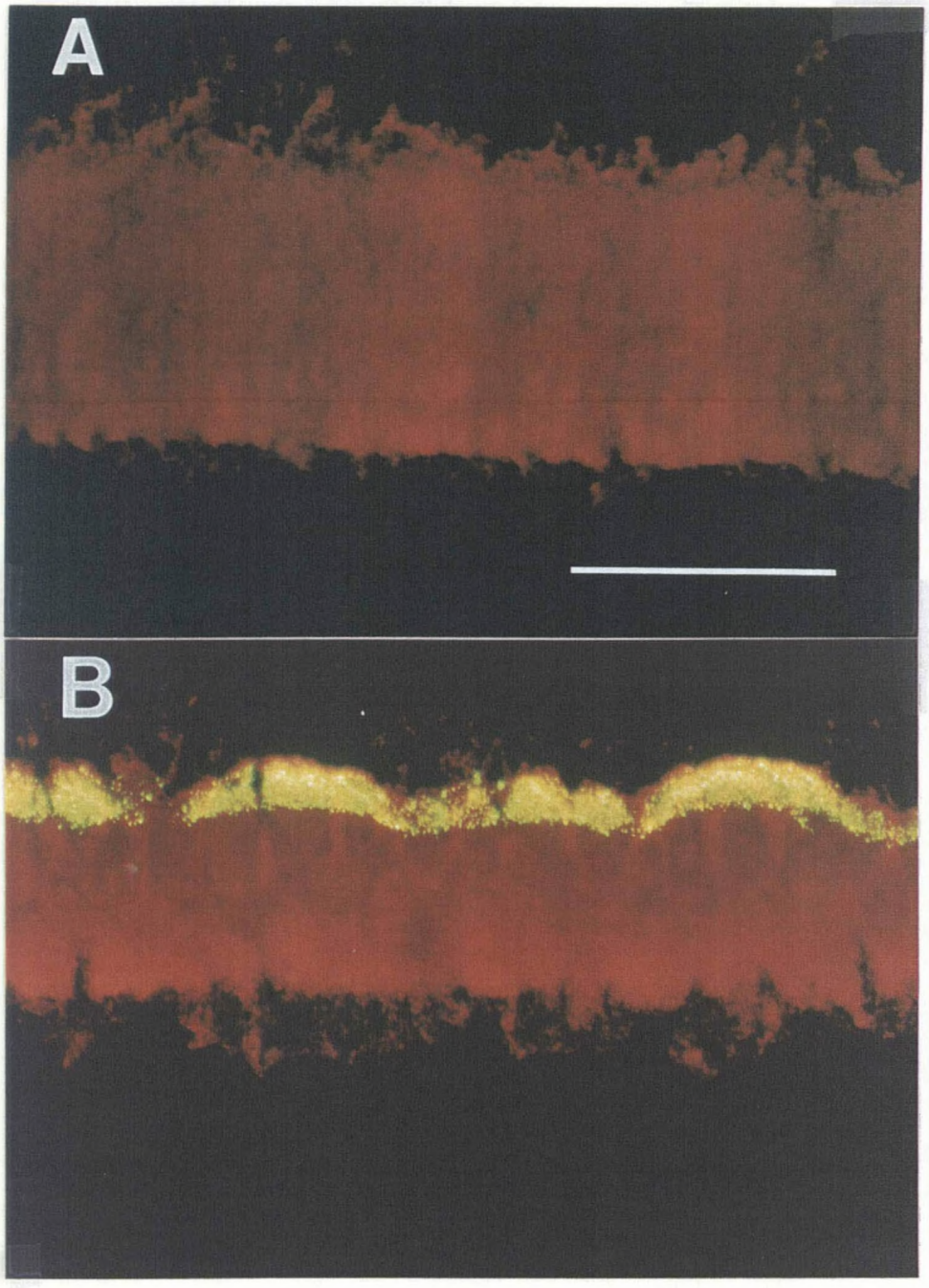


Figure 2.4. Photographs of *P.aeruginosa* biofilm cross-sections of biofilms induced for 0 (A), 12 (B), 24 (C), 36 (D) hours of phosphaste starvation. The green-yellow color represents Apase positive cells and the red color represents all cells. The images are oriented with the substratum at the bottom of the photographs. Bar = 100μm

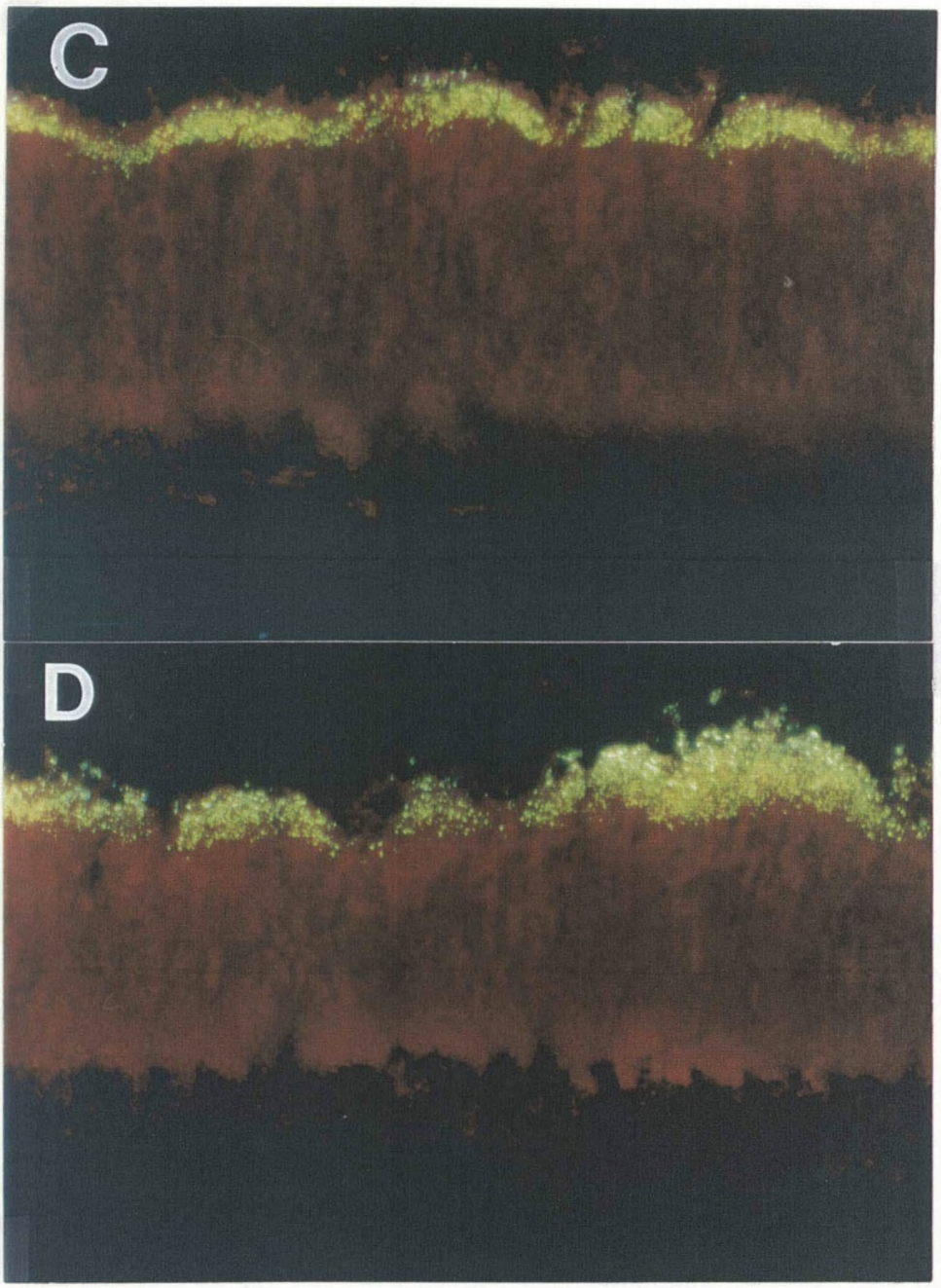


Figure 2.4. Photographs of *P.aeruginosa* biofilm cross-sections of biofilms induced for 0 (A), 12 (B), 24 (C), 36 (D) hours of phosphaste starvation. The green-yellow color represents Apase positive cells and the red color represents all cells. The images are oriented with the substratum at the bottom of the photographs. Bar = 100μm

Biofilm subjected to low phosphate medium in a nitrogen atmosphere exhibited no visible phosphatase activity (Figure 2.5C). On the other hand, when the reactor atmosphere was pure oxygen, not only was the zone of APase expression expanded but also localized sites of APase activity could be found much deeper inside the biofilm (Figure 2.5D).

Image analysis was applied to 10 images like those in Figure 2.6 to quantitate the dimension of the zone of APase expression under different gaseous environments. A representative image analysis result, showing a profile for phosphatase activity along with a profile for the entire biofilm, is shown in Figure 2.6. The mean biofilm thickness ranged from 117 to 151 μm (Table 2.2). The mean dimension of the APase activity band was approximately 30 μm when grown in air. With a pure oxygen environment, the zone of APase activity was expanded approximately 1.5 fold (Table 2.2).

Dissolved Oxygen Penetration Profile.

We measured the dissolved oxygen profile within the biofilm under ambient aerobic conditions and superimposed image analysis data of APase activity with the dissolved oxygen concentration profile (Figure 2.7). Dissolved oxygen concentration decreased from approximately 0.25 mg/L at the biofilm-bulk fluid interface to essentially zero (less than 0.01 mg/L) at a point approximately 60 μm above the substratum. The band of APase expression in the upper region of the biofilm coincided with dissolved oxygen concentrations of greater than 0.05 mg/L.

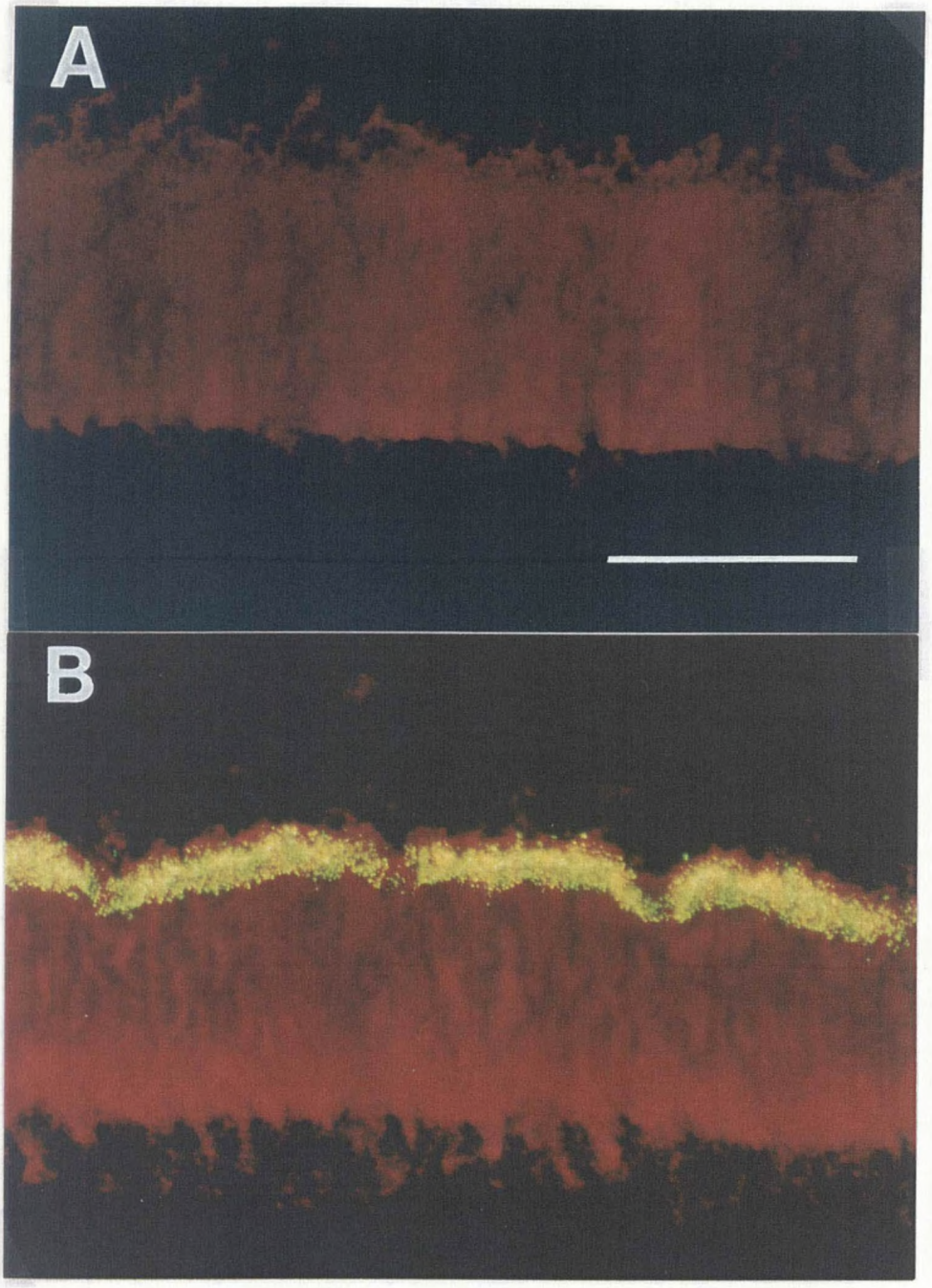


Figure 2.5. Photographs of *P.aeruginosa* biofilm cross-sections stained for APase activity under different conditions. (A) high phosphate medium with ambient air; (B) low phosphate medium with ambient aerobic atmosphere; (C) low phosphate medium under pure nitrogen atmostphere; (D) low phosphate medium under pure oxygen atmosphere. The yellow color represents Apase positive cells and the red color represents all cells. The images are oriented with the substratum at the bottom of the photographs. Bar=100 μm.

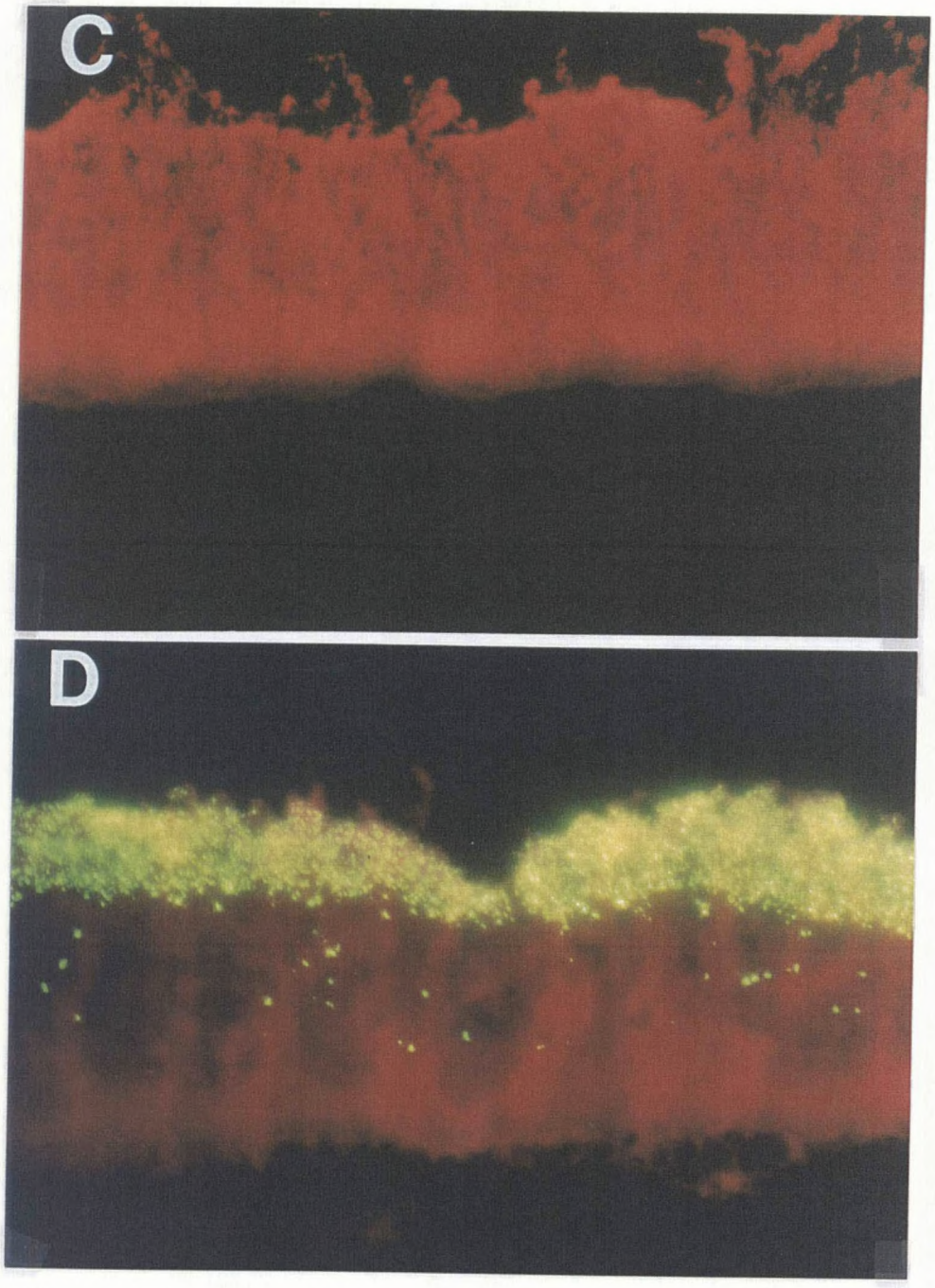


Figure 2.5. Photographs of *P.aeruginosa* biofilm cross-sections stained for APase activity under different conditions. (A) high phosphate medium with ambient air; (B) low phosphate medium with ambient aerobic atmosphere; (C) low phosphate medium under pure nitrogen atmostphere; (D) low phosphate medium under pure oxygen atmosphere. The yellow color represents APase positive cells and the red color represents all cells. The images are oriented with the substratum at the bottom of the photographs. Bar = 100 μm.

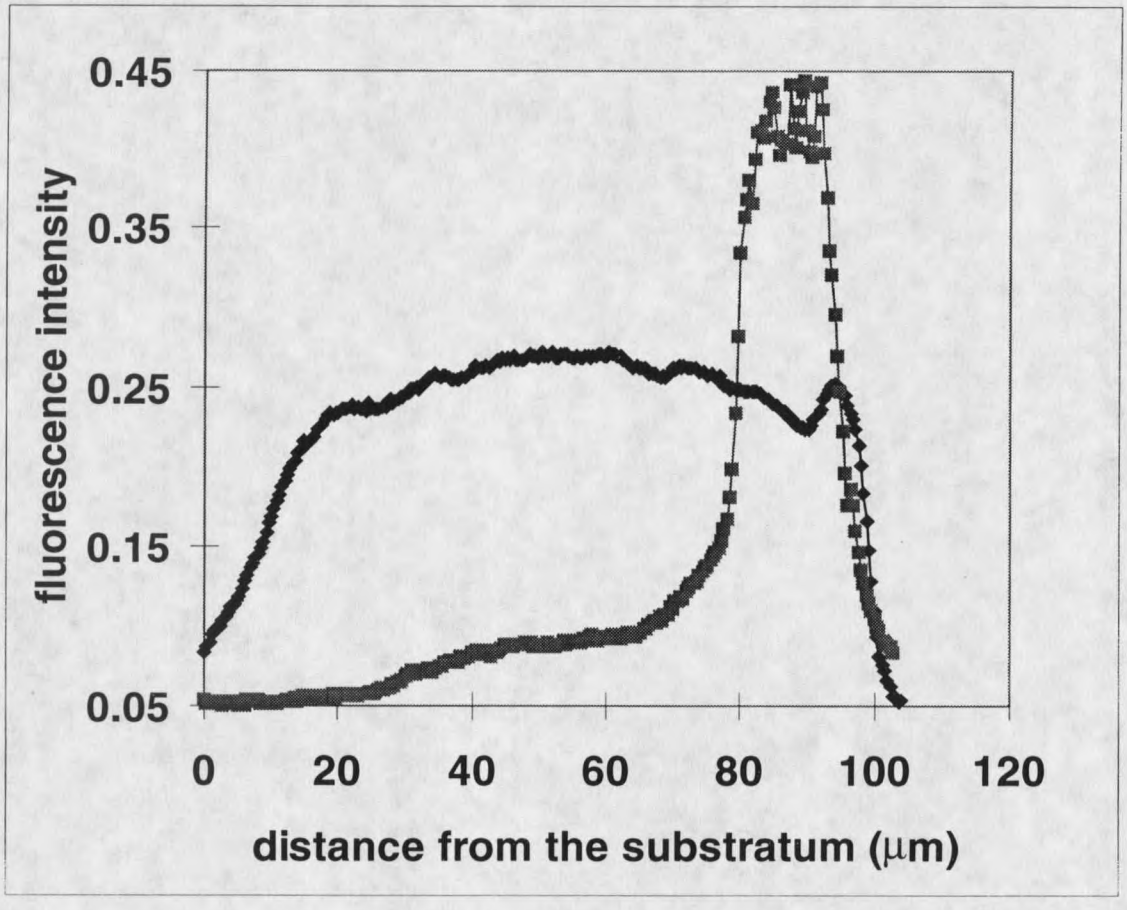


Figure 2.6. A representative image analysis result of APase activity in *P.aeruginosa* biofilms with phosphate starvation under ambient aerobic condition. (◆) represents biofilm cells stained with tetramethyl rhodamine , while (■) represents APase positive cells. The substratum is at the "0" point.

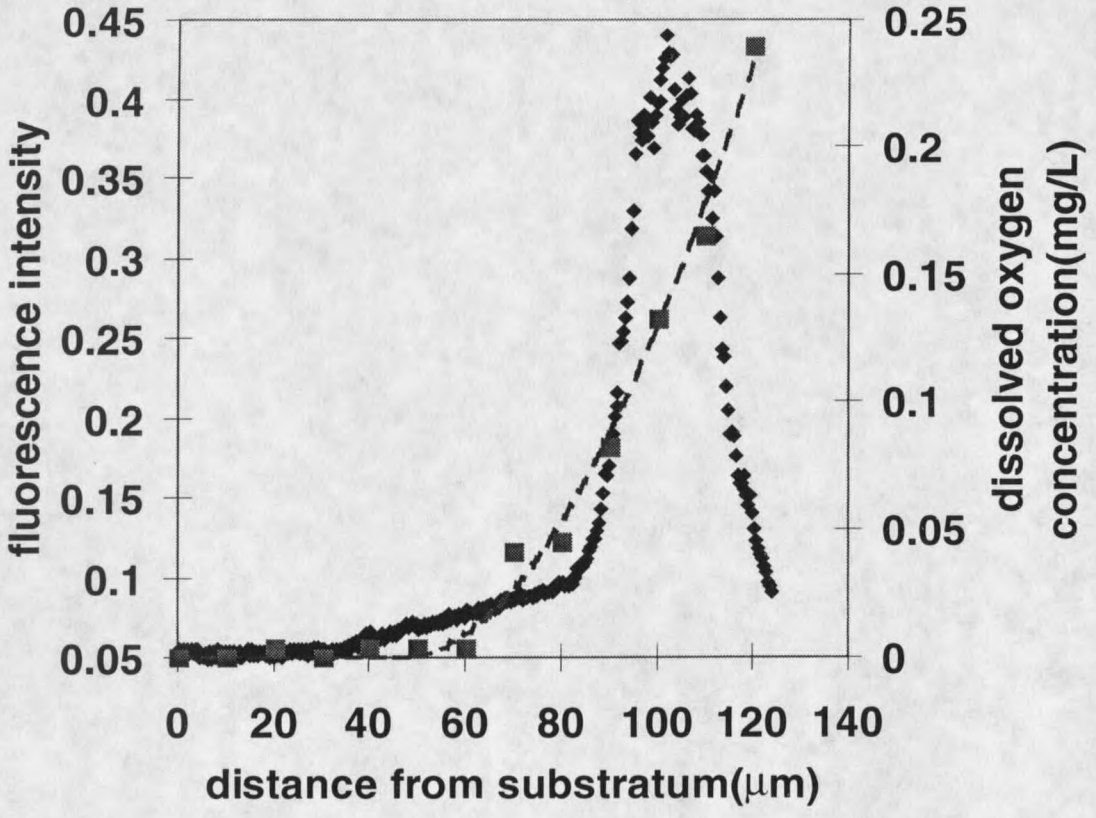


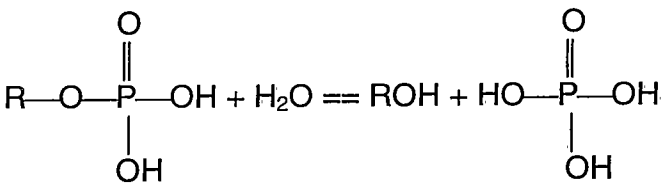
Figure 2.7. Correlation of dissolved oxygen profile with image analysis result of APase activity under aerobic conditions. (◆) APase activity, (■) dissolved oxygen, (-) trend line representing dissolved oxygen concentration. The substratum is at the "0" point.

Table 2.2. Thickness of the zone of APase expression under different gaseous conditions.

Condition	Biofilm thickness(μm)	APase band thickness(μm)
Air	117.13 ± 11.54	29.89 ± 4.39
N_2	142.04 ± 19.14	1.82 ± 3.11
O_2	150.59 ± 30.61	46.43 ± 5.72

Discussion

Alkaline phosphatase from *E. coli* is an enzyme that has been known and characterized since the 1960's (Reid and Wilson, 1971). Horiuchi et al. (1959) and Torriani (1960) found that orthophosphate repressed the formation of a nonspecific phosphomonoesterase in *E. coli* and a maximum rate of synthesis of the enzyme occurred only when the phosphate concentration became low enough to limit cell growth. Under phosphate limitation conditions, alkaline phosphatase accounts for about 6% of the total protein synthesized by the cell (Garen and Levinthal, 1960). The alkaline phosphatase of *E.coli* is a Zn – metalloprotein composed of two identical subunits (Reid and Wilson, 1971). The equilibrium catalyzed by alkaline phosphatase is as following:



The maximum hydrolytic activity of the enzyme is above pH 8, which is why the enzyme has the name of alkaline phosphatase. The nucleotide sequence of APase of *E.coli* has been determined (Chang et al., 1986). Pre-APase has total of 471 amino acids including a signal sequence of 21 amino acids. In *E. coli* cells, the monomers of the enzyme are synthesized inside the endoplasm and transported to the periplamic region, where dimerization and accurate folding occur before an active enzyme can form (Reid and Wilson, 1971). This characteristic has been widely employed to make protein fusions to study protein secretion (Hoffman and Wright, 1985; Derman and Beckwith, 1995; Strom and Lory, 1987; Boudineaud, et al. 1993). In *E. coli* it is induced under the control of a complex regulatory circuit and functions in scavenging phosphate from organic phosphate esters under phosphate starvation (Moat and Foster, 1995).

Alkaline phosphatase was first discovered in *P. aeruginosa* by Hou in 1966 (Hou et al., 1966). APase activity is repressed at the high phosphate medium ([Pi] = 7mM) easily inducible in planktonic suspensions of *P. aeruginosa* under phosphate starvation ([Pi] = 0.07mM) (Hou et al., 1966; Huang et al., 1998). In *P.aeruginosa* biofilms, the enzyme-labeled-fluorescence technique coupled with cryoembedding and cryosectioning has enabled the visualization of the spatial pattern of alkaline

phosphatase expression (Huang et al. 1998). The pattern is distinct in *P. aeruginosa* biofilms under an atmosphere of ambient air. We hypothesized that this pattern is due to oxygen limitation because: i) oxygen is often limiting in aerobic biofilms because of its rapid consumption, ii) in the drip-flow system both nutrients and oxygen come from the top of the biofilm; cells near the bulk fluid/biofilm interface have greater access to oxygen and can consume it, iii) oxygen is limiting deep within biofilms as suggested by de Beer et al. (1994) and iv) enzyme biosynthesis requires both nutrients and oxygen since *P. aeruginosa* is an obligate aerobe under the experiment conditions used (no nitrate and arginine available).

To test this hypothesis we designed a simple experiment using planktonic bacteria to see if we could switch APase production off and on by anaerobic and aerobic conditions. The result shown in Figure 2.4 supported our hypothesis. Pure nitrogen stopped APase production immediately and APase production was resumed when the culture was exposed to air. We then exposed biofilms to different gaseous environments to see how the pattern of APase production would change in the attached population. With pure nitrogen, the expression of alkaline phosphatase was totally blocked. This showed that enzyme synthesis within the *P.aeruginosa* biofilm required oxygen. The experiment of pure oxygen environment led to a very interesting observation. The dimension of the APase expression band increased 1.5 fold as measured by image analysis. Disperse green crystals, indicating isolated sites of APase activity were found deep within the biofilm. Collective APase specific activity of the

entire biofilm under ambient aerobic conditions was approximately 1/15 that of comparable planktonic bacteria, which makes sense because only the upper 1/5~1/4 layer of the biofilm was expressing the enzyme. Also, 1.0g/L glucose was used in planktonic culture to achieve enough cell mass. Alkaline phosphatase production of the whole biofilm was increased 2-fold under pure oxygen. This supports our speculation that oxygen could penetrate deeper within the biofilm when pure oxygen was used but the physiological heterogeneity of the community with oxygen-starved cells deep within the biofilm might lead to a different response. Hence, it was of interest to measure the dissolved oxygen profile under a pure oxygen atmosphere. A good correlation was observed between the oxygen penetration profile, when measured under ambient aerobic conditions, and the band of alkaline phosphatase expression. These findings also correspond somewhat to studies on microbial mats where changes in guild activity reflect changing chemical composition with increasing depth in the community (Canfield and Des Marais 1991; D'Amelio et al. 1989; Ward et al. 1992).

The spatial patterns of phosphate starvation gene expression in *P.aeruginosa* biofilms are distinct because we chose *P. aeruginosa*, which can only use oxygen as an electron acceptor under the experimental condition, as our test microorganism to study the role of oxygen limitation in the expression of the phosphate starvation response. These results may also be related to the reduced susceptibility of bacterial biofilms to antimicrobial agents. Specifically, it could be important to determine the role of limiting nutrient in the establishment of physiological gradients to understand mechanisms of

recalcitrance. Since the spatial physiological pattern of biofilms of different microorganisms may not be the same as pure *P. aeruginosa* biofilms (Huang et al. 1998), that goal is further complicated in natural biofilm communities composed of both aerobes and anaerobes. However, the results reported here from *P. aeruginosa* biofilms gave a representative picture and support the concept of physiological heterogeneity within biofilms (Huang et al. 1998; Wentland et al. 1996)

Acknowledgments

This work was supported through cooperative agreement EEC- 8907039 between the National Science Foundation and Montana State University and by the industrial associates of the Center for Biofilm Engineering.

We thank Betsy Pitts (Center for Biofilm Engineering, Montana State University, Bozeman, MT) for PCR-amplifying the 16S rDNA of the isolate and Mary Bateson (Department of Microbiology, Montana State University, Bozeman, MT) for assistance with the phylogenetic analysis.

References Cited

Boudineaud, J. P., D. Heierli, M. Gamper, H. J. Verhoogt, A. J. Driessen, W. N. Konings, C. Lazdunski, and D. Haas. 1993. Characterization of the arcD arginine: ornithine exchanger of *Pseudomonas aeruginosa*. Localization in the cytoplasmic membrane and a topological model. *J. Biol. Chem.* **268**: 5417-5424.

Brown, M. R. W., and P. Gilbert. 1993. Sensitivity of biofilms to antimicrobial agents. *J. Appl. Bacteriol. Symp. Suppl.* **74:** 87S-97S.

Canfield, D. E., and D. J. Des Marais. 1991. Aerobic sulfate reduction in microbial mats. *Science* **251:** 1471-1473.

Chang, C. N., W. J. Kuang, and E. Y. Chen. 1986. Nucleotide sequence of the alkaline phosphatase gene of *Escherichia coli. Gene* **44**: 121-125.

Costerton, J. W. 1984. The formation of biocide-resistant biofilms in industrial, natural and medical systems. *Dev. Ind. Microbiol.* **25:** 363-372.

D'Amelio, E. D., Y. Cohen, and D. J. Des Marais. 1989. Comparative functional ultrastructure of two hypersaline submerged cyanobacterial mats: Guerrero Negro, Baja California Sur, Mexico, and Solar Lake, Sinai, Egypt, p. 97-113. *In* Y. Cohen, and E. Rosenberg (ed.), Microbial mats: physiological ecology of benthic microbial communities. Am. Soc. Microbiol., Washington, D. C..

de Beer, D., P. Stoodley, and Z. Lewandowski. 1994. Effects of biofilm structures on oxygen distribution and mass transport. *Biotechnol. Bioeng.* **43:** 1131-1138.

Derman, A. I., and J. Beckwith. 1995. *Escherichia coli* alkaline phosphatase localized to the cytoplasm slowly acquires enzymatic activity in cells whose growth has been suspended: a caution for gene fusion studies. *J. Bacteriol.* 177: 3764-3770.

Garen, A., and C. Levinthal. 1960. BBA. **38**: 460

Harkin, G., and P. Shope. 1993. The Mark image analysis system. Technical report, Center for Biofilm Engineering, Montana State University, Bozeman, MT.

Hoffman, C. S., and A. Wright. 1985. Fusions of secreted proteins to alkaline phosphatase: an approach for studying protein secretion. *Proc. Natl. Acad. Sci.* USA. 82: 5107-5111.

Horiuchi, T., S. Horiuchi, and D. Mizuno. 1959. *Nature.* **183**: 1529.

Hou, C. I., A. F. Gronlund, and J. J. R. Campbell. 1966. Influence of phosphate starvation on cultures of *Pseudomonas aeruginosa. J. Bacteriol.* **92(4):** 851-855.

Huang, C. -T., K. D. Xu, G. A. McFeters, and P. S. Stewart. 1998. Spatial patterns of alkaline phosphatase expression within bacterial colonies and biofilms in response to phosphate starvation. *Appl. Environ. Microbiol.* **64**: 1526-1531.

LeChevallier, M. W., C. D. Cawthon, and R. G. Lew. 1988. Inactivation of biofilm bacteria. *Appl. Environ. Microbiol.* **54:** 2492-2499.

Maidak, B. L., N. Larsen, M. J. McCaughey, R. Overbeek, G. J. Olson, K. Fogel, J. Blandy, and C. R. Woese. 1994. The Ribosomal Database project. *Nucleic Acids Res.* **22**: 3485-3487.

Moat, A. G., and J. W. Foster. 1995. p. 196-197. *In* Microbial physiology, 3rd Ed, John Wiley & Sons, Inc., New York, NY.

Murga, R., P. S. Stewart, and D. Daly. 1995. Quantitative analysis of biofilm thickness variability. *Biotechnol. Bioeng.* **45**: 503-510.

Neidhardt, F. C., P. L. Bloch, and D. F. Smith. 1974. Culture medium for enterobacteria. *J. Bacteriol.* **119:** 736-747.

Nickel, J. C., I. Ruseska, J. B. Wright, and J. W. Costerton. 1985. Tobramycin resistance of *Pseudomonas aeruginosa* cells growing as a biofilm on urinary catheter material. *Antimicrob. Agents Chemother.* **27:** 619-624.

Revsbech, N. P. 1989. An oxygen microsensor with a guard cathode. *Limnol. Oceanogr.* **34:** 474-478.

Reid, T. W. and I. B. Wilson. 1971. *E. coli* alkaline phosphatase. In The Enzymes. Ed. P. D. Boyer. Vol. IV. p. 373-416. Academic Press, Inc., London, UK.

Strom, M. S., and S. Lory. 1987. Mapping of export signals of *Pseudomonas aeruginosa* pilin with alkaline phosphatase fusions. *J. Bacteriol.* 169: 3181-3188.

Torriani, A. 1960. BBA. **38**: 460

Ward, D. M., J. Bauld, R. W. Castenholz, and B. K. Pierson. 1992. Modern phototrophic microbial mats: anoxygenic, intermittently oxygenic/anoxygenic, thermal, eukaryotic, and terrestrial, p. 309-324. *In* J. W. Schopf and C. Klein (ed.), The proterozoic biosphere, a multidisciplinary study. Cambridge Univ. Press, New York, NY.

Wentland, E. J., P. S. Stewart, C.- T. Huang, and G. A. McFeters. 1996. Spatial

variations in growth rate within *Klebsiella pneumoniae* colonies and biofilm. *Biotechnol. Prog.* **12**:316-321.

Yu, F. P., G. M. Callis, P. S. Stewart, T. Griebe, and G. A. McFeters. 1994. Cryosectioning of biofilm for microscopic examination. *Biofouling* **8**: 85-91

CHAPTER 3

SPATIAL PHYSIOLOGICAL HETEROGENEITY REVEALED BY ACRIDINE ORANGE STAINING AND FLUORESCENT-IN-SITU-HYBRIDIZATION (FISH)

Introduction

Microbiologists have dedicated years of effort to developing methods to estimate bacterial growth rates independent of culture technique. A common method of estimating growth rate is by determining the nucleic acid concentrations. An earliest observation in microbiology was the correlation of RNA content with growth rate (Schaechter et al., 1958). Studies done by Rosset et al. (1966) showed a linear relationship between the ratio of the amount of RNA to DNA and growth rate of *E. coli.* Leick (1968) confirmed these results by extracting nucleic acids from 12 different bacteria including *E. coli*, *Bacillus subtilis*, *Aerobacter aerogenes*, *Micrococcus anhaemolyticus*, *Pseudomonas aeruginosa* and *Lactobacillus bulgaricus* and found a similar trend between the RNA: DNA ratio and growth rate. Most data have been obtained from cultures growing at fairly high rates, but the correlation also seems valid for the growth rate range more realistic for the marine environment. Kerhof and Ward (1993) found a similar correlation between the RNA/DNA ratio and the growth rate in *Pseudomonas stutzeri* growing with generation times between 6 and 60 hours. The

works mentioned above were performed by extracting RNA and DNA and measuring the amount by biochemical or fluorescent methods.

To determine RNA content or RNA/DNA ratio in whole cells, there are nonspecific fluorescent staining methods and phylogenetic specific fluoresent-in-situ-hybridization (FISH) methods. Commonly used fluorescent stains for measuring RNA content are acridine orange and pyronin Y. Moubouquette et al. (1990) developed an *in situ* method of measuring RNA content of bacteria immobilized within calcium alginate beads using the fluorescent stain pyronin Y. Acridine orange (AO) is a metachromatic stain that fluoresces with a different color depending on the type of nucleic acid to which it is bound to. When AO is bound to RNA it fluoresces orange (650nm), when it is bound to DNA it fluoresces green (526nm) (Haugland, 1992). It has been reported that many factors may influence the chromatic response of acridine orange when it is used to stain bacteria, including fixation, staining concentration, chorine treatment and boiling (McFeters et al., 1990). McFeters et al. (1990) suggested that AO should be used to determine the amount of RNA under controlled conditions. Wentland et al. (1995, 1996) suggested that AO staining method was acceptable for discerning qualitative trends in growth pattern within well-defined microbial aggregates.

Oligonucleotide probes complementary to specific regions of rRNAs were developed in late 80's to early 90's to identify uncultivated microorganisms in situ. The pioneering work of Amann group (Amann et al., 1991) was to study the uncultivated symbiotic bacterium *Holospora*. They extracted the total nucleic acids from an

ecosystem and PCR amplified, cloned and sequenced the rDNA of *Holospora*. The sequences were then used to design species- as well as genus-specific rRNA hybridization probes, which enabled them to detect and differentiate individual cells in the host nuclei *in situ*. Recent advances in computer-assisted microscopy have made FISH more and more available to study natural samples. Examples of identification and enumeration of microorganisms using FISH include sulfate-reducing bacteria in multispecies biofilms grown in laboratory reactors (Amann et al., 1992) and in environmental biofilms from a sewage treatment plant (Ramsing et al., 1993), *Bifidobacterium* spp. in human fecal samples (Langendijk et al., 1995), *Salmonella* in foods (Lin and Tsen, 1995), *Legionella pneumophila* in the protozoan *Acanthamoeba castellanii* in an artificial water microcosm (Grimm et al., 1998), *Pseudomonas aeruginosa* and *Pseudomonas cepacia* (*Burkholderia cepacia* now) in soil (Hahn et al., 1992), *Vibrio vulnificus* on membrane filters (Heidelberg et al., 1993), the domains of *Bacteria*, *Archaea*, and *Eucarya* and the beta and gamma subclasses of *Proteobacteria* in drinking water (Manz et al., 1993), some photosynthetic eukaryotes from marine samples (Simon et al., 1995) and nitrifying bacteria within sludge flocs (Mobarry et al. 1996).

Another use of FISH is to estimate RNA content by fluorescence intensity so as to estimate growth rate and activity. In *E. coli* (Delong et al., 1989) and a sulfate-reducing bacterium (Poulsen et al., 1993) the signal intensities of FISH were found to

correlate linearly with growth rate. FISH was also found to be valid to infer physiological state of *Pseudomonas fluorescens* in a mesocosm and *E. coli* growing in the large intestines of streptomycin-treated mice (Boye et al., 1995; Pouslen et al., 1995).

The purpose of this work is to observe the spatial pattern of growth using AO and FISH staining, utilizing the knowledge of correlation of RNA content to growth rate and compare the results of these two methods.

Materials and Methods

Bacterial Strains and Media.

Pure cultures of *Pseudomonas aeruginosa* ERC1, *Escherichia coli*, *Klebsiella pneumoniae* Kp1 were used in this part of the project. *E.coli* was obtained from the culture collection of Dr. Gordon A. McFeters' lab, Department of Microbiology, Montana State University-Bozeman. It was isolated from a drinking water distribution system in New Haven, CT and identified with API20E, API No. #4144572. *K.pneumoniae* Kp1 isolated from drinking water, was obtained from Dr. D. Smith, South Central Connecticut Water Authority, New Haven, CT and stored in the Culture Collection of Center for Biofilm Engineering. Glucose minimal medium consisted of 1.363 g/L Na_2HPO_4, 0.656g/L KH_2PO_4, 0.011 g/L $MgSO_4 \cdot 7H_2O$, 0.036g/L NH_4Cl, 0.1ml stock solution of trace element and 0.1g/L glucose. The composition of trace elements was as described previously (Wentland, 1995). Glucose minimal medium was used from overnight culture

to biofilm growth. LB medium (Geenstein and Besmond, 1995) was used for the growth of *E. coli*, *K. pneumoniae* and *P. aeruginosa* as FISH single cell controls.

Planktonic Culture and Sampling procedure.

E. coli, K. pneumoniae and *P. aeruginosa* were grown in Bellco 250 ml culture flasks by subculturing overnight cultures. Growth was monitored by taking absorbance at 600nm with a spectrophotometer (Spectronic Instrument, Inc.). Mid log-phase cultures were fixed in 4% paraformaledhyde for 1 hour at 4 C, then spun down and resuspended in 1x PBS to wash out the paraformaldehyde, then spun down and resuspended in 50% 1xPBS, 50% ethanol and stored at –20ºC. PBS was prepared using PBS tablets (Sigma, St. Louis, MO). Thirty mililiters of 4% paraformaldehyde solution was prepared by preheating 20 ml distilled water to 60-80°C and adding 1 drop of NaOH (6M) solution. Paraformaldehyde (1.3g) was added to this alkaline water and stirred to dissolve. When the solution became clear, 10 ml of 3x PBS and 1 drop of HCl (6M) was added. The prepared paraformaldehyde solution was kept at 4ºC and used within 24 hours.

Biofilm Culture and Sampling Procedure.

P.aeruginosa ERC1 biofilm was grown in the drip-flow reactor as described in Chapter 2. After four days of growth, the biofilms were cryoembedded and cryosectioned. All biofilm experiments were duplicated.

Cryoembedding and Cryosectiong Procedure.

Biofilms were cryoembedded and cryosectioned as described in Chapter 2. When sections were used for FISH staining, biofilms were cut in 3 µm sections instead of 5 µm. Biofilm sections were collected on 8-well Superfrost slides (Fisher Scientific)

Acridine Orange Staining Procedure.

AO staining was performed according to Wentland (1995). Biofilm sections were fixed for 10 minutes at 4°C in a fixative consisting of 10% formadehyde, 5% glacial acetic acid, and 85% ethanol. Slides were then rinsed with two changes of 85% ethanol and allowed to air dry. Fixed sections were stored under refrigeration. A stock solution of 0.02% AO (Sigma) in phosphate buffer (pH 7.2) was formulated and incubated at 35°C overnight. The stock solution was then filtered through a 0.2-um syringe filter to remove any particulates. From the stock solution, a fresh solution of 0.0004% AO was prepared. Biofilm sections were stained by locating the cross section on the glass slide and placing 3 µL drops in succession along the length of the cross section. Sections were stained for 5 minutes before excess staining solution was blotted from the slide.

Hybridization of Whole cells and Biofilms.

Whole-cell in situ hybridization was performed according to Flood (1998). Biofilm sections on slides were immediately fixed with 4% paraformaldehyde solution, washed

once with phosphate-buffered-saline PBS (130mM sodium chloride, 10mM sodium phosphate [pH7.2]). The planktonic cell suspensions were dropped in 10 µl on the wells of Superfrost slides and air-dried. Then biofilm sections and slides with planktonic suspensions were dehydrated in 50, 80, 96% (vol/vol) ethanol (3 minutes each) by immersing the slides in a Coplin staining jar with ethanol. The slides were air dried thoroughly before hybridization. The following oligonucleotides were used: i) Eub338, complementary to a region of the 16S rRNA conserved in the domain *Bacteria* (Amman et al., 1990); and ii) non-Eub 338, complementary to Eub338, serving as a negative control for nonspecific binding. The probes were labeled with tetramethylrhodamine-5-isothiocyanate (Genetic Research, Inc.) For in situ hybridization, aliquots of 10 µL of hybridization solution which contained 5 ng probe, 20% formamide, 0.9M NaCl and 0.01% SDS in 20mM Tris-HCl [pH7.2] were blotted on the fixed biofilm sections and planktonic suspensions. The slides were placed in 50 ml polypropylene centrifuge tubes (Fisher Scientific) with filter paper moistened with approximate 2 ml hybridization buffer and incubated for 1.5h at 46°C. After hybridization, the slides were carefully removed and rinced once with some of the washing buffer (20mM Tris-HCl [pH7.2], 0.01% SDS, 0.225M NaCl). They were then immersed in 50 ml of washing buffer at 48°C for 20 minutes. After the wash the slides were briefly rinsed with distilled water, air dried and mounted.

Microscopy.

An Olympus BH-2 microscope (Lake Success, NY) with epifluorescence illumination was used for the examination of the biofilm sections. AO-stained sections were visualized using an Olympus B filter cubic unit containing an excitation filter (BP490), a dichroic mirror (DM500), and a barrier filter (AFC +0515). Tetramethyl-rhodamine from the *in situ* hybridization was visualized with a G filter containing an excitation filter (BP-545), a dichroic mirror (DM-570), and a barrier filter (O-590).

Image Analysis.

Image analysis of FISH images was performed with Image Tool 2.0 software. An image of a ruler was first taken to calibrate the distance in μm to pixel. The fluorescence intensity along pixel was measured with the built-in "line profile" function. A line was drawn across the biofilm section and the "line profile" function gave the number of fluorescence intensity along the line. The result was opened in Microsoft Excel and graph was generated.

Results

AO Staining Results of Biofilm Sections.

A representative 4-day *P. aeruginosa* biofilm section stained with acridine orange is shown in Figure 3.1. The surface layer and substratum layer of the biofilm were stained orange, whereas inner parts of the biofilm were stained green.

FISH Staining Result of Planktonic Cells and Biofilm Sections.

Exponential-phase *E. coli*, *P. aeruginosa, K. pneumoniae* grown in LB medium were all stained with the rhodamine labeled Eub338 probe and appeared red. The image of *P. aeruginosa* stained with FISH probe is shown in Fig 3.2. The signals of the Eub338 probe were bright, whereas no signal was observed from the antiEub338 probe stained cells.

FISH staining results of *P. aeruginosa* biofilm sections were shown in Figure 3.3. There was a gradient of fluorescent signal intensity across the section. The surface has higher fluorescent intensity than the lower part of the biofilm. No signal was observed from the antiprobe stained biofilm sections. The FISH staining image of the biofilm was quantified with Image Tool Software and the result is shown in Figure 3.4.

Since we could not separate the orange and green colors of AO staining by different filters, the orange zones at the surface of AO stained sections were measured manually with a ruler and quantified. Ten random-chosen sections from AO or FISH staining samples were quantified, the result was summarized into Table 3.1

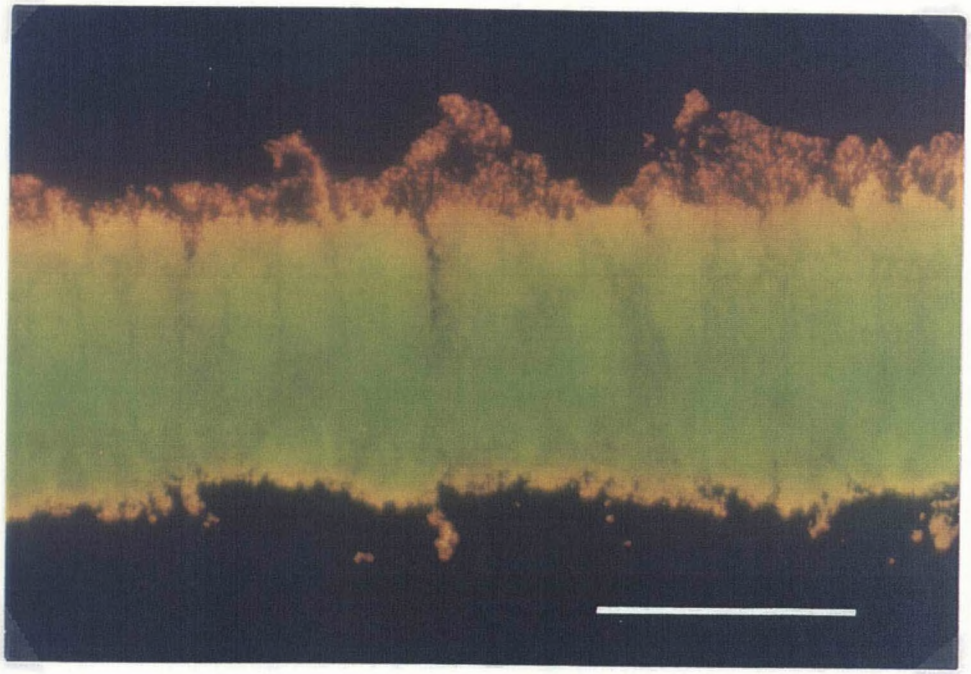


Figure 3.1. A representative image of a 4-day old biofilm section stained with acridine orange. Orange color represents high RNA, whereas green color represents low RNA. The substratum is at the bottom of the photograph. Bar = 100μm

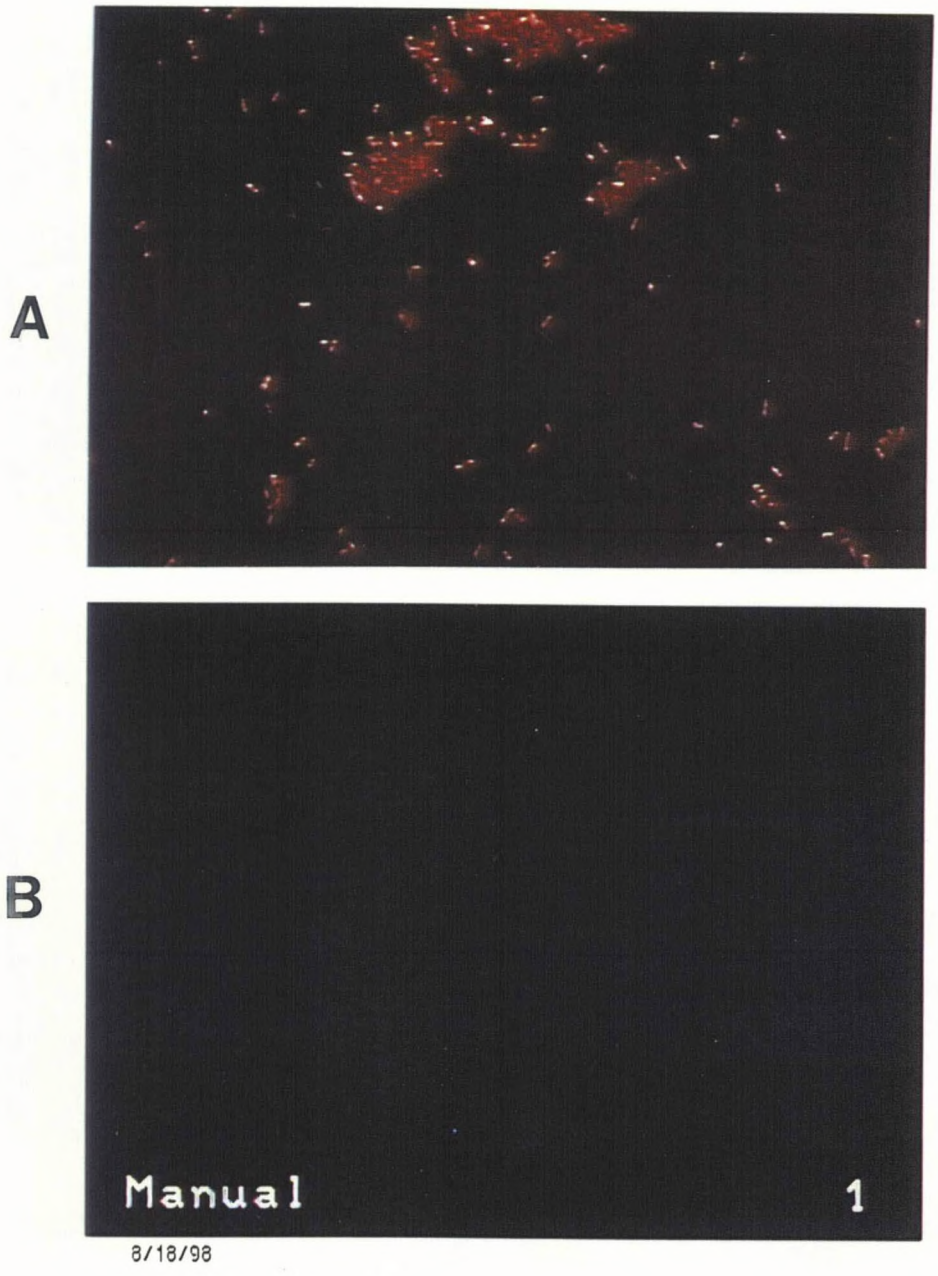


Figure 3.2. Photographs of *P.aeruginosa* planktonic cells stained with Eub338 probe (A) and anti-Eub338 probe (B). X40 magnification.

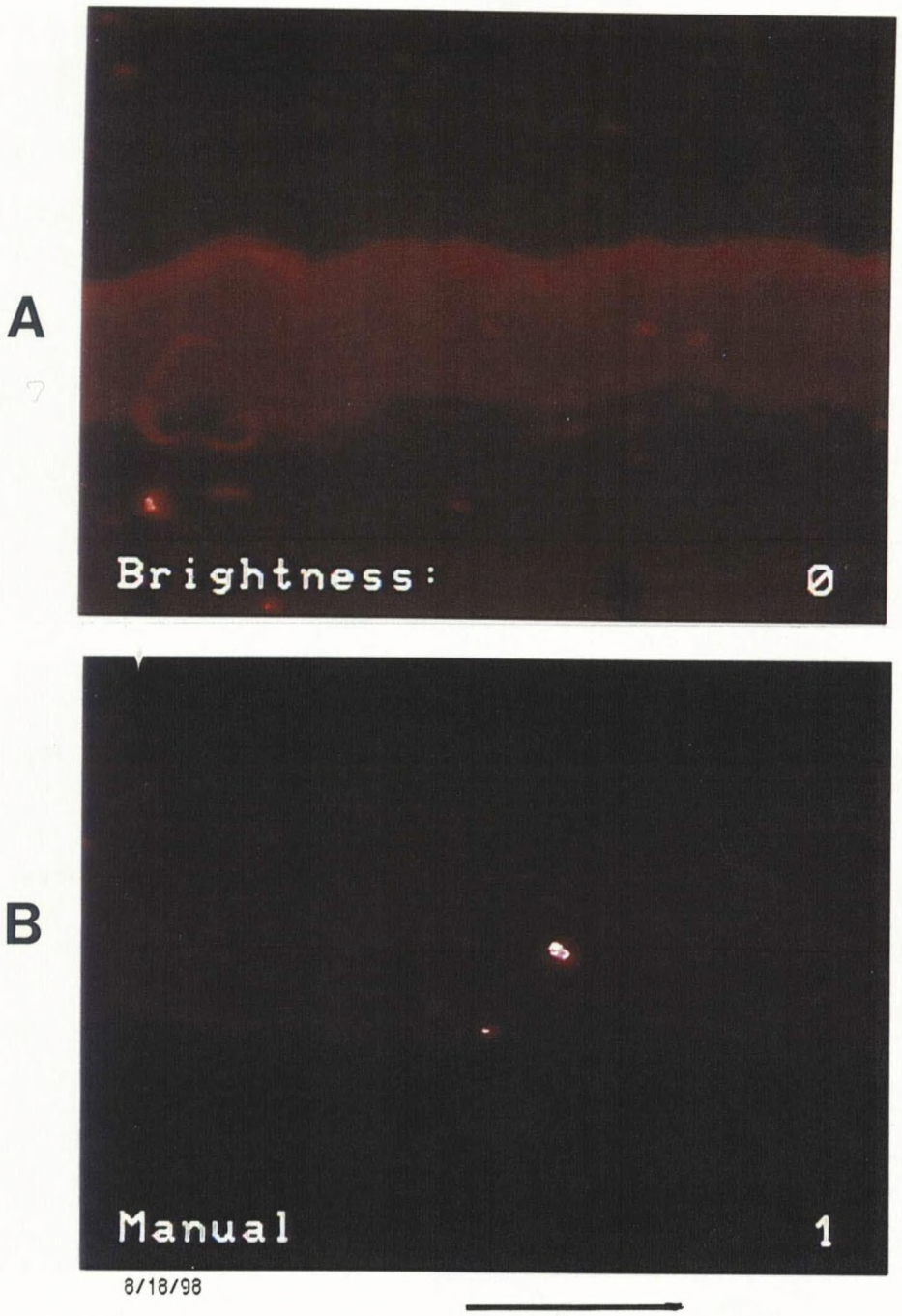


Figure 3.3. A representative image of a 4-day old *P.aeruginosa* biofilm section stained with Eub338 probe (A) and anti-Eub338 probe (B). The substratum was oriented at the bottom of the photograph, bar = 100 μm.

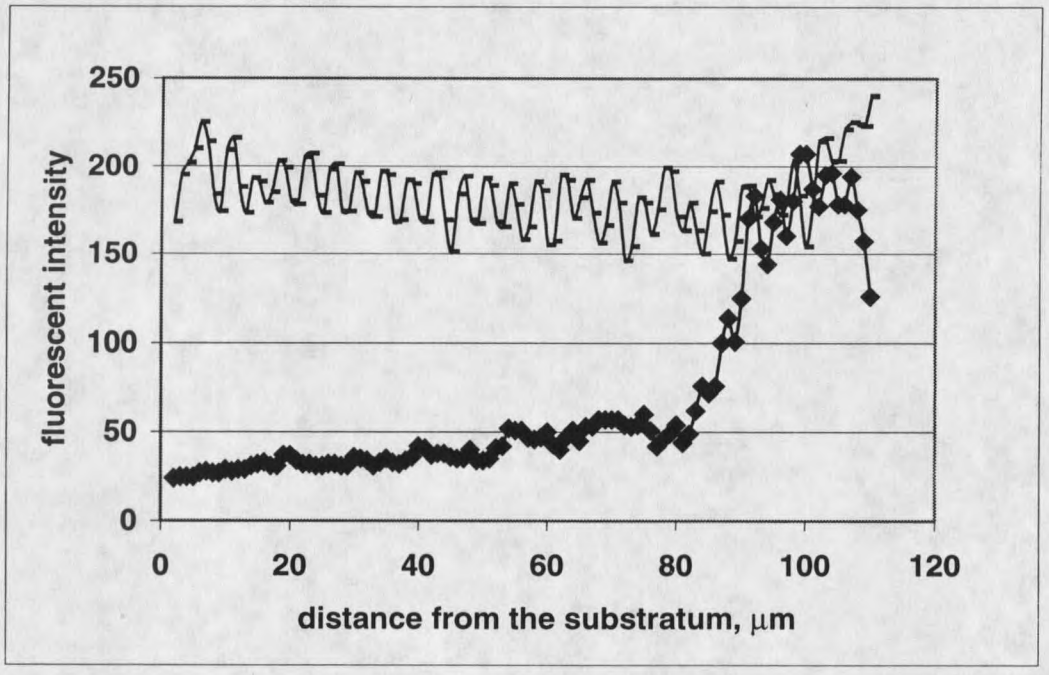


Figure 3.4 Image analysis result of a FISH/DAPI stained *P.aeruginosa* biofilm section. (♦) represents FISH fluorescent Intensity, (–) represents DAPI intensity. Substratum is at "0" position.

Table 3.1 Summary of image analysis results of AO and FISH

	AO staining		FISH staining	
Sample No.	Thickness (μm)	Active zone (μm)	Thickness (μm)	Active zone (μm)
1	92	23	110.3	23.0
2	130	19	98.6	20.7
3	105	20	85.2	21.6
4	110	20	78.5	20.8
5	78	18	115.4	20.2
6	135	25	108.1	22.4
7	108	20	130.5	19.1
8	126	21	120.2	23.4
9	120	21	110.8	22.8
10	110	17	119.7	18.5
AVR. ± STDV	111.4 ± 16.5	20.4 ± 2.2	107.73 ± 15.34	21.25 ± 1.59

Discussion

Using AO and FISH staining we revealed a spatial pattern of heterogeneity which reflects growth rate in a thick biofilm. Since we did not make an independent correlation of growth rate and the color of AO staining or FISH fluorescent intensity, the results are suggestive but not conclusive. AO staining showed that the 20-25 μm upper layer of the biofilm was orange indicating faster growing cells whereas the majority of the inner part of the biofilm was green indicating slower growing cells. The bacteria immediately adjacent to the substratum were also consistently stained orange for unknown reasons. We speculate that either they are fast growing because their growth was enhanced by

surface association or there is some staining artifact. FISH staining showed consistent results with AO; the surface layers of the cells of the biofilm in this system appeared to have more RNA indicating faster growth.

The Eub338 probe has been shown to be a robust and reliable probe (Flood, 1999). Our result using planktonic bacteria as a control showed little background nonspecific staining. The biofilm sections stained with antiEub338 probe also served as a negative control, indicating little nonspecific binding. Since yeast cells have thick cell walls that will prevent oligonucleotide probe permealizing, they will not serve as a good negative control. From literature and other researcher's preliminary work (Flood, 1999), the 20% formamide combined with temperature at 46°C should be stringent for Eub338 probe.

Moller et al. (1995) compared quantitative results of acridine orange staining for RNA to 16S hybridizaiton in *Pseudomonas putida* and found that acridine orange staining gave a good indication of total RNA content within a cell.

The dimension of zones of growth rate revealed by AO and FISH are consistent in our work: the faster growing cells are located in the upper 20-25 um layer of the biofilm sections, revealed both by AO and the FISH staining technique.

References Cited

Amann, R. I., J. Stomley, R. Devereux, R. Key, and D. A. Stahl. 1992. Molecular and microscopic identification of sulfate-reducing bacteria in multispecies biofilms. *Appl. Environ. Microbiol.* **58**: 614-623.

Amann, R., N. Springer, W. Ludwig, H-D. Görtz, and K-H. Schleifer. 1991. Identification *in situ* and phylogeny of uncultured bacterial endosymbionts. *Nature.* **351**: 161-164

Boye, M., T. Ahl, and S. Molin. 1995. Application of a strain-specific rDNA oligonucleotide probe targeting *Pseudomonas fluorescens* Ag1 in a mesocosm study of bacterial release into environment. *Appl. Environ. Microbiol.* **61**: 1384-1390

Delong, E. F., G. S. Wickham, and N. R. Pace. 1989. Phylogenetic stains: ribosomal RNA-based probes for identification of single cells. *Science* **243**: 1360-1363.

Flood, J. 1997. Eutrophic wetland biofilms. Ph.D. thesis. University of New South Wales, New South Wales, Australia

Flood, J. 1999. Personal communication.

Grimm, D., H. Merkert, W. Ludwig, K. H. Schleifer, J. Hacker, and B. C. Brand. 1998. Specific detection of *Legionella pneumophila*: construction of a new 16S rRNA-targeted oligonucleotide probe. *Appl. Environ. Microbiol.* **64**: 2686-90.

Hahn, D., R. I. Amann, W. Ludwig, A. D. Akkermans, and K. H. Schleifer. 1992. Detection of micro-organisms in soil after in situ hybridization with rRNA-targeted, fluorescently labelled oligonucleotides. *J. Gen. Microbiol.* **138**: 879-887.

Haugland, R. P. 1992. Handbook for Fluorescent Probes and Research Chemicals. P. 221-227. Larison, K. D. Editor. Molecular Probes, Inc., Eugene, OR.

Heidelberg, J. F., K. R. O'Neill, D. Jacobs, and R. R. Colwell. 1993. Enumeration of *Vibrio vulnificus* on membrane filters with a fluorescently labeled oligonucleotide probe specific for kingdom-level 16S rRNA sequences. *Appl. Environ. Microbiol.* **59**: 3474-3476.

Kerkhof, L. and B. B. Ward. 1993. Comparison of nucleic acid hybridization and fluorometry for measurement of the relationship between RNA/DNA ratio and growth rate in a marine bacterium. *Appl. Environ. Microbiol.* **59**: 1303-1309.

Langendijk, P. S., F. Schut, G. J. Jansen, G. C. Raangs, G. R. Kamphuis, M. H. F. Wilkinson, and G. W. Welling. 1995. Quantitative fluorescence in situ hybridization of *Bifidobacterium* spp. with genus-specific 16S rRNA-targeted probes and its application in fecal samples. *Appl. Environ. Microbiol.* **61**: 3069-3075.

Leick, Vagn. 1968. "Ratios between contents of DNA, RNA and protein in different microorganisms as a function of maximal growth rates". *Nature.* **217**: 1153-1155.

Lin, C.-K., and H.-Y. Tsen. Development and evaluation of two novel oligonucleotide probes based on 16S rRNA sequence for the identification of *Salmonella* in foods. *J. Appl. Bacteriol.* **78**: 507-520.

Manz, W., U. Szewzyk, P. Ericsson, R. I. Amann, K.-H. Schleifer, and T.-A. Stenström. 1993. In situ identification of bacteria in drinking water and adjoining biofilms by hybridization with 16S and 23S rDNA-directed fluorescent oligonucleotide probes. *Appl. Environ. Microbiol.* **59**: 2293-2298.

Mobarry, B. K., M. Wagner, V. Urbain, B. E. Rittmann, and D. A. Stahl. 1996. Phylogenetic probes for analyzing abundance and spatial organization of nitrifying bacteria. *Appl. Environ. Microbiol.* 62: 2156-2162.

Møller, S., C. S. Kristensen, L. K. Poulsen, J. M. Carstensen, and S. Molin. 1995. Bacterial growth on surfaces: automated image analysis for quantification of growth rate-related parameters. *Appl. Environ. Microbiol.* **61**: 741-748

Monbouquette, H. G., G. D. Sayles and D. F. Ollis. 1990. Immobilized cell biocatalyst activation and pseudo-steady-state behavior: model and experiment. *Biotechnol. Bioeng.* **35**: 609-629.

Poulsen, L. K., T. R. Licht, C. Rang, K. A. Krogfelt, and S. Molin. 1995. Physiological state of *Escherichia coli* BJ4 growing in the large intestines of streptomycin-treated mice. *J. Bacteriol.* **177**: 5840-5845.

Ramsing, N. B., M. Kühl, and B. B. Jørgensen. 1993. Distribution of sulfate-reducing bacteria, O_2, and H_2S in photosynthetic biofilms determined by oligonucleotide probes and microelectrodes. *Appl. Environ. Microbiol.* **59**: 3840-3849.

Rosset, R., J. Julien, and R. Monier. 1966. Ribonucleic acid composition of bacteria as a function of growth rate. *J. Mol. Biol.* **18**: 308-320.

Schaechter, M., O. Maaloe, and N. O. Kjeldgaard. 1958. Dependency on medium and temperature of cell size and chemical composition during balanced growth of *Salmonella typhimurium. J. Gen. Microbiol.* **19**: 592-606.

Simon, N., N. LeBot, D. Marie, F. Partensky, and D. Vaulot. 1995. Fluorescent in situ hybridization with rRNA-targeted oligonucleotide probes to identify small phytoplankton by flow cytometry. *Appl. Environ. Microbiol.* **61**: 2506-2513.

CHAPTER 4

PHYSIOLOGICAL HETEROGENEITY OF RESPIRATORY ACTIVITY REVEALED BY CTC STAINING

Introduction

In Chapter 2, a sharp oxygen gradient was shown in the biofilm and the three-fourths lower 3/4 of the biofilm was experiencing oxygen limitation. It is logical to hypothesize that there is a physiological gradient in respiration rate or oxygen consumption rate in this pure culture *P.aeruginosa* biofilm.

Estimation of microbial respiration rate or respiratory activity is frequently required in microbial ecological studies to estimate system productivity, biomass turnover, or substrate utilization potentials. Recently tetrazolium salts have been widely employed to observe and enumerate respirometrically active bacteria in aquatic environmental samples (Swannell and Williamson, 1988; Harvey and Young, 1980; Quinn, 1984; Stubberfield and Shaw, 1990; Zimmermann et al., 1978; Rodgriguez et al., 1992). These redox dyes have been used in many bio-, cyto-, and histo-chemical studies since 1941, when Kuhn and Jerchel (1941) drew attention to their possible value in biochemical research. This approach relies on the fact that tetrazolium salts can accept electrons from different sites along the electron transport system (ETS) and are

reduced to colored formazans which can be viewed under a microscope, or extracted in an organic solvent (commonly ethanol) and quantified spectrophotometrically (Nachlas et al., 1960; Lippold, 1982).

INT (2-(4-iodophenyl)-3-(4-nitrophenyl)-5-phenyl tetrazolium chloride) and CTC (5-cyano-2, 3-ditolyl tetrazolium chloride) are two tetrazolium salts that have been used commonly as indicators of bacterial respiratory activity and viability (Boucher et al., 1994; Kaprelyants and Kell, 1993; Rodriguez et al., 1992). Both salts are reduced to their insoluble red (INF), or fluorescent-orange (CTF) formazans by components of the prokaryotic respiratory chain (Packard, 1985; Smith, 1995). CTC appears to be reduced by the primary dehydrogenases (succinate, NAD(P)H, and possibly others) in *Escherichia coli*, while INT may also be reduced by ubiquinone, and possibly cytochromes b555, 556 (Smith, 1995). These sites of reduction are similar to those suggested for eukaroytic cells (Nachlas, et al. 1960; Packard, 1985; Pearse, 1972; Seidler, 1991).

Althought INT-formazan may be observed microscopically with bright-field optics as opaque red intracellular deposits and the INT procedure has proved extremely useful in many environmental studies, it can not be applied to study biofilm bacteria on opaque substrata without removal of the cells. CTC, because of the fluorescent nature of its reduced formazan, has been successfully applied to study respiratory activity of biofilms (Rodgriguez, et al., 1992; Yu and McFeters, 1994; Huang, 1995;).

In order to visualize the spatial pattern of respiratory activity in biofilms, CTC was applied to 4-day old pure culture *P.aeruginosa* biofilms followed by cryoembedding and cryosectioning. Image analysis was applied to the CTC-stained biofilm sections to quantify the spatial pattern.

Materials and Methods

Bacterial Strains, Media and Biofilm Growth Procedure.

A pure culture of *Pseudomonas aeruginosa* ERC1 strain was used thoroughout. It was described in Chapter 2. Glucose minimal medium was used to grow biofilm. The composition of the medium was described in Chapter 3. Glucose was added to give a final concentration of 1g/L after filter sterilization. Biofilm was grown in drip-flow reactor for four days total including one day preincubation. All the experiments were duplicated.

CTC Staining Procedure.

CTC staining was performed according to Yu (1994). Four-day old biofilms on the coupons were transferred to a homemade staining box containing 0.04% (approx. 4mM) CTC (Polysciences, Inc.) in reagent-grade water. After incubation at 35°C for up to 2 hours, the CTC solution was removed and replaced with 5% formalin to fix the biofilms for 5 minutes, then counterstained with 4', 6-diamidino-2-phenylindole (DAPI) (1 μg/ml, final concentration) for 3 minutes.

Preparation of Biofilm Sections for Microscopy.

The biofilms stained with CTC were subsequently cryoembedded and cryosectioned as described in Chapter 2.

Microscopy.

Biofilm sections stained with CTC/DAPI were visualized under an Olympus BH-2 microscope with epifluorescence illumination. An Olympus B filter cubic unit with excitation filter (BP490), a dichroic mirror (DM500) and a barrier filter (AFC +O515) were used to simultaneously visualize the CTC-formazan and DAPI fluorescence. All bacteria appeared green when stained with DAPI, whereas the respiring cells were green but contained red intracellular CTC-formazan crystals. Filter block G containing an excitation filter (BP-545), a diachronic mirror (DM-570), and a barrier filter (O-590) was used to visualize the red CTC-formazan crystals by excluding DAPI fluorescence, whereas the U filter cubic unit with excitation filter (UG-1), a dichroic mirror (DM400) and a barrier filter (L420) was used for visualizing the DAPI fluorescence.

Image Analysis.

The images of biofilm sections captured at the same spot by the G or U filter were digitalized by a cooled color CCD camera (Optronics, Goleta, CA) and saved as 8-bit gray scale TIFF files. The DAPI and CTC-formazan fluorescence intensity was

determined by MARK image analysis software (Harkin and Shope 1993) as described in Chapter 2.

Results

There was a distinct pattern of CTC staining indicating respiratory activity within the biofilm sections observed. An intense layer of red CTC-formazan formed at the biofilm-bulk liquid interface (Panel A, Figure 4.1); less intense scattered CTC-formazan appeared thoroughout the rest of the biofilm section. DAPI staining of same spot of the biofilm section revealed a uniform blue intensity thorough the biofilm except the cells at the substratum appeared brighter (Panel B, Figure 4.1). When the biofilm section was observed with the B cubic filter to visualize CTC-formazan and DAPI simultaneously, CTC-formazan appeared orange and DAPI appeared green (Panel C, Figure 4.1). An intense orange layer was at the upper layer of the biofilm section, whereas the background was green DAPI staining. Image analysis was performed to quantify the zone of higher respiratory activity. A representative image analysis result is shown in Figure 4.2. Image analysis was performed on ten randomly chosen biofilm sections (Table 4.1). The intense CTC-formazan zone indicating higher respiratory activity was found to be 24.77 ± 3.06 μm from the surface, biofilm thickness was found to be 96.74 ± 11.25 μm from the substratum.

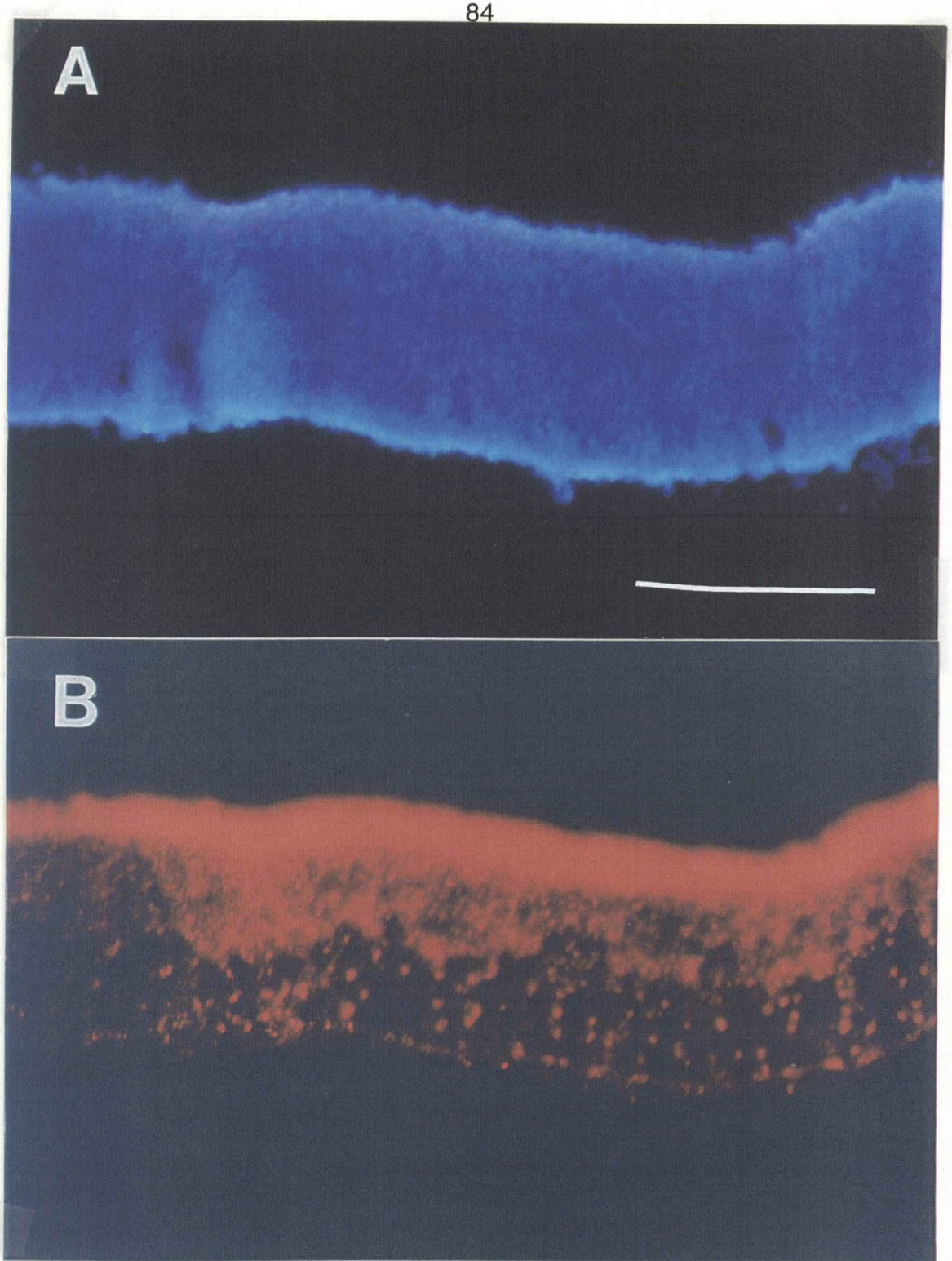


Figure 4.1. Photographs of a 4-day old *P.aeruginosa* biofilm stained with CTC/DAPI. (A) DAPI staining visualized with U cubic filter; (B) CTC-formazan formed across biofilm visualized with G cubic filter; (C) CTC/DAPI staining simultaneously visualized with B cubic filter. The substratum is at the bottom of the photographs. Bar = 100μm

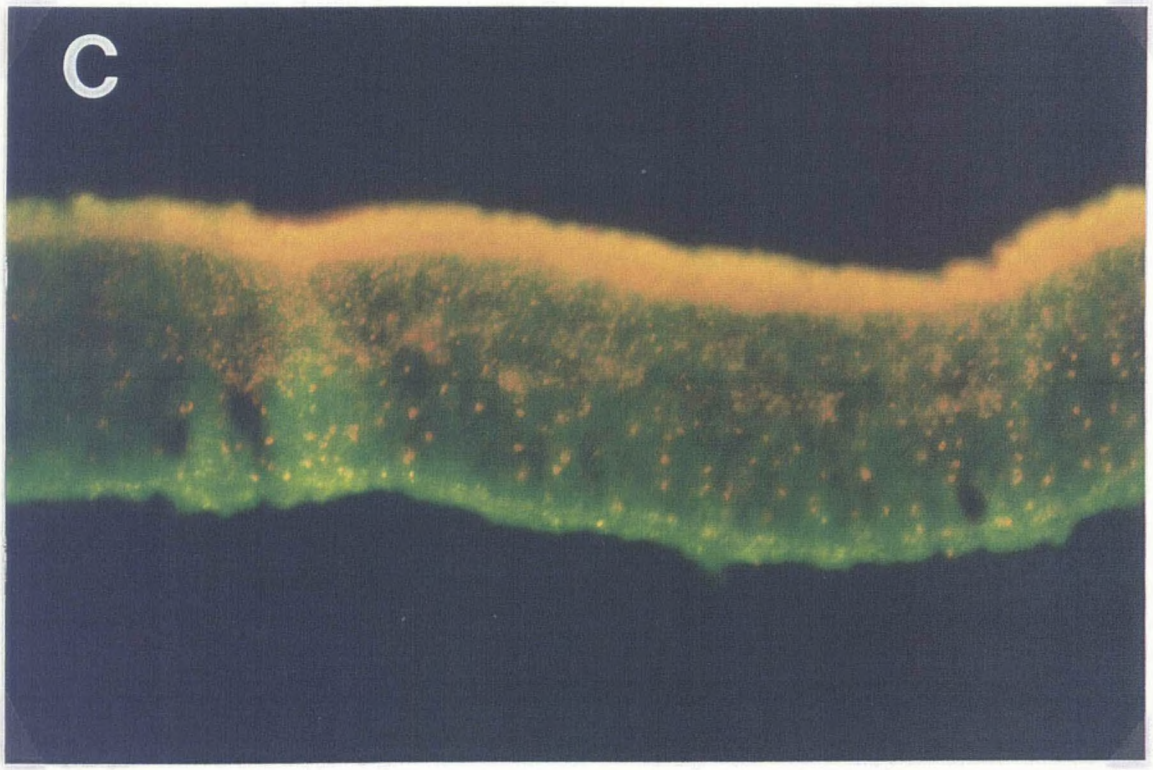


Figure 4.1. Photographs of a 4-day old *P.aeruginosa* biofilm stained with CTC/DAPI. (A) DAPI staining visualized with U cubic filter; (B) CTC-formazan formed across biofilm visualized with G cubic filter; (C) CTC/DAPI staining simultaneously visualized with B cubic filter. The substratum is at the bottom of the photographs. Bar = 100μm

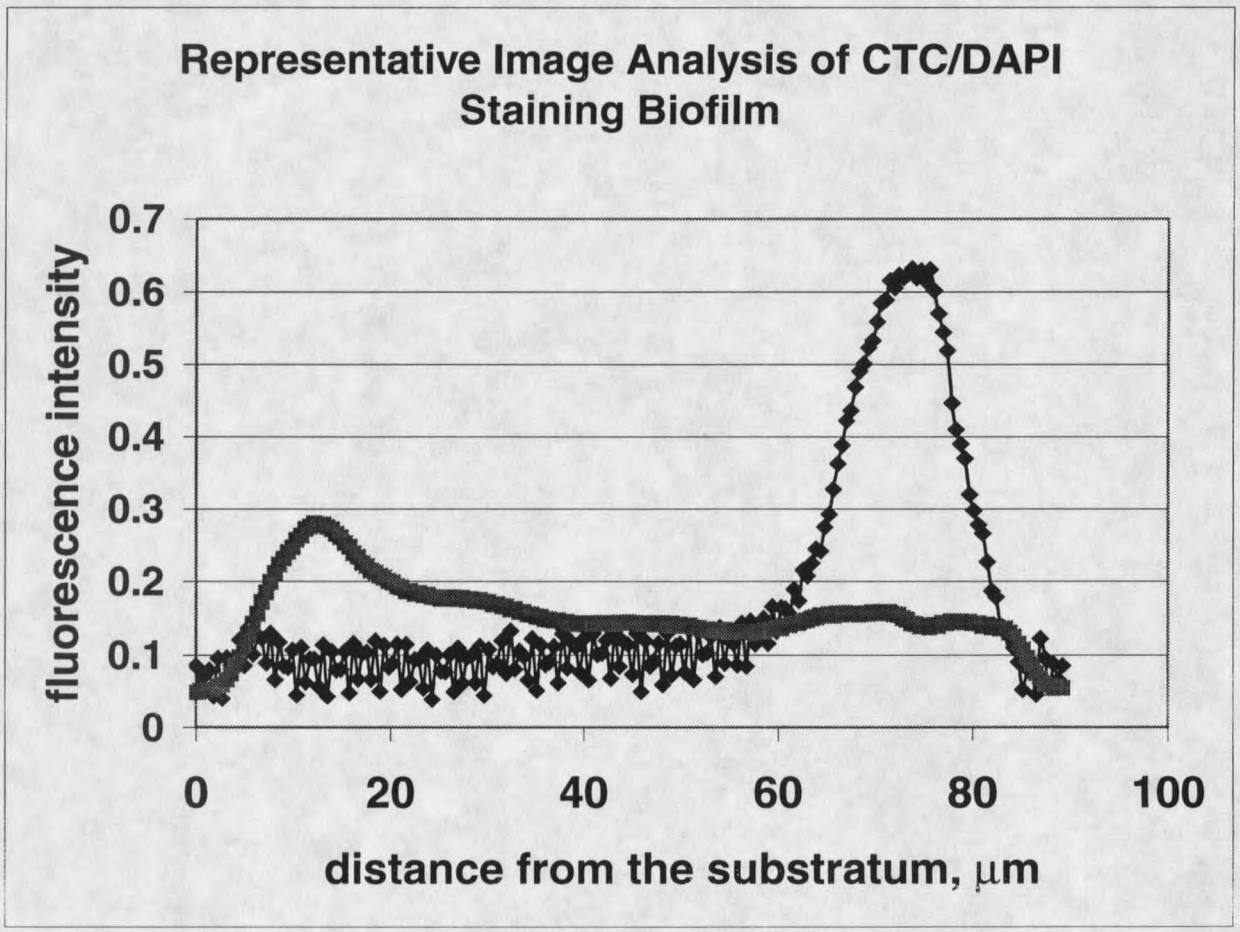


Figure 4.2. Image analysis result of CTC/DAPI staining of a 4-day old biofilm. (■) represents CTC staining and (♦) represents DAPI staining. Substratum is at "0" point.

Table 4.1 Summary of image analysis results of CTC staining

Sample No.	Overall Thickness (μm)	Active Zone Thickness by CTC Staining (μm)
1	84.2	23.7
2	98.8	26.6
3	109.3	23.2
4	98.4	21.5
5	105.2	28.3
6	90.5	23.6
7	72.9	21.4
8	96.8	19.2
9	92.7	24.8
10	112.6	26.4
AVR ± STDV	96.14 ± 11.25	23.87 ± 2.61

Discussion

A distinct non-uniform pattern of respiratory activity revealed by CTC staining in this thick *P.aeruginosa* biofilm.

One mol of oxygen consumption is equivalent to 2 mol of INT reduction, and since the tetrazolium reduction is accomplished during a measured reaction time, the results can be expressed as moles of CTC per time, electron quivalents per time or moles of oxygen per time. This means this kind of ETS measurement yields results dimensionally equivalent to respiration rates.

Smith (1995) systematically studied the sites of reduction for INT and CTC in *E.coli* ETS systems by examining the effects of various inhibitors of electron transport

and uncouplers of oxidative phosphorylation with well described sites of action. His result indicated CTC was reduced by NADH dehydrogenase. He also found that CTC reduction was highly coupled to oxygen consumption rate measured with oxygen electrode. In another investigation with marine *P.perfectomarinus*, Packard et al. (1983) showed that respiration and ETS activity are correlated at the r = 0.98 level for aerobically grown cultures. Working with sewage effluent, Jones and Simon (1979) found similar result: ETS activity was highly correlated with both short-term oxygen consumption and long-term BOD measurements.

As discussed above, CTC reduction is directly coupled to respiration rate. The oxygen penetration gradient of the *Pseudomonas aeruginosa* biofilm grown in drip-flow reactor was shown previously (see Chapter 2). Using CTC staining the biofilm was again found to be spatially heterogeneous in respiratory activity. The upper layer, quantified to be about 24.77 ± 3.06 μm by image analysis, of the biofilm has much higher and more intense respiratory activity. The thickness of intense respiratory activity is consistent with alkaline phosphase activity and FISH result discussed before (see Chapter 2 and 3). Although when Huang et al. (1995) employed CTC to stain biofilm before and after monochloramine disinfection to observe the loss of viability, he found uniform CTC staining pattern of biofilms before disinfection, the biofilm in his system was relatively thin (approximately 25-40 μm).

References Cited

Boucher, S. N., E. R. Slater, A. H. L. Chamberlain, and M. R. Adams. 1994. Production and viability of coccoid forms of *Campylobacter jejuni.. J. Appl. Bacteriol.* **77**: 303-307.

Harkin, G., and P. Shope. 1993. The Mark image analysis system. Technical report, Center for Biofilm Engineering, Montana State University, Bozeman, MT.

Harvey, R. W. and L. Y. Young. 1980. Enumeration of particle-bound and unattached respiring bacteria in the salt marsh environment. *Appl. Environ. Microbiol.* **40**: 156-160.

Huang, C.-T., F. P. Yu, G. A. McFeters and P. S. Stewart. 1995. Nonuniform spatial patterns of respiratory activity within biofilm during disinfection. *Appl. Environ. Microbiol.* **61**: 2252-2256.

Jones, J. G., and B. M. Simon. 1979. The measurement of electron transport system activity in freshwater benthic and planktonic samples. *J. Appl. Bacteriol.* **46**: 305-315.

Kaprelyant, A. S., and D. B. Kell. 1993. The use of 5-cyano-2, 3-ditolyl tetrazolium chloride and flow cytometry for the visualization of respiratory activity in individual cells of *Micrococcus luteus. J. Microbiol. Meth.* **17**: 115-122.

Kuhn, R., and D. Jerchel. 1941. *Ber. Dtsch. Chem. Ges.*, **74**: 941-949.

Lippold, H. J. 1982. Quantitative succinic dehydrogenase histochemistry. A comparison of different tetrazolium salts. *Histochem.* **76**: 381-405.

Nachlas, M. M., S. I. Margulies, and A. M. Seligman. 1960. Sites of electron transfer to tetrazolium salts in the succinoxidase system. *J. Bio. Chem.* **235**: 2739-2743.

Packard, T. T., P. C. Garfield, and R. Martinez. 1983. Respiration and respiratory enzyme activity in aerobic and anaerobic cultures of the marine denitrifying bacterium, *Pseudomonas perfectomarinus. Deep-Sea Res.*, **30**: 227-243.

Packard, T. T. 1985. Measurement of electron transport activity of microplankton. In Advances in aquatic microbiology. Ed. Jannasch, H. W. and P. J. Williams, P. J. Vol. 3, pp. 207-262. London, Academic Press Inc.

Pearse, A. G. E. 1972. Principles of oxidoreductase histochemistry, pp. 880-920. *In* Histochemistry, theoretical and applied. Pearse, A. G. E. (ed.) Vol. 2. Baltimore, U. S. A., Williams and Wilkins Co.

Quinn, J. P. 1984. The modification and evaluation of some cytochemical techniques for the enumeration of metabolically active heterotrophic bacteria in the aquatic environment. *J. Appl. Bacteriol.* **57**: 51-57.

Rodriguez, G. G., D. Phipps, K. Ishiguro, and H. F. Ridgway. 1992. Use of a fluorescent redox probe for direct visualization of actively respiring bacteria. *Appl. Environ. Microbiol.* **58**: 1801-1808

Seidler, E. 1991. The tetrazolium-formazan system: Design and histochemistry. Prog. *Histochem. Cytochem.* **24**: 1-86.

Smith, J. J. 1995. Survival, physiological response and recovery of enteric bacteria exposed to a polar marine environment. Ph.D. thesis, Montana State University, Bozeman, MT.

Stubberfield, L. C. F., and P. J. A. Shaw. 1990. A comparison of tetrazolium reduction and FDA hydrolysis with other measures of microbial activity. *J. Microbiol. Methods.* **12**: 151-162.

Swannell, R. P. J., and F. A. Williamson. 1988. An investigation of staining methods to determine total cell numbers and the number of respiring micro-organisms in samples obtained from the field and the laboratory. *FEMS Microbiol. Ecol.* **53**: 315-324.

Yu, F. P. 1994. Rapid *in situ* physiological assessment of disinfection in bacterial biofilms. Ph.D. thesis, Montana State University, Bozeman, MT

Yu, F. P., and G. A. McFeters. 1994. Rapid in situ assessment of physiological activities in bacterial biofilms using fluorescent probes. *J. Microbiol. Methods.* **20**: 1-10.

Zimmermann, R., R. Iturriaga, and J. Becker-Birck. 1978. Simultaneous determination of the total number of aquatic bacteria and the number thereof involved in respiration. *Appl. Environ. Microbiol.* **36**: 926-935.

CHAPTER 5

ANALYSIS OF GENE EXPRESSION AND PROTEIN LEVELS OF THE STATIONARY PHASE SIGMA FACTOR, RpoS, IN CONTINUOUSLY-FED *PSEUDOMONAS AERUGINOSA* BIOFILMS

Introduction

Biofilms are a collection of microorganisms and the extracellular polymers they secrete, attached to either an inert or living substratum (Costerton et al., 1995; Geesey, 1982). The industrial and medical significance of bacterial biofilms has gradually emerged since their first description (Zobell, 1936) and the first recognition of their ubiquity (Costerton et al., 1978). Biofilm-related problems cost US industry billions of dollars annually by corroding pipes, reducing heat transfer or hydraulic pressure in industrial water systems, plugging water injection jets and clogging filters. In addition, biofilms cause major medical problems through infecting host tissues, harboring bacteria that contaminate drinking water and causing rejection of medical implants (Costerton et al., 1999). Biofilm-related problems are exacerbated by biofilm recalcitrance to antimicrobial agents. It is well documented that microorganisms in biofilms are generally less susceptible to antimicrobial agents than their free-living counterparts (Brown and Gilbert, 1993; Costerton, 1984; LeChevallier et al., 1988).

Two hypothesized mechanisms of biofilm resistance to antimicrobial agents are poor penetration of the agent into the biofilm and physiological changes of microorganisms in the biofilm rendering at least some of the cells less susceptible. The binding, absorption or reaction of an antimicrobial agent within a biofilm can cause reduced penetration of antimicrobial agents (Stewart, 1996). This has been shown by experiments like the one performed by de Beer et al. (1994), in which the incomplete penetration of chlorine into biofilms during disinfection was measured with a chlorine microelectrode. Limited penetration of chlorine has subsequently been shown to be a result of neutralization of the chlorine in the biofilm matrix (Chen and Stewart, 1996; Stewart et al., 1998; Xu et al., 1996). Although reduced penetration of antimicrobial agents can explain some cases of biofilm resistance, transport limitation is not a universal explanation. Nichols (1989) mathematically modeled the penetration of two antibiotics into a *P. aeruginosa* biofilm. The amino-glycoside, tobramycin and a β-lactam, cefsulodin were considered. The authors concluded from their model that transport limitation of these two antibiotics was not the only factor contributing to the reduced susceptibility of the biofilms. Using a total internal reflection infrared spectroscopy approach, Vrany et al (1997) observed rapid transport (<20 minutes) of two fluoroquinolones, levofloxacin and ciprofloxacin, into a 15-25 μm thick *P. aeruginosa* biofilm. Differences in levels of recalcitrance observed for this system were suggested to be due to the particular physiological status which bacteria assume in the biofilm mode of growth. Therefore, physiological and genetic modifications of biofilms

resulting in biofilm resistance are receiving more and more attention (Anwar et al., 1992; Gilbert et al., 1990).

In thick biofilms, striking gradients in physiological status have been shown by researchers employing different physiological indicators (Huang et al., 1998; Kinniment et al., 1992; Wentland et al., 1996; Wimpenny et al., 1993). Slow growth and starvation were hypothesized to occur in the biofilm zones where nutrients had been depleted by cells that have easier access to nutrients (Anwar et al., 1992; Gilbert et al., 1990). The purpose of the work reported in this paper was to investigate the gene expression and protein levels of stationary phase sigma factor RpoS in a mature *P. aeruginosa* biofilm.

Materials & Methods

Bacterial Strains and Growth media.

The strains used in this study are listed in Table 5.1; *Pseudomonas aeruginosa* ERC1 was transformed with plasmids pMAL.S (*rpoS-lacZ*) and pMP220 (vector control) (Latifi et al., 1996) using electroporation. For cultures of plasmid-containing KX101 and KX101c, media were supplemented with tetracycline (100 µg/ml). To grow SS24, gentamycin (15 µg/ml) was added to the media. LB medium was prepared as described by Geenstein and Besmond (1995). Glucose minimal medium consisted of 13.632g of Na_2HPO_4, 6.568 g of KH_2PO_4, 0.36 g of NH_4Cl, 0.056g of $MgSO_4 \circ 7H_2O$ and 1ml of

trace element solution (Wentland, 1995) per liter. Glucose was added to give a final concentration of 1g/L after filter sterilization.

Table 5.1: Bacterial strains and plasmids

Strains or plamids	Description	Reference
P.aeruginosa		
ERC	Wild type	48
KX101	ERC carrying $_P$MAL.S	This study
KX101c	ERC carrying $_P$MP220	This study
PAO1	Wild type	20
SS24	Like PAO1 but *rpoSS101*:: *aacCI*	38
Plasmids		
$_P$MAL.S	1kb *Kpn*I-*Bam*HI fragment, containing the *rpoS* promoter, from $_P$DB18R in $_P$MP220	27
$_P$MP220	IncP T_C^R for *lacZ* transcriptional fusions	27

T_C^R, tetracycline resistant

Planktonic Culture Procedure.

All planktonic cultures were grown in Bellco 250 ml culture flasks by subculturing overnight cultures. Growth was monitored by reading the absorbance at 600nm with a spectrophotometer (Spectronic Instrument, Inc.). Except for analyzing *rpoS* expression in LB medium during the planktonic growth stages when KX101 and KX101c were grown at 37 °C, all other experiments were carried out at room temperature, i.e., 22.2 ± 3 °C. For western blots, PAO1 and SS24 were grown in LB media until stationary phase as positive and negative controls, respectively. ERC1 was grown in either 1/5-

strength LB, glucose minimal medium, or 1/10-strength glucose minimal medium. To study the effect of oxygen limitation on the accumulation of RpoS during planktonic growth, pure nitrogen was sparged into a mid-log phase ERC1 culture growing in LB medium at room temperature (22.2 ± 3 °C). ERC1 grown in LB medium in a culture flask that was left in the ambient air environment throughout growth was used as a control. Samples were taken from the experimental and control cultures every hour to monitor cell density. Adjusted volumes of samples (to give equivalent amounts of biomass) were then taken for western blots.

Biofilm Culture Procedure.

The drip-flow reactor (Xu et al., 1998) was used to grow biofilms. After inoculation with an overnight culture (3 x 10^{8} cells/ml) and static incubation for 24 hours, stainless steel coupons in the reactor chambers were continuously fed with medium that dripped onto the biofilm at a constant flow rate of 50ml/h. For western blots; ERC1 was grown in 1/5LB medium, glucose-minimal medium and 1/10 glucose-minimal medium.

β-Galactosidase Activity and Total Protein Assay.

In planktonic experiments, 2-ml aliquots were sampled, centrifuged and then resuspended in 1ml of TEP solution (10mM Tris-Cl [pH 8.0], 1mM EDTA [pH8.0], 1mM phenylmethylsulfonyl fluoride). In biofilm experiments, attached cells were scraped into

20ml of phosphate-buffered saline (PBS) with a rubber scraper. After being treated with a homogenizer (Tissuemizer, type SDT 1810; Tekmar Co., Cincinnati, Ohio) with an output speed of 13,500 rpm in an ice bath for 3 min, 2-ml aliquots were centrifuged and resuspended in 1ml of TEP solution. Bacterial suspensions in TEP solution were disrupted by ultrasonic treatment with an ultrasonic cell disrupter (TORBEO, 36810 series; Cole-Parmer, Vernon Hills, Ill.) and then centrifuged. The supernatant was used for enzyme and total protein assays. The β-galactosidase activity was calculated based on the conversion of the substrate *o*-nitrophenyl-β-D-galactopyranoside (ONPG, Sigma) to *o*-nitrophenol (Wood et al., 1991). Two hundred microliters of the supernatant were mixed with 2.5 ml reagent A (0.1M Na_2HPO_4 adjusted to pH 7.3 with 0.1M NaH_2PO_4), 100 µl reagent B (3.6M β-mercaptoethanol), 100 µl reagent C (30mM $MgCl_2$) and 200 µl reagent D (33.2 mM ONPG in reagent A). The well-vortexed mixture was then placed in a spectrophotometer (Spectronic Instrument, Inc.) with wavelength set at 410 nm; the spectrophotometer automatically calculated the change in absorbance over a two-minute interval. Total protein was determined with Sigma (St. Louis, MO) diagnostic kit No. 690, which was a modified micro-Lowry method. The specific activity of the β-galactosidase was expressed as ΔA_{410} ml mg^{-1} min^{-1}.

SDS-PAGE and Western Blot.

Planktonic cultures and biofilm PBS resuspensions were collected by centrifugation. Volumes were adjusted to give the same cell density equivalent to an

OD_{600} of 2.0. Pellets were then resuspended in 100 µl Nanopure water and 100 µl protein sample buffer (50mM Tris-HCl [pH6.8], 2% SDS, 1% 2-mercaptoethanol, 10% glycerol, 0.025% bromophenol blue) to achieve cell lysates. Equal amounts of pellets were also resuspended in 1ml TEP buffer for total protein assay. Ten microliter aliquots of cell lysates were seperated by sodium dodecyl sulfate-polyacrylamide gel electrophoresis (SDS-PAGE) with 3% stacking gels and 12% resolving gels. Proteins were transferred to nitrocellulose membranes overnight at 4 °C. Blots were blocked for 40 minutes at room temperature with 3% gelatin containing TTBS (Tris-buffered saline with 0.05% Tween-20), rinsed with TTBS and incubated with anti-RpoS IgG diluted 1:5000 in 1% gelatin in TTBS. Anti-RpoS antiserum was obtained by injecting purified RpoS into a rabbit and RpoS-specific IgG was purified from anti-RpoS antiserum using RpoS-immobilized AminoLink column (Pierce, Inc., Rockford, IL). The membranes were rinsed 8 times, 5 minutes each with TTBS, then incubated with peroxidase-conjugated anti-rabbit IgG (Bio-Rad Labs, Hercules, CA) diluted 1:6000 in 1% gelatin in TTBS. RpoS reacting bands were detected with a chemiluminescent method using homemade enhanced chemiluminescence substrate (Ausubel et al., 1995). The membranes were exposed to Fuji X-ray Film for 15 seconds. The films were then scanned with a Bio-Rad Fluor-S Multiimager (Bio-Rad Labs, Hercules, CA) according to manufacturer's directions.

Statistical Analysis.

Statistical analyses were performed to compare the specific β-galactosidase activity of biofilms with planktonic culture stationary phase average level using two-sample t-test within Minitab12 software (Minitab Inc.). The level of significance was set at $p<0.05$ for all comparisons.

Results

rpoS Expression in Planktonic Culture.

To investigate *rpoS* expression during the growth phases of a planktonic culture, we grew KX101 and KX101c in full strength LB broth and measured β-galactosidase specific activity from early log phase to stationary phase (Fig. 5.1). Bacteria entered stationary phase approximately 10 hours after subculturing. The background level of β-galactosidase activity expressed from the promoterless control plasmid KX101c was very low throughout the experiment. *rpoS* expression in KX101 began increasing 3 hours after subculturing (mid-log phase) and kept increasing through late log phase until it peaked at the transition from log to stationary phase. The peak level of *rpoS* expression in LB broth was six times the initial level. *rpoS* expression decreased in stationary phase to 60% of the peak level where it plateaued before largely disappearing at 32 hours.

rpoS Expression in Biofilms.

In 3-day biofilms grown in 1/5 LB, *rpoS* expression was found to be approximately 3 times higher than the average level, almost twice higher than the peak level measured in a stationary phase planktonic culture grown in 1/5 LB (Fig. 5.2). Three and half-day old biofilm had a slightly less *rpoS* expression than 3-day old biofilm, but still significantly higher than the average level of stationary-phase planktonic culture ($p = 0.0016$)(Fig. 5.2).

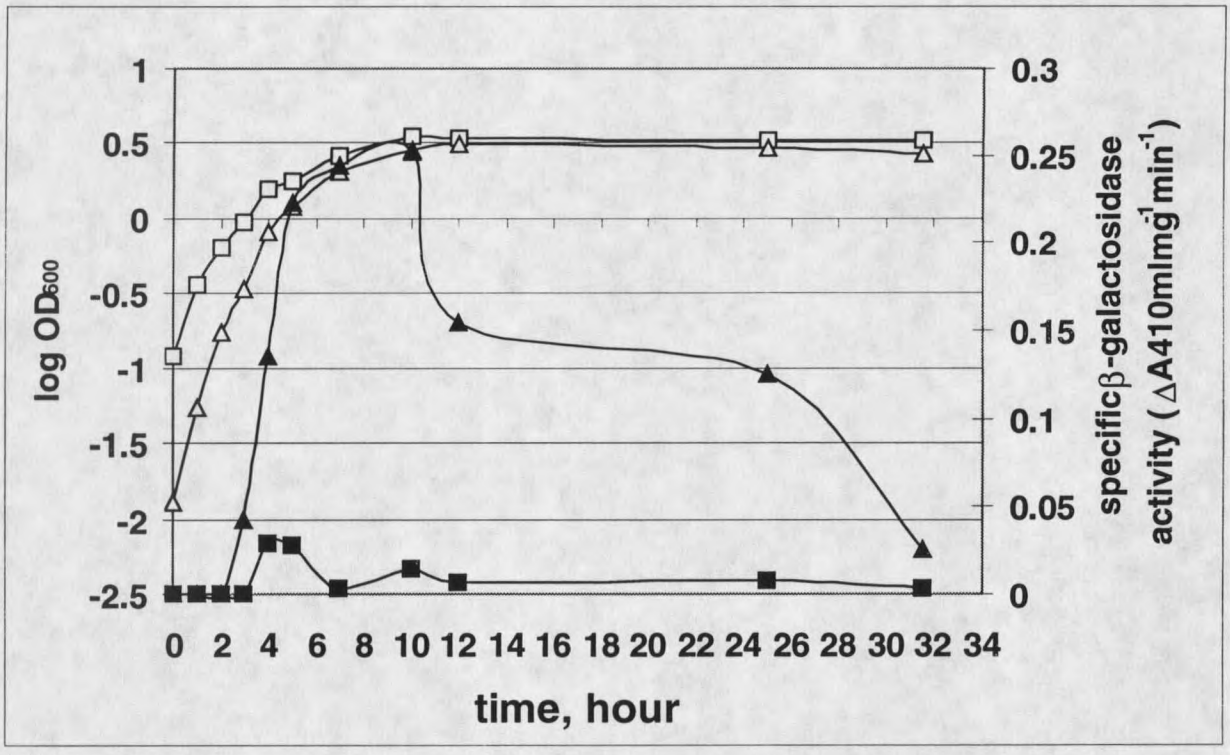


Figure 5.1. *rpoS* expression in planktonic KX101 and KX101c during growth in full strength LB. The cell density is expressed as $\log OD_{600}$, specific β-galactosidase activity is expressed as $\Delta A_{410} ml mg^{-1} min^{-1}$; (Δ) and (▲) represents $\log OD_{600}$ and specific β-galactosidase activity of KX101, respectively; (□) and (■) represents $\log OD_{600}$ and specific β-galactosidase activity of KX101c, respectively.

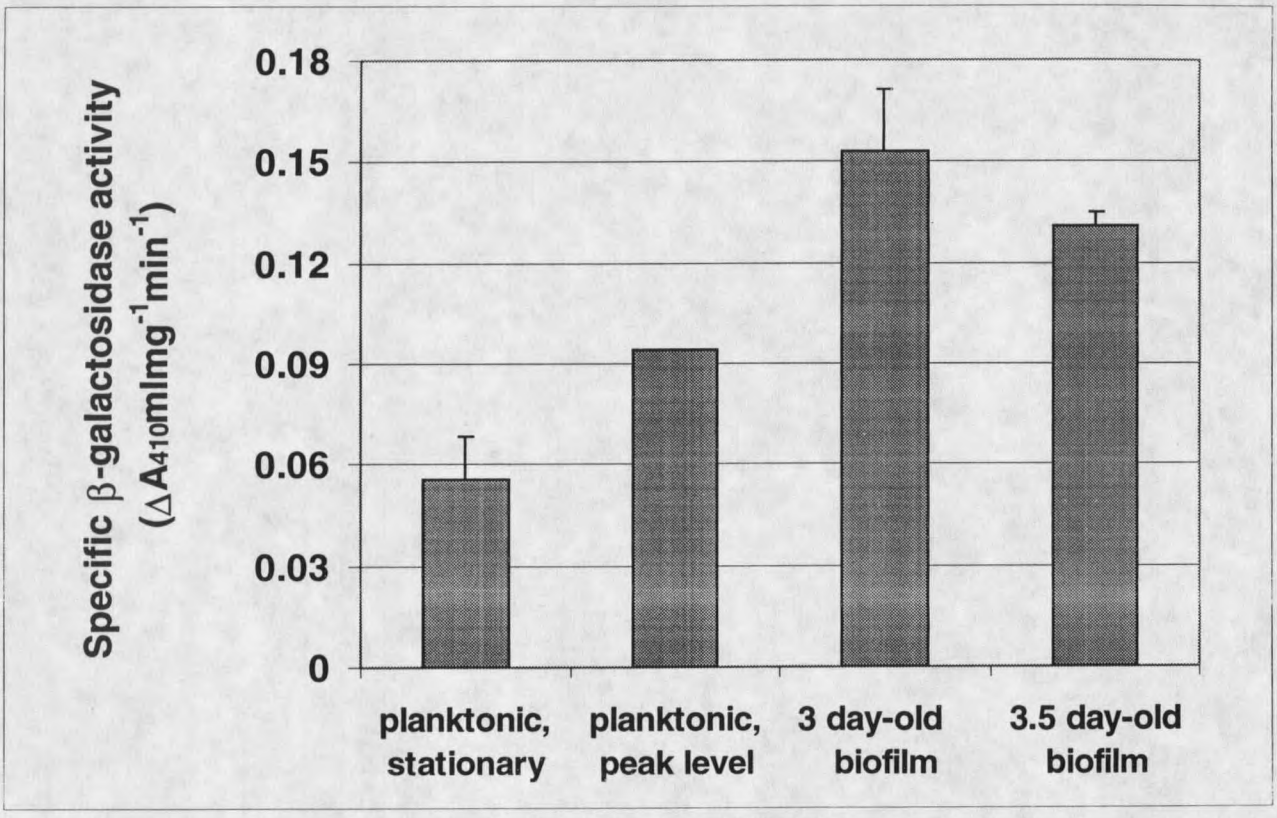


Figure 5.2. Comparison of *rpoS* expression in stationary-phase planktonic culture and biofilms grown in 1/5-strength LB medium. The first bar at the left is the average level of *rpoS* expression of planktonic culture within 20-hour stationary phase (excluding the lowest level of *rpoS* expression). (n=4 for planktonic, stationary; n=3 for 3 day and 3.5 day biofilms; bar = S.D.)

Presence and Levels of RpoS in Mature Biofilms Grown in Complex and Minimal Media.

To investigate the presence and relative levels of the RpoS protein in mature biofilms a polyclonal antibody reactive with *P. aeruginosa* RpoS was used to probe western blots of total cell proteins. A protein with molecular weight of 43~44 kD reactive with this antibody RpoS was present in *rpoS*$^+$ strains but not in *rpoS*$^-$ mutant derivatives (compare lanes 1 and 2 of Fig. 5.3). The relative levels of RpoS in biofilms and planktonic culture grown in 1/5LB are shown in Fig. 5.3. In planktonic culture, the level of RpoS increased from mid log phase up to the transition to stationary phase. No RpoS band was detected in stationary phase, but an antibody-reacting protein with lower molecular weight (39~40kD) was apparent (Lane 3 to 5, Fig. 5.3). In 2.5, 3, 3.5-day old biofilms, RpoS was consistently detected and the levels were slightly higher than that of a mid-log phase planktonic culture. The same protein with lower molecular weight which was found in stationary phase planktonic culture (Fig. 5.3, lane 5) was also detected in 3.5-day old biofilm (lane 8, Fig. 5.3). RpoS was not detected in a 3.5-day SS24 (*rpoS*$^-$) biofilm (lane 9, Fig. 5.3).

In a minimal medium-grown culture, a single protein band of molecular weight at 43~44 KD was found (Fig. 5.4). In planktonic culture, RpoS increased from mid-log phase to transition phase, then decreased at stationary phase (Fig. 5.4, lanes 2 to 4). Three-day old biofilm had a comparable amount of RpoS to stationary phase planktonic culture. Four and 4.5-day old biofilms had less RpoS.

In our previous work, one-tenth strength glucose minimal media was used to grow biofilms. When grown on 1/10 glucose minimal medium, RpoS was present at elevated levels in 3, 4, and 4.5-day biofilms (lane 4 to 6, Fig 5.5), exceeding those of a mid-log phase planktonic culture and similar to a stationary phase planktonic culture.

Effect of Oxygen Limitation on RpoS Levels During Planktonic Culture.

When nitrogen was sparged into a mid-log phase LB grown planktonic culture, growth was arrested immediately. In contrast a control culture kept growing until stationary phase (upper panel in Fig. 5.6). The result from western blot analysis showed that nitrogen treatment prevented RpoS accumulation (A in lower panel in Fig. 5.6), whereas in the control culture, levels of RpoS increased normally from mid-log phase to late log-phase and to stationary phase (B in lower panel in Fig. 5.6). The cross-reactive band with lower molecular weight was also found in the last two samples of the control culture (B in lower panel in Fig. 5.6).

Discussion

The *rpoS* gene is expressed and the RpoS protein is present in continuously-fed *Pseudomonas aeruginosa* biofilms. The level of *rpoS* gene expression in a 3-day old biofilm was found to be three-fold higher than the average level of a stationary phase planktonic culture grown in the same medium. Normalized RpoS levels in mature

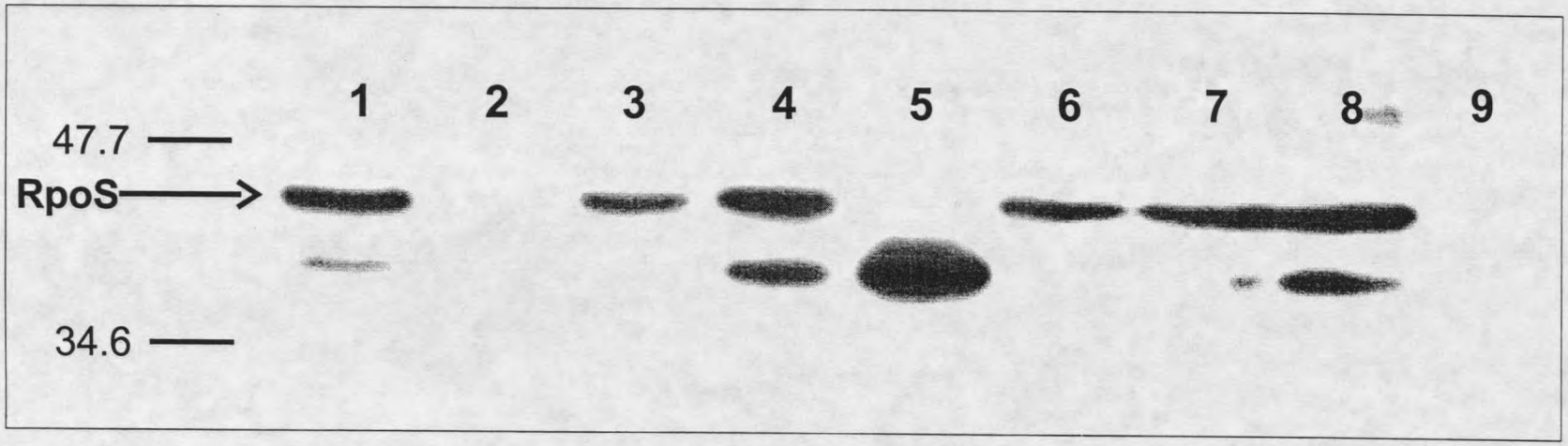


Figure 5.3. Western blot analysis of RpoS levels in 1/5LB grown planktonic and biofilm cultures. The arrrow indicates RpoS. The positions of molecular weight markers (in kilodaltons) are indicated on the left. Lane 1: stationary-phase PAO1; lane 2: stationary-phase SS24; lane 3-5: mid-log, transition, stationary phase ERC1; lane 6-8: 2.5, 3, 3.5-day ERC1 biofilm; lane 9: 3.5-day SS24 biofilm.

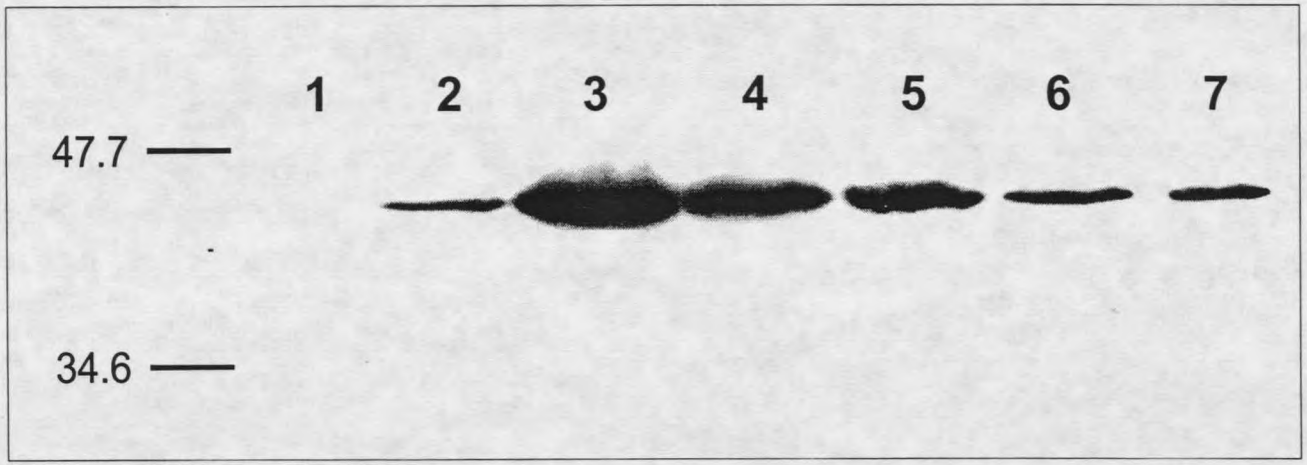


Figure 5.4. Western blot analysis of RpoS level in 1g/L glucose minimal media grown planktonic and biofilm cultures. The positions of molecular weight marker (in kilodalton) are indicated on the left. Lane 1: stationary-phase SS24; lane 2-4: mid-log, transition, stationary phase ERC1; lane 5-7: 3, 3.5, 4--day ERC1 biofilms. .

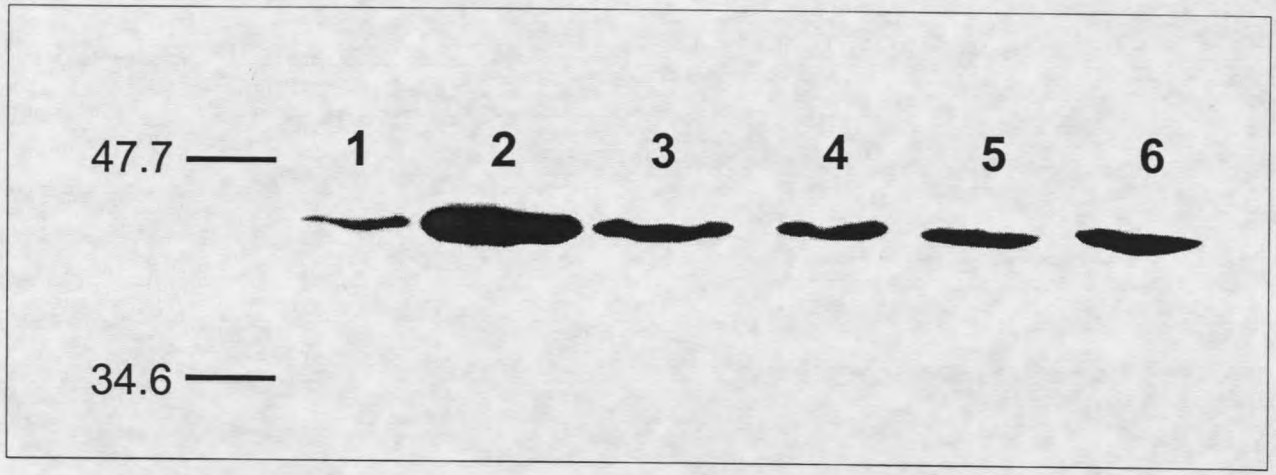


Figure 5.5. Western blot analysis of RpoS levels in 0.1g/L glucose minimal media grown biofilms. The positions of molecular weight marker (in kilodaltons) are indicated on the left. Lane 1-3: mid-log, transition, stationary-phase ERC1 grown in 1g/L glucose minimal medium; lane 4-6: 3, 4, 4.5-day ERC1 biofilms grown in 0.1g/L glucose minimal medium..

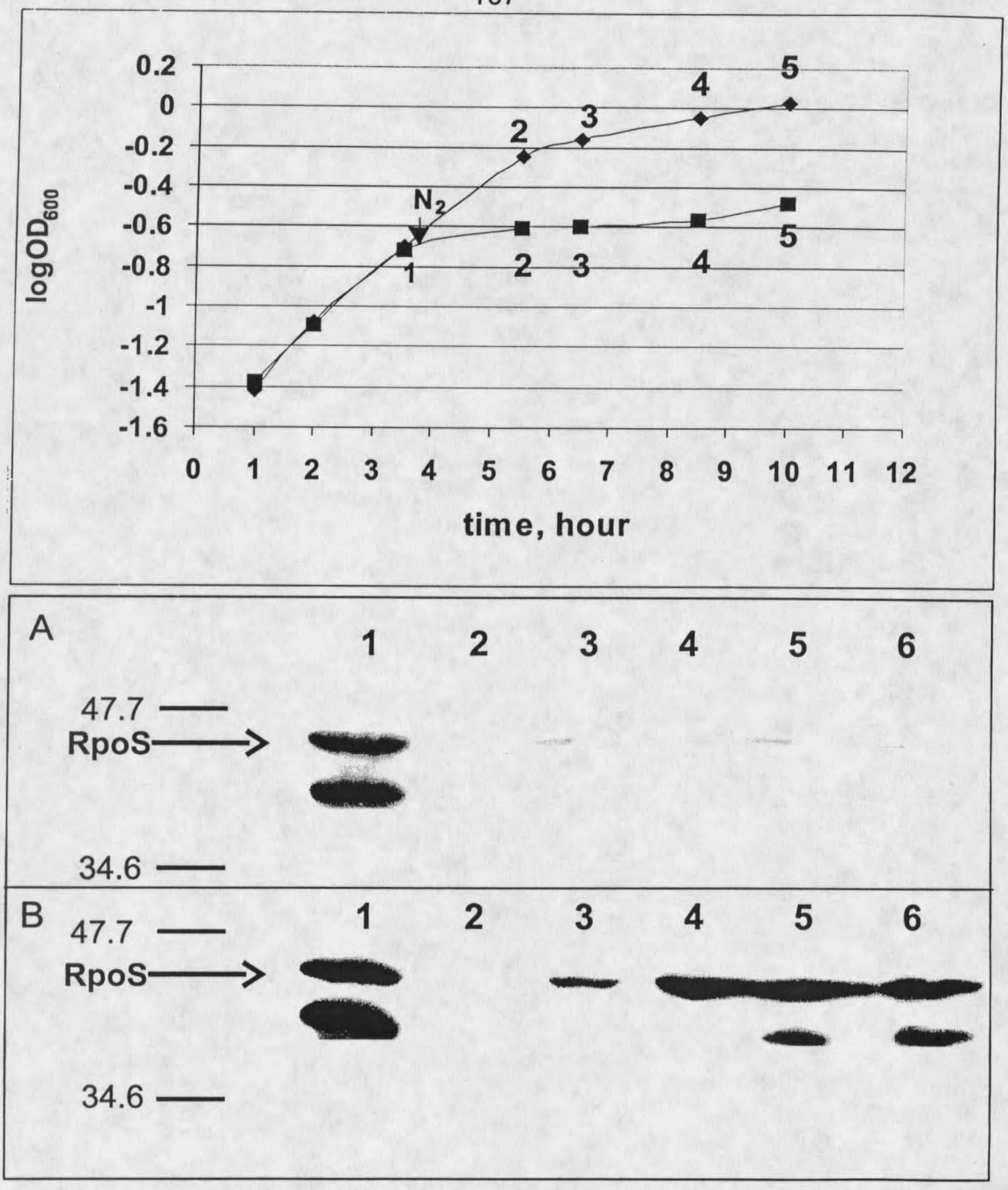


Figure 5.6. Effect of oxygen limitation on growth and RpoS accumulation. The upper panel shows the growth curve of LB medium under ambient air or nitrogen. The growth is expressed as $logOD_{600}$; (◆) represents the growth of ERC1 in LB under ambient air condition without interuption (control culture); (■) represents the growth of ERC1 in LB under ambient air condition for 3.5 hours before pure nitrogen was introduced and left inside the culture flask (experimental culture). The arrow indicates when pure nitrogen was introduced. The lower panel shows western blots of samples taken from the cultures above: A) lane 1: stationary-phase PAO1 as positive control, lane 2-6 corresponding to samples 1-5 from experimental culture; B) lane 1: stationary-phase PAO1 as positive control, lane 2-6 corresponding to samples 1-5 from control culture.

biofilms were always higher than those of mid-log phase planktonic culture grown in the same media. In stationary phase planktonic cultures grown in complex medium, a second protein band that cross-reacted with the RpoS antibody was evident in a western blot. This same band was never seen in mid-log phase planktonic cultures but was consistently detected in biofilms grown on the same medium. These results suggest that *P. aeruginosa* biofilms exhibited some stationary phase character, at least as indicated by gene expression and protein levels of the stationary phase sigma factor.

Working with the same *P. aeruginosa* model system, Xu et al (1998) demonstrated that these biofilms exhibit marked spatial heterogeneity with respect to protein synthesis and oxygen concentration. Only the upper 30 microns (out of the total biofilm thickness of approximately 120 microns) was capable of de novo protein synthesis. Oxygen penetration was limited to a zone of similar dimension, also located at the biofilm-bulk fluid interface. These observations lead us to hypothesize that the expression of *rpoS* is spatially heterogeneous within the biofilm. The biofilm is likely to harbor regions in which bacteria are rapidly growing, regions in which bacteria are in stationary phase, and a gradient of physiological states in between.

Both *rpoS* expression as measured by a reporter gene assay and RpoS levels revealed by a western blot peaked in early stationary phase or near the transition from late log phase to stationary phase. This same pattern was observed in complex and minimal media. Previous research on the regulation of RpoS levels in *E. coli* cells has suggested that regulation occurs at three levels (Lange and Hengge-Aronis, 1994;

Takayanagi, 1994): transcription, translation and protein stability. Lange and Hengge-Aronis (1994) reported that in complex medium *rpoS* transcription was stimulated during entry into stationary phase whereas in minimal medium it was not significantly induced. *rpoS* translation was stimulated during transition into stationary phase in both media. RpoS was also found to be a highly unstable protein in exponentially growing cells (with a half-life of 1.4 minutes), that was stabilized (with a half-life of 10.5 minutes) in stationary phase (Lange and Hengge-Aronis, 1994). Zgurskaya et al (1997) recently found the increase in RpoS level during stationary phase was solely due to a large increase in its stability. The data reported here for *P. aeruginosa* suggest that RpoS is regulated at the transciptional and post-transcriptional levels.

On western blot membranes, the putative RpoS band of *P. aeruginosa* was found at a position of 43-44 kD. *E.coli* RpoS migrates to 42 kD position in 12% SDS-PAGE gel in spite of its 38 kD molecular weight (Brown and Elliott, 1996; Nguyen et al., 1993) and *P.aeruginosa* RpoS migrates to a position of slightly higher molecular weight (Tanaka and Takahashi, 1994). In complex medium but not in minimal medium, we found an anti-RpoS cross reacting protein band with lower molecular weight (39-40 kD) than RpoS itself. This protein band was always detected beginning in late log phase in complex medium-grown cultures. It is hypothesized to be a degradation product of RpoS.

The environmental stimulus leading to the induction of *rpoS* in *P. aeruginosa* biofilms is not clear from our experiments. Unlike a traditional batch culture, there can

be no system-wide depletion of nutrients in the continuous flow reactor used to grow biofilms. The fluid residence time in this system is less than two minutes (data not shown), so fresh medium was always available. It is possible for gradients in nutrient concentration to be established within the biofilm. For example, incomplete penetration of oxygen into these same *P. aeruginosa* biofilms has been previously demonstrated using oxygen microelectrode technology (Xu et al., 1998). In *E. coli* anaerobiosis stimulated *rpoS* expression during exponential growth in LB medium (Mulvey et al., 1990). In the same medium, however, anaerobiosis alone did not induce RpoS in *P. aeruginosa* (Figure 5.6). We attribute this difference between *E. coli* and *P. aeruginosa* to the fact that *E. coli* performs fermentation under anaerobic conditions whereas *P. aeruginosa* does not perform fermentation under most anaerobic conditions (Brock et al., 1994). Neither does carbon limitation within the biofilm appear likely as a stimulus for *rpoS* induction. Similar levels of RpoS were seen in biofilms grown on 1/10 strength minimal medium (40 mg C l^{-1}), full strength minimal medium (400 mg C l^{-1}), and 1/5 strength LB (approximately 2000 mg C l^{-1}). We suggest that a quorum sensing regulatory mechanism is responsible for the elevated levels of RpoS in mature biofilms. Latifi et al. (1996) reported a hierarchical quorum-sensing cascade in *P. aeruginosa* involved in the elevated expression of *rpoS*. A density-dependent phenotype in *P. aeruginosa* biofilms was shown recently by Davies et al (1998). Given the extraordinarily high cell densities encountered in biofilms, which are of the order of

magnitude of 10^{11} cells/ml, it may be possible for signaling molecules to accumulate to levels sufficient for gene induction even in a continuous flow system.

Bacteria are subject to an array of stresses within their natural environment, and it has been demonstrated previously that stationary-phase (starving) cells survive these insults better than their exponential-phase counterparts (Jenkins et al., 1988). RpoS is thought to play a central role in development of starvation-mediated general resistance in *E. coli* (Lange and Hengge-Aronis, 1994; McCann et al., 1991). Our demonstration of RpoS in *P. aeruginosa* biofilms may aid in explaining why these biofilms are so resistant to antimicrobial agents and can establish persistent infections. It is interesting to note that *rpoS* was strongly expressed in the sputum samples from cystic fibrosis patients with chronic *P. aeruginosa* lung infection (Foley et al., 1999).

Acknowledgements

This work was supported through cooperative agreement EEC-8907039 between the National Science Foundation and Montana State University and by the industrial associates of the Center for Biofilm Engineering.

We thank Dr. Lazdunski (Laboratoire d'Ingéniérie et Dynamique des Systèmes membranaires, Centre National de la Recherche Scientifique, France) for sending us pMAL.S and pMP220.

References Cited

Altuvia, S., M. Almirón, G. Huisman, R. Kolter, and G. Storz. 1994. The *dps* promoter is activated by OxyR during growth and by IHF and σ^S in stationary phase. *Mol. Microbiol.* **13**: 265-272.

Anwar, H., J. L. Strap, and J. W. Costerton. 1992. Establishment of aging biofilms: possible mechanism of bacterial resistance to antimicrobial therapy. *Antimicrob. Agents Chemother.* **36**: 1347-1351.

Atlung, T., and L. Brøndsted. 1994. Role of the transcriptional activitor AppY in regulation of the *cyx appA* operon of *Escherichia coli* by anaerobiosis, phosphate starvation, and growth phase. *J. Bacteriol.* **176**: 5414-5422.

Ausubel, F. M., R. Brent, R. E. Kingston, D. D. Moore, J. G. Seidman, J. A. Smith, and K. Struhl. 1995. Current Protocols in Molecular Biology. 3rd edition. pp. A1-37. Greene Publishing Associates, Inc. and John Wiley & Sons, Inc.

Brock, T. D., M. T. Madigan, J. M. Martinko, and J. Parker. 1994. Biology of Microorganisms. Seventh Edition, pp.775-777

Brown, L., and T. Elliott. 1996. Efficient translation of the RpoS sigma factor in *Salmonella typhimurium* requires host factor I, an RNA-binding protein encoded by the *hfq* gene. *J. Bacteriol.* **178**: 3763-3770

Brown, M. R. W., and P. Gilbert. 1993. Sensitivity of biofilms to antimicrobial agents. *J. Appl. Bacteriol. Symp. Suppl.* **74**: 87S-97S.

Chen, X., and P. S. Stewart. 1996. Chlorine penetration into artificial biofilm is limited by a reaction-diffusion interaction. *Environ. Sci. Technol.* **30**: 2078-2083.

Costerton, J. W., G. G. Geesey, and K.-J. Cheng. 1978. How bacteria stick. *Sci. Am.* **238**: 86-95.

Costerton, J. W. 1984. The formation of biocide-resistant biofilms in industrial, natural and medical systems. *Dev. Ind. Microbiol.* **25**: 363-372.

Costerton, J. W., Z. Lewandoski, D. E. Caldwell, D. R. Korber, and H. M. Lappin-Scott. 1995. Microbial biofilms. *Ann. Rev. Microbiol.* **49**: 711-745.

Costerton, J. W., P. S. Stewart, and E. P. Greenberg. 1999. Bacterial biofilms: A common cause of persistent infections. *Science* **284**:1318-1322.

Davies, D. G., M. R. Parsek, J. Pearson, B. H. Iglewski, J. W. Costerton, and E. P. Greenberg. 1998. The involvement of cell-to-cell signals in the development of a bacterial biofilm. *Science* **280**: 295-298.

de Beer, D., R. Srinivasan, and P. S. Stewart. 1994. Direct measurement of chlorine penetration into biofilm during disinfection. *Appl. Env. Microbiol.* **60**: 4339-4344.

Foley, I., P. Marsh, E. M. H. Wellington, A. W. Smith, and M. R. W. Brown. 1999. General stress response master regulator *rpoS* is expressed in human infection: a possible role in chronicity. *J. Antimicrob. Chemother.* **43**: 164-165.

Geenstein, D., and C. Besmond. 1995. *Escherichia coli*, Plasmids and Bacteriophages. In Short Protocols in Molecular Biology (Ausubel, F., Brent, R., Kingston, R. E., Moore, D. D., Seidman, J. G., Smith, J. A. and Struhl, K. Eds, 3rd Ed), pp.1-3. John Wiley & Sons, Inc.

Geesey, G.G. 1982. Microbial exopolymers: ecological and economic considerations. *ASM News* **48**: 9-14.

Gilbert, P., P. J. Collier, and M. R. W. Brown. 1990. Influence of growth rate on susceptibility to antimicrobial agents: biofilms, cell cycle, dormancy, and stringent response. *Antimicrob. Agents Chemother.* **34**: 1865-1868.

Hengge-Aronis, R., W. Klein, R. Lange, M. Rimmele, and W. Boos. 1991. Trehalose synthesis genes are controlled by the putative sigma factor encoded by *rpoS* and are involved in stationary phase thermotolerance in *Escherichia coli*. *J. Bacteriol.* **173**: 7918-7924.

Hengge-Aronis, R. 1996. Regulation of gene expression during entry into stationary phase. In *Escherichia coli* and *Salmonella*: Cellular and Molecular Biology (Neidhardt, F. C., Curtiss III, R., Ingraham, J. K., Lin, E. C. C., Low, K. B., Magasanik, B. et al., Eds), pp. 1497-1512. ASM Press, Washington, D. C.

Holloway, B. W. 1955. Genetic recombination in *Pseudomonas aeruginosa*. *J. Gen. Microbiol.* **13**: 572-581.

Huang, C.-T., K. D. Xu, G. A. McFeters, and P. S. Stewart. 1998. Spatial patterns of alkaline phosphatase expression within bacterial colonies and biofilms in response to phosphate starvation. *Appl. Environ. Microbiol.* **64**: 1526-1531.

Jenkins, D. E., J. E. Schultz, and A. Matin. 1988. Starvation induced cross-protection against heat or H_2O_2 challenge in *Escherichia coli*. *J. Bacteriol.* **170**: 3910-3914.

Jung, J. U., C. Gutierrez, F. Matin, M. Ardourel, and M. Villarejo. 1990. Transcription of *osmB*, a gene encoding an *Escherichia coli* lipoprotein, is regulated by dual signals. *J. Biol. Chem.* **265**: 10574-10581.

Kaasen, I., P. Falkenberg, O. B. Styrvold, and A. R. Strøm. 1992. Molecular cloning and physical mapping of the *otsBA* genes, which encode the osmoregulatory trehalose pathway of *Escherichia coli*: evidence that transcription is activated by KatF (AppR). *J. Bacteriol.* **174**: 889-898.

Kinniment, S. L., and J. W. T. Wimpenny. 1992. Measurements of the distribution of adenylate concentrations and adenylate energy charge across *Pseudomonas aeruginosa* biofilms. *Appl. Environ. Microbiol.* **58**: 1629-1635.

Lange, R., and R. Hengge-Aronis. 1994. The cellular concentration of the σ^S subunit of RNA polymerase in *Escherichia coli* is controlled at the levels of transcription, translation, and protein stability. *Genes Dev.* **8**: 1600-1612

Latifi, A., M. Foglino, K. Tanaka, P. Williams, and A. Lazdunski. 1996. A hierarchical quorum-sensing cascade in *Pseudomonas aeruginosa* links the transcriptional activators LasR and RhlR (VsmR) to expression of the stationary-phase sigma factor RpoS. *Mol. Microbiol.* **21**: 1137-1146.

LeChevallier, M. W., C. D. Cawthon, and R. G. Lee. 1988. Inactivation of biofilm bacteria. *Appl. Env. Microbiol.* **54**: 2492-2499.

Loewen, P. C., and B. L. Triggs. 1984. Genetic mapping of *katF*, a locus that with *katE* affects the synthesis of a second catalase species in *Escherichia coli*. *J. Bacteriol.* **160**: 668-675.

McCann, M. P., J. P. Kidwell, and A. Matin. 1991. The putative σ factor *katF* has a central role in development of starvation-mediated general resistance in *Escherichia coli*. *J. Bacteriol.* **173**: 4188-94

Mulvey, M. R., J. Switala, A. Borys, and P. C. Loewen. 1990. Regulation of transcription of *katE* and *katF* in *Escherichia coli. J. Bacteriol.* **172**: 6713-20.

Nguyen, L. H., D. B. Jensen, N. E. Thompson, D. R. Gentry, and R. R. Burgess. 1993. *In vitro* functional characterization of overproduced *Escherichia coli katF/rpoS* gene product. *Biochem* **32**: 11112-11117.

Nichols, W. W. 1989. Susceptibility of biofilms to toxic compounds. In Structure and Function of Biofilms. Eds. W. G. Characklis and P. A. Wilderer. pp. 321-331. John Wiley & Sons, Inc..

Raina, S., D. Missiaka, L. Baird, S. Kumar, and C. Georgopoulos. 1993. Identification and transcriptional analysis of the *Escherichia coli htrE* operon which is homologous to *pap* and related pilin operons. *J. Bacteriol.* **175**: 5009-5021.

Sak, B. D., A. Eisenstark, and D. Touati. 1989. Exonuclease III and the catalase hydroperoxide in *Escherichia coli* are both regulated by the *katF* product. *Proc. Natl. Acad. Sci. USA.* **86**: 3271-3275.

Stewart, P. S. 1996. Theoretical aspects of antibiotic diffusion into microbial biofilms. *Antimicrob. Agents Chemother.* **40**: 2517-2522.

Stewart, P. S., L. Grab, and J. A. Diemer. 1998. Analysis of biocide transport limitation in an artificial biofilm system. *J. Appl. Bacteriol.* **85**: 495-500.

Suh, S.-J.; L. Silo-Suh, D. E.Woods, D. J. Hassett, S. E. H. West, D. E. Ohman. 1998. Effect of *rpoS* mutation on the stress response and expression of virulence factors in *Pseudomonas aeruginosa. Mol. Microbiol.* **In Press**.

Takayanagi, Y., K. Tanaka, and H. Takahashi. 1994. Structure of the 5' upstream region and the regulation of the *rpoS* gene of *Escherichia coli. Mol. Gen. Genet.* **243**: 525-531.

Tanaka, K., and H. Takahashi. 1994. Cloning, analysis and expression of a *rpoS* homologue gene from *Pseudomonas aeruginosa* PAO1. *Gene* **150**: 81-85.

Vrany, J. D., P. S. Stewart, and P. A. Suci. 1997. Comparison of recalcitrance to ciprofloxacin and levofloxacin exhibited by Pseudomonas biofilms displaying rapid-transport characteristics. *Antimicro. Agents. Chemother.* **41**: 1352-1358.

Weichart, D., R. Lange, N. Henneberg, and R. Hengge-Aronis. 1993. Identification and characterization of stationary phase-inducible genes in *Escherichia coli. Mol. Microbiol.* **10**: 407-420.

Wentland, E. J. 1995. Visualization and quantification of spatial variations in growth rate within *Klebsiella pneumoniae.* Master thesis. Montana State University-Bozeman, MT

Wentland, E. J., P. S. Stewart, C.-T. Huang, and G. A. McFeters. 1996. Spatial variations in growth rate within *Klebsiella pneumoniae* colonies and biofilm. *Biotechnol. Prog.* **12**: 316 –321

Wimpenny, J. W. T., S. L. Kinniment, and M. A. Scourfield. 1993. The physiology and Biochemistry of biofilm. *Society for Applied Bacteriology Technical Series,* **30,** pp. 51-95.

Wood, T. K., and S. W. Peretti. 1991. Effect of chemically-induced, cloned-gene expression on protein synthesis in *E.coli. Biotechnol. Bioeng.* **38**: 397-412.

Xu, X., P. S. Stewart, and X. Chen. 1996. Transport limitation of chlorine limitation of *Pseudomonas aeruginosa* entrapped in alginate beads. *Biotechnol. Bioeng.* **49**: 93-100.

Xu, K. D., P. S. Stewart, F. Xia, C.-T. Huang, G. A. McFeters. 1998. Spatial physiological heterogeneity in *Pseudomonas aeruginosa* biofilm is determined by oxygen availability. *Appl.Env. Microbiol.* **64**: 4035-4039

Yim, H. H., R. L. Brems, and M. Villarejo. 1994. Molecular characterization of the promoter of *osmY*, an *rpoS* dependent gene. *J. Bacteriol.* **176**: 100-107.

Zgurskaya, H. I., M. Keyhan, and A. Matin. 1997. The σ^S level in starving *Escherichia coli* cells increased solely as a result of its increased stability, despite decreased synthesis. *Mol. Microbiol.* **24**: 643-651.

Zobell, C. E., Anderson, D. Q. 1936. Observations on the multiplication of bacteria in different volumes of stored seawater and the influence of oxygen tension and solid surfaces. *Bio. Bull. Woods Hole* **71**: 324-42.

CHAPTER 6

SUMMARY AND DISCUSSION

Biofilm has recently become a hot area in microbiological and biotechnology research (Costerton et al., 1999). This interest is largely due to the biofilm-related problems in industry and health care including biofouling, microbial corrosion, and chronic infections on medical implants. Biofilm related problems are exacerbated by biofilm resistance to antimicrobial agents. Although biofilm resistance could be explained partially by transport limitation of antimicrobial agents, physiological and genetic mechanisms remain unclear. In a thick aging biofilm, nutrient limitation was hypothesized to be involved in biofilm resistance.

The main goal of this study was to achieve a comprehensive understanding of spatial physiological heterogeneity and nutrient limitation in thick biofilms, thereby providing insight into possible physiological mechanisms of the recalcitrance of thick biofilms. Two specific objectives were 1) to demonstrate spatial physiological heterogeneity with different fluorescent probes including alkaline phosphatase activity, CTC, fluorescent-in-situ-hybridization and acridine orange; determine if this spatial physiological heterogeneity is caused by oxygen gradient in the biofilm (Chapter 2, 3, 4) and 2) to investigate the gene expression and protein levels of starvation sigma factor

RpoS in the biofilms (Chapter 5). These two objectives were met and are summarized below.

Pseudomonas aeruginosa biofilms were grown in the drip-flow reactor as a model laboratory biofilm for physiological studies. This drip-flow reactor allowed us to achieve a 100-150 μm thick biofilm in four days. The biofilm was grown for four days before being subjected to phosphate starvation. The biofilm was then stained with an alkaline phosphatase fluorogenic substrate. This substrate stained all and alkaline phosphatase-positive cells in the biofilm simultaneously. By coupling with cryoembedding and cryosectioning, the spatial pattern of alkaline phosphatase activity was demonstrated. In the four-day old biofilm, the alkaline phosphatase zone was limited to the upper layer of the biofilm. This zone did not expand significantly for 24 and 36-hour starvation over that from 12 hours of starvation. This excluded the possibility that the lower part of the biofilm did not experience phosphate starvation. By image analysis, the zone of active alkaline phosphatase synthesis was quantified to be 30 μm in a 117 μm-thick biofilm. Limitation of induced enzyme activity to this zone was hypothesized to be due to a nutrient limitation in deeper layers of the biofilm. In this system, oxygen was calculated to be the limiting nutrient. By switching the ambient air to pure nitrogen, we found the alkaline phosphatase synthesis was blocked completely. When pure oxygen was provided to the biofilm, the zone of enzyme synthesis was expanded 1.5 fold. We think the pattern of active enzyme synthesis was effected by oxygen availability (Chapter 2), because oxygen is often limiting in aerobic biofilms due

to its rapid consumption and *P.aeruginosa* is an obligate aerobe under the experimental conditions (no nitrate or arginine available). Bacterial alkaline phosphatase is a common enzyme that exists in a variety of bacteria (Reid and Wilson, 1971) including aerobes and anaerobes. When Bourdineaud et al. (1993) studied arginine metabolism of *P. aeruginosa* PAO1, they made a protein fusion of alkaline phosphatase to the arginine deiminase (key enzyme involved in arginine metabolism of *P.aeruginosa*) and found alkaline phosphatase activity. Since they performed the experiment under anaerobic condition for the study of arginine metabolism, this provided evidence of active alkaline phosphatase activity under anaerobic condition. The pattern of alkaline phosphatase synthesis provided the pattern of de nove protein synthesis in the mature *P.aeruginosa* biofilm.

When biofilm sections of the same age were stained with acridine orange, the surface layer was stained orange, whereas the inner part of the biofilm was stained green. We did not correlate the orange/green intensity ratio with growth rate before staining biofilm as Wentland has done (Wentland, 1995). Nevertheless, the AO staining pattern suggests, based on other researcher's studies, that the surface layer may be faster growing and the inner part of the biofilm cells may be slower growing. We also found the substratum layer of the biofilm was stained orange. This could be due to high activity stimulated by surface or it could be an artifact. The bilayer phenomenon was also observed in some sections of APase staining and CTC staining samples (data not shown). Image analysis was not carried out on AO-stained photographs because we

could not separate green and orange color by different filters. By measuring the orange zone manually, the faster growing zone was found to be 20 ± 2 μm in a 111 ± 17 μm thick biofilm. FISH results were consistent with the AO staining result. Higher fluoresent intensity was located at the surface layer of the biofilm, which was quantified to be 21 ± 2 μm by image analysis. The pattern of AO and FISH indicated the pattern of RNA content in the mature *P.aeruginosa* biofilm (Chapter 3).

The biofilm was stained with CTC for respiratory activity staining. CTC staining revealed a distinct pattern, in which the greater fluorescent intensity occurred in the upper layer of the biofilm. Image analysis showed the dimension zone (25 ± 3 μm in 97 ± 11 μm) of actively respiring cells was consistent with the APase result (Chapter 4).

The results of Chapter 2, 3 & 4 were summarized as follow (Table 6.1).

Table 6.1 Active zones measured by different staining methods

	Apase	AO	FISH	CTC
Active Zone (Mean ± Standard Error)	30 ± 4	20 ± 2	21 ± 2	24 ± 3
Overall Thickness (Mean ± Standard Error)	117 ± 12	112 ± 17	108 ± 15	96 ± 11

The overall physiological patterns demonstrated using these different staining methods were consistent. However, the active zones that APase staining and CTC

demonstrated were more intense, while the fluorescent intensity of the active zone FISH revealed was less intense. The active zones measured by different methods were statistically significantly different ($p<0.05$) from each other except the ones measured by AO and FISH ($p=0.36$). This may be due to differing thresholds of nutrient limitation that each parameter responds to. Upon oxygen limitation active protein synthesis and respiratory activity are likely the first activities inhibited, while the change of RNA content could take longer. Lisle (1998) found that the 16S rRNA-based cell counts were insignificantly less than or equal to the total cells counts when *Escherichia coli* O157:H7 was starved for carbon for 14 days.

The results of Chapter 2, 3 & 4 and reports of density-dependent gene regulation (Davies et al., 1998) point to the likely upregulation of the starvation sigma factor, rpoS. The gene expression and protein level of RpoS were investigated and compared with planktonic culture (Chapter 5). The level of *rpoS* gene expression, measured with a *rpoS–lacZ* transcriptional fusion in a 3-day old biofilm was found to be three-fold higher than the average level of a stationary phase planktonic culture grown in the same medium. RpoS levels in mature biofilms, studied with western blot, were always higher than those of mid-log phase planktonic cultures grown in the same media. In stationary phase planktonic cultures grown in complex medium, a second protein band that cross-reacted with the antiRpoS antibody was evident in a western blot. This same band was never seen in mid-log phase planktonic cultures but was consistently detected in biofilms grown in the same medium. When we sparged nitrogen into mid-log phase

planktonic cultures, we found oxygen limitation did not induce RpoS in planktonic culture. These results suggested that *P.aeruginosa* biofilms exhibited some stationary phase character. The high level of RpoS existing in the biofilm may be due to quorum-sensing, since oxygen limitation alone was insufficient to lead to high level of RpoS.

This study aids in a comprehensive understanding of the physiological status of a thick biofilm. My results are consistent with Kinniment and Wimpenny's findings (Kinniment and Wimpenny 1992). They found the distribution of adenylate concentration and adenylate energy charge across the *Pseudomonas aeruginosa* biofilm was heterogeneous, with total adenylates peaking just below the interface. Examination by TEM of the same *P.aeruginosa* biofilm revealed that healthy cells were present in the upper two-thirds of the biofilm (approximately 100 μm thick). Below this the majority of the cells appeared to be lysed. There was a sharp division between the two zones.

Evidence of spatial physiological heterogeneity provides a powerful explanation for biofilm resistance to antimicrobial agents. The lower part of the biofilm, where cells are starved and slower growing is likely the part rendering biofilm resistance. Further experiments should investigate if there is difference in terms of antimicrobial susceptibility between the faster and slower growing cells in the same biofilm.

The study of stationary phase sigma factor, RpoS provided some insight into molecular mechanism of biofilm resistance. Recently there were some studies regarding the genetic mechanisms of biofilm formation (O'Toole and Kolter, 1998; Pratt and Kolter, 1998). However, there are not findings revealing the genetic mechanisms of

biofilm resistance. Cochran found AlgT and RpoS provided monolayer biofilms protection from hydrogen peroxide but not monochloramine (Cochran 1998). It is interesting to note that *rpoS* was strongly expressed in the sputum samples from cystic fibrosis patients with chronic *P.aeruginosa* lung infection (Foley et al. 1999). Future experiments should investigate where RpoS is found in the thick biofilm and the role of RpoS in protecting thick biofilms.

References Cited

Bourdineaud, J.-P., D. Heierli, M. Gamper, H. J. C. Verhoogt, A. J. M. Driessen, W. N. Konings, C. Lazdunski, and D. Haas. 1993. Characterization of the *arcD* arginine:ornithine exchanger of *Pseudomonas aeruginosa. J. Biol. Chem.* **268**: 5417-5424.

Cochran, W. L. 1998. Physiological basis for biofilm resistance to antimicrobial agents. PhD thesis. Montana State University-Bozeman, Montana.

Costerton, J. W., P. S. Stewart, and E. P. Greenberg. 1999. Bacterial biofilms: a common cause of persistent infections. *Science* **284**: 1318-1322.

Davies, D. G., M. R. Parsek, J. Pearson, B. H. Iglewski, J. W. Costerton, and E. P. Greenberg. 1998. The involvement of cell-to-cell signals in the development of a bacterial biofilm. *Science* **280**: 295-298.

Foley, I., P. Marsh, E. M. H. Wellington, A. W. Smith, and M. R. W. Brown. 1999. General stress response master regulator *rpoS* is expressed in human infection: a possible role in chronicity. *J. Antimicrob. Chemother.* **43**: 164-165.

Kinniment, S. L., and J. W. T. Wimpenny. 1992. Measurements of the distribution of adenylate concentrations and adenylate energy charge across *Pseudomonas aeruginosa* biofilms. *Appl. Environ. Microbiol.* **58**: 1629-1635.

Lisle, J. T., S. C. Broadway, A. M. Prescott, B. H. Pyle, C. Fricker, and G. A. McFeters. 1998. Effects of starvation on physiological activity and chlorine disinfection resistance in *Escherichia coli* O157:H7. *Appl. Environ. Microbiol.* **64**: 4658-4662.

O'Toole, G. A., and R. Kolter. 1998. Flagellar and twitching motility are necessary for *Pseudomonas aeruginosa* biofilm development. *Mol. Microbiol.* **30**: 295-304

Pratt, L. A., and R. Kolter. 1998. Genetic analysis of *Escherichia coli* biofilm formation: role of flagella, motility, chemotaxis and type I pili. *Mol. Microbiol.* **30**: 285-293.

Reid, T. W., and I. B. Wilson. 1971. *E. coli* alkaline phosphatase. In The Enzymes. Ed. P. D. Boyer. Vol. IV. p. 373-416

Wentland, E. J. 1995. Visualization and quantification of spatial variations in growth rate within Klebsiella pneumoniae. Master thesis, Montana State University-Bozeman, MT.

APPENDIX

Repeatibility of Biofilm Thickness among Different Chambers in Drip-flow Reactor

The thickness of biofilms grown in 4 different chambers was measured to examine the repeatability among different chambers. The biofilms from each chamber were cryosectioned and stained with DAPI. The sections were viewed under an Olympus microscope with U filter cubic unit containing an excitation filter (334-365nm), a dichroic mirror (DM-400), and a barrier filter (L-420). Thirty images from each biofilm section was taken with Image Pro 3.0 software and saved as grayscale TIFF files. An image of a ruler was first taken to calibrate how many pixels were equal to one micrometer. The images were then analyzed with MARK program (Murga et al., 1995) to obtain thickness measurement. The thickness variability is shown in Table 2.1.

Table 7.1. Variability of biofilm thickness among different chambers of a drip-flow reactor

	Thickness (μm)
Chamber 1	128. 6 ± 35.5
Chamber 2	116.3 ± 31.2
Chamber 3	105.0 ± 31.5
Chamber 4	119.2 ± 32.0

Biofilm Accumulation Curve

To observe the growth of biofilm on the coupon, a stainless steel coupon was removed from one reactor chamber each day until day 4 and the biofilm was scraped into 20 ml PBS buffer with a rubber scraper. The cells were homogenized, diluted and plated on R2A. The log(CFU)/cm^2 was calculated and presented against day to generate a biofilm accumulation curve.

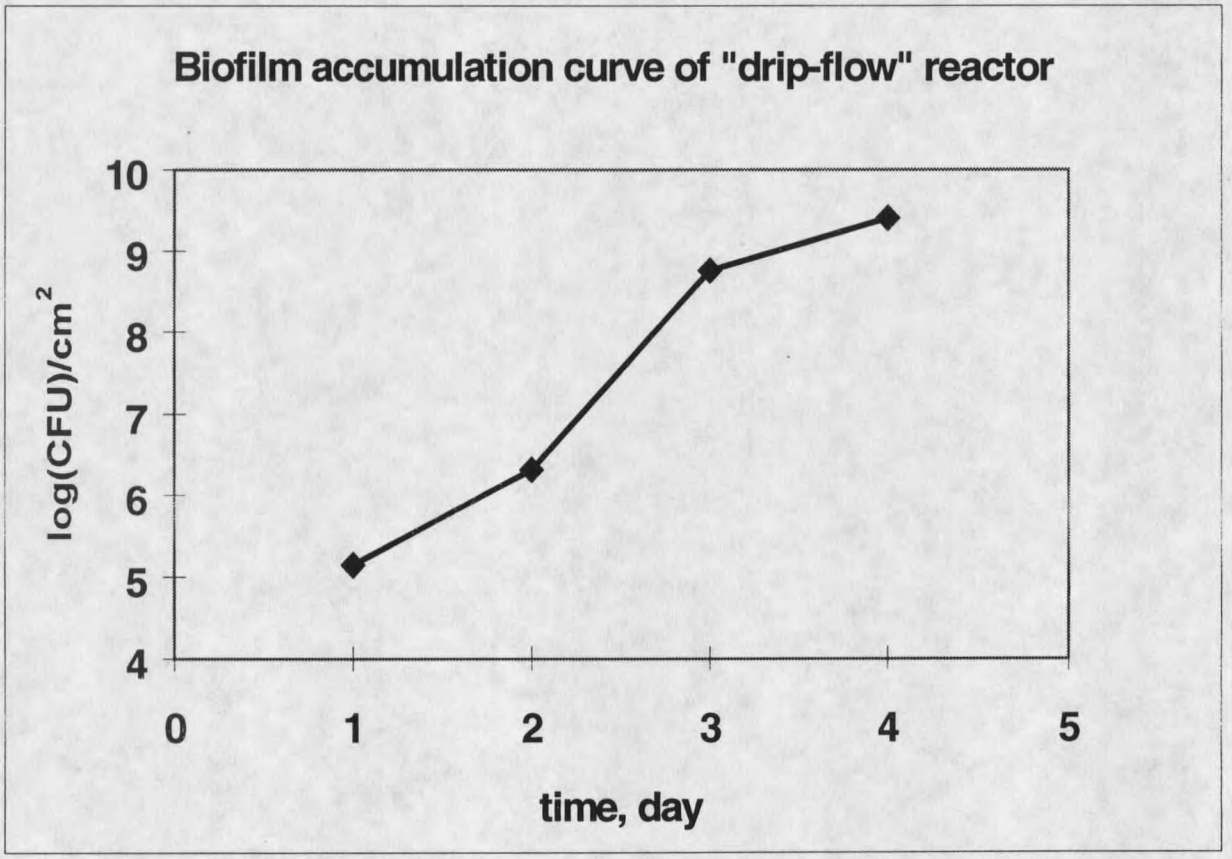


Figure 7.1. Accumulation curve of biofilms grown in the drip-flow reactor.

Quantification of Western Blot Bands

The results of western blot images were analyzed with ImageQuan 3.0 Software to get a quantitative value for the band intensity. However, since western blot is a semi-quantitative assay and we did not have purified RpoS to make a standard curve, the results were not presented in the main body of the thesis. The data is presented in the appendix as following:

Table 7.2. Raw data of the quantitative result of the two bands in Figure 5.3

OBJECT NAME	VOLUME	**PERCENT**	BACK-GROUND	# PTS IN OBJECT	AVER	PEAK VALUE AT X-Y	PEAK X-POS	PEAK Y-POS	SUM ABOVE BKGND	PTS ABOVE	PTS EQUAL	PTS BELOW
~0066	-333777	**29.602**	246	7227	199.8	255	476	52	50967	5663	0	1564
~0067	0	**0**	255	7227	255	255	178	48	0	0	7227	0
~0068	-70635	**6.264**	255	7227	245.2	255	276	46	0	0	6950	277
~0069	-248787	**22.064**	251	7227	216.6	255	380	52	24552	6138	0	1089
~0070	-99873	**8.857**	254	7227	240.2	255	574	56	6807	6807	0	420
~0071	-116778	**10.357**	249	7227	232.8	255	672	56	39594	6599	0	628
~0072	-257706	**22.855**	248	7227	212.3	255	770	56	42126	6018	0	1209
~0073	0	**0**	255	7227	255	255	870	56	0	0	7227	0

Table 7.3. Raw data of the quantitative result of the first band in Figure 5.3

OBJECT NAME	VOLUME	**PERCENT**	BACK-GROUND	# PTS IN OBJECT	AVER	PEAK VALUE AT X-Y	PEAK X-POS	PEAK Y-POS	SUM ABOVE BKGND	PTS ABOVE	PTS EQUAL	PTS BELOW
~0078	-155985	**29.36**	247	3675	204.6	255	778	62	23584	2948	0	727
~0079	0	**0**	255	3675	255	255	180	54	0	0	3675	0
~0080	-65835	**12.392**	253	3675	235.1	255	282	54	6776	3388	0	287
~0081	-160695	**30.246**	253	3675	209.3	255	384	54	6032	3016	0	659
~0082	53805	**-10.127**	238	3675	252.6	255	478	54	61897	3641	0	34
~0083	-75915	**14.289**	247	3675	226.3	255	576	56	26096	3262	0	413
~0084	-126660	**23.84**	247	3675	212.5	255	672	56	24504	3063	0	612
~0085	0	**0**	255	3675	255	255	878	58	0	0	3675	0

Table 7.4. Raw data of the quantitative result of the band in Figure 5.4

OBJECT NAME	VOLUME	PERCENT	BACK-GROUND	# PTS IN OBJECT	AVER	PEAK VALUE AT X-Y	PEAK X-POS	PEAK Y-POS	SUM ABOVE BKGND	PTS ABOVE	PTS EQUAL	PTS BELOW
~0050	-867674	**33.626**	199	7301	80.16	255	588	56	128520	2295	0	5006
~0051	-22723	**0.881**	233	7301	229.9	255	748	74	144804	6582	0	719
~0052	-716578	**27.77**	233	7301	134.9	255	444	56	84942	3861	0	3440
~0053	-567214	**21.982**	254	7301	176.3	255	296	56	5048	5048	0	2253
~0054	-222830	**8.636**	250	7301	219.5	255	150	56	31420	6284	0	1017
~0055	-183372	**7.106**	252	7301	226.9	255	4	58	19488	6496	0	805

Table 7.5. Raw data of the quantitative result of the band in Figure 5.5

OBJECT NAME	VOLUME	PERCENT	BACK-GROUND	# PTS IN OBJECT	AVER	PEAK VALUE AT X-Y	PEAK X-POS	PEAK Y-POS	SUM ABOVE BKGND	PTS ABOVE	PTS EQUAL	PTS BELOW
~0040	-973284	**37.523**	242	5967	78.89	255	384	240	23998	1846	0	4121
~0041	-136425	**5.26**	255	5967	232.1	255	230	242	0	0	5432	535
~0042	-434775	**16.762**	255	5967	182.1	255	534	242	0	0	4262	1705
~0043	-305490	**11.778**	255	5967	203.8	255	682	244	0	0	4769	1198
~0044	-301920	**11.64**	250	5967	199.4	255	826	244	23330	4666	0	1301
~0045	-441915	**17.037**	255	5967	180.9	255	962	248	0	0	4234	1733

Figure 5.3, 2 bands

lane	intensity
2	0
3	6.264
4	22.064
5	29.602
6	8.857
7	10.357
8	22.855
9	0

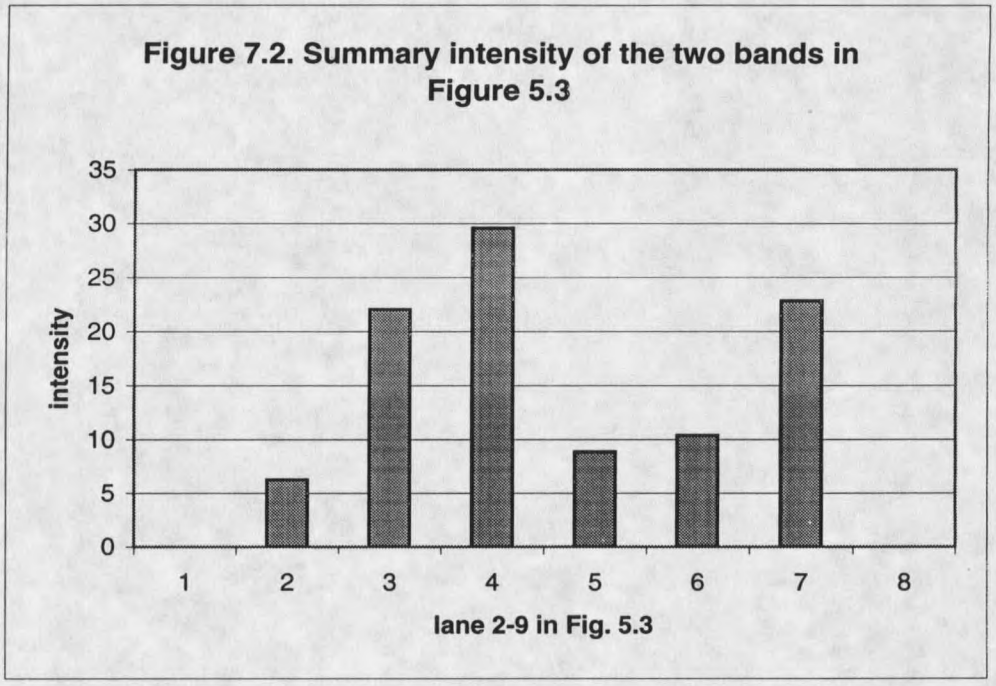


Figure 5.3, 1st band

lane	intensity
2	0
3	12.392
4	30.246
5	0
6	14.289
7	23.84
8	29.36
9	0

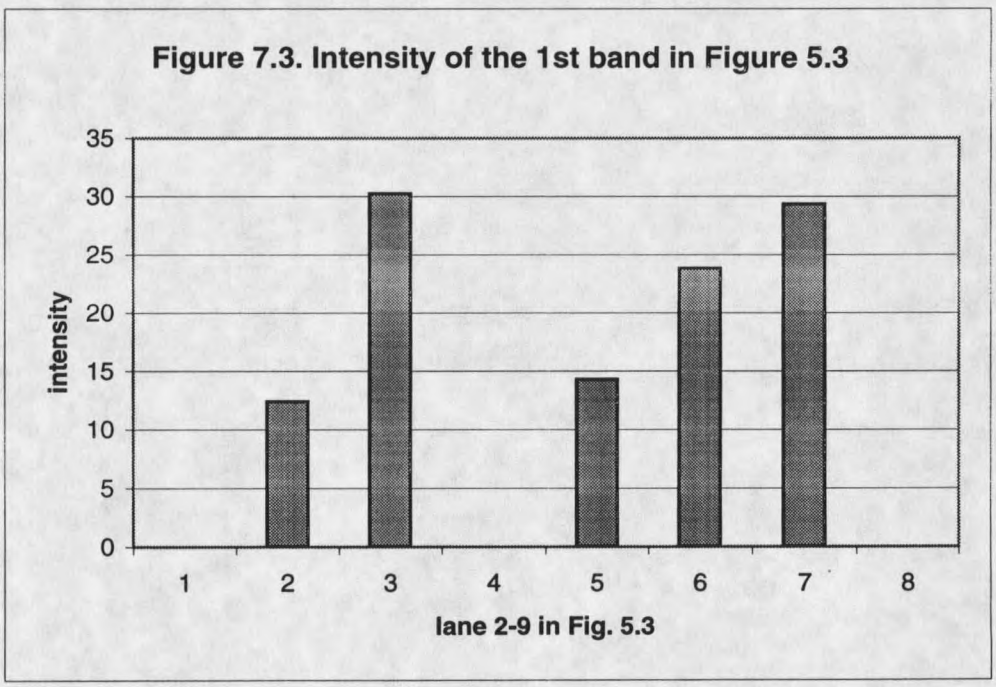


Figure 5.4.

lane	intensity
1	0
2	0.881
3	33.626
4	27.77
5	21.982
6	8.636
7	7.106

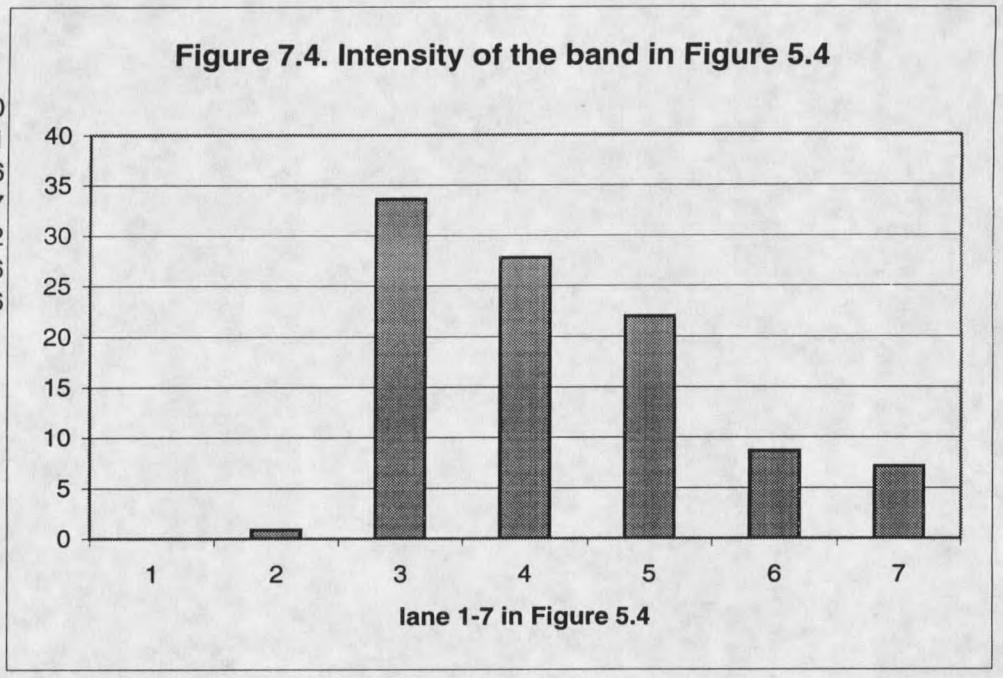
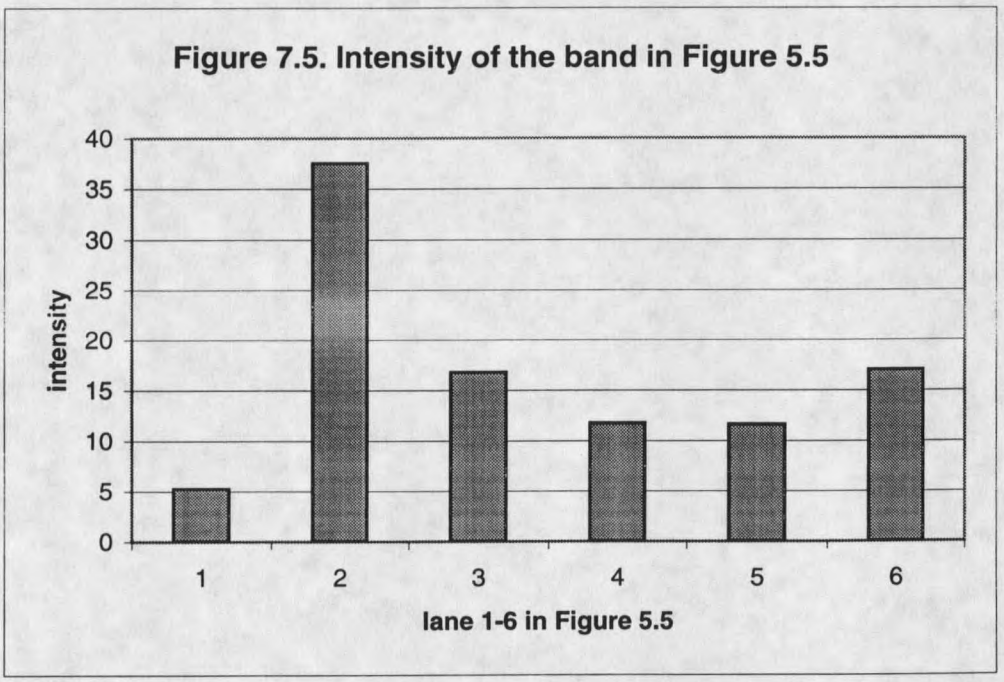


Figure 5.5.

lane	intensity
1	5.26
2	37.523
3	16.762
4	11.778
5	11.64
6	17.037



MONTANA STATE UNIVERSITY - BOZEMAN
3 1762 10331163 3